ARCHAEOMETRIC STUDIES ON SELECTED SAMPLES OF HUMAN BONES EXCAVATED FROM THE RUINS OF THE ROMAN AMPHITHEATRE IN İZNİK

A THESIS SUBMITTED TO
THE GRADUATE SCHOOL OF NATURAL AND APPLIED SCIENCES
OF
MIDDLE EAST TECHNICAL UNIVERSITY

BY

UĞUR BÜLENT AKSOY

IN PARTIAL FULFILLMENT OF THE REQUIREMENTS
FOR
THE DEGREE OF DOCTOR OF PHILOSOPHY
IN
ARCHAEOMETRY

AUGUST 2020

Approval of the thesis:

ARCHAEOMETRIC STUDIES ON SELECTED SAMPLES OF HUMAN BONES EXCAVATED FROM THE RUINS OF THE ROMAN AMPHITHEATRE IN İZNİK

submitted by **UĞUR BÜLENT AKSOY** in partial fulfillment of the requirements for the degree of **Doctor of Philosophy in Archaeometry Department, Middle East Technical University** by,

Prof. Dr. Halil Kalıpçılar
Dean, Graduate School of **Natural and Applied Sciences** _____

Prof. Dr. Musa Doğan
Head of Department, **Archaeometry** _____

Assoc. Prof. Dr. Kaan Sayıt
Supervisor, **Archaeometry, METU** _____

Assoc. Prof. Dr. Kameray Özdemir
Co-Supervisor, **Anthropology, Hacettepe University** _____

Examining Committee Members:

Prof. Dr. Musa Doğan
Archaeometry, METU _____

Assoc. Prof. Dr. Kaan Sayıt
Archaeometry, METU _____

Prof. Dr. Deniz Burcu Erciyas
Settlement Archaeology, METU _____

Assoc. Prof. Dr. Ali Akın Akyol
Con. and Res. of Cult. Prop. Dept., HBVU _____

Assoc. Prof. Dr. Handan Üstündağ
Archaeology, Eskişehir Anadolu U. _____

Date: 01.08.2020

I hereby declare that all information in this document has been obtained and presented in accordance with academic rules and ethical conduct. I also declare that, as required by these rules and conduct, I have fully cited and referenced all material and results that are not original to this work.

Name, Surname: Uğur Bülent Aksoy

Signature:

ABSTRACT

ARCHAEOMETRIC STUDIES ON SELECTED SAMPLES OF HUMAN BONES EXCAVATED FROM THE RUINS OF THE ROMAN AMPHITHEATRE IN İZNİK

Aksoy, Uğur Bülent
Doctor of Philosophy, Archaeometry
Supervisor: Assoc. Prof. Dr. Kaan Sayıt
Co-Supervisor: Assoc. Prof. Dr. Kameray Özdemir

August 2020, 141 pages

In this study, major, minor, and trace elements were analysed in 21 bones belonging to 19 individuals with different sex, age, and location excavated from the Roman Theatre in İznik. Additionally, five soil samples taken from different parts of the site were analysed with applied chemical and physical analysis using archaeometric methods to determine and investigate the implication of toxic elements (Pb, As, Cd, etc.), and their accumulation in bone hydroxyapatite due to diagenic and/or biogenic basis.

The elemental composition of the İznik bones were determined using both XRF (X-ray fluorescence spectrometry) and ICP-OES (inductively coupled plasma optical emission spectrometry) methods, simultaneously. One of the soil samples and four of the bone samples were analyzed by Ultra Trace Aqua Regia ICP-MS to obtain a control group. Before the elemental analysis, the organic phase of the bone matrix was removed and the analysis was based solely on bone hydroxyapatite.

Cortical bones (femora) and trabecular bones (costa) were examined separately. The elemental analysis focused on the matrix elements of Ca and P, diagenetic related elements Mn, Fe, K, Pb, Al, U, Zr, and Y, and dietary elements Zn, Ba, Mg and Sr. To define uncontaminated bone matrix, the Ca/P mass ratio in the crystal structure of bone hydroxyapatite was calculated.

To obtain diagenetic implication in the surrounding soil of the burial, electrical conductivity, hydrogen-ion activity, and soil type analysis were performed. Furthermore, diagenetic alteration of bone apatite was physically tested, due to the changes of porosity and recrystallization, by using FTIR (Fourier Transform Infrared) spectroscopy and porosity measurements. The results were evaluated with principal component analysis (PCA). In the correlation matrix, the diagenetic effects of different elements on the bone samples was determined statistically.

Keywords: Diagenesis, Trace Elements, Femora, Hydroxyapatite, Dietary, Costa, X-Ray.

ÖZ

İZNİK ROMA ANTİK TİYATROSU KAZILARINDAN ELDE EDİLMİŞ İNSAN KEMİKLERİ ÜZERİNE ARKEOMETRİK ÇALIŞMALAR

Aksoy, Uğur Bülent
Doktora, Arkeometri
Tez Danışmanı: Doç. Dr. Kaan Sayıt
Ortak Tez Danışmanı: Doç. Dr. Kameray Özdemir

Ağustos 2020, 141 sayfa

Bu çalışmada, İznik Roma antik tiyatrosu 1988-1990 kazı çalışmalarında gün ışığına çıkartılmış kemikler arasından seçilen 19 bireye ait toplam 21 adet kemik ve bu kemiklerin gömü alanlarından elde edilmiş 5 toprak örneğinin, fiziksel ve kimyasal analizleri arkeometrik bakış açısı ile incelenmiştir. Elde edilen veriler doğrultusunda, söz konusu bireylere ait kemiklerde eser miktarda bulunan arsenik, kurşun, kadmiyum ve benzeri toksik elementlerin, bireylerin yaşam süresi içerisinde mi, yoksa kemiklerin toprak altında geçirdikleri süre içerisinde mi biriktikleri yönünde bulgulara ulaşilmasi hedeflenmektedir.

İznik kemiklerinin element analizleri, aynı anda X-ışını fluoresans (XRF) ve indüktif eşleşmiş plazma atomik emisyon spektroskopi (ICP-OES) yöntemleri kullanılarak analiz edilmiştir. Sonuçların kontrolü için bir adet toprak örneği ve 4 adet kemik örneği indüktif eşleşmiş plazma kütle spektroskopi (ICP-MS) yöntemi ile hidroklorik ve nitrik asit (aqua regia) çözeltisinde ayrıştırılarak analiz edilmiştir. Çalışmalar sırasında kemiğin organik bileşeni arkeometrik yöntemlerle uzaklaştırılmış ve analizler kemiğin inorganik yani hidroksiapatit mineral yapısı üzerine odaklanmıştır.

Element analizlerinden önce kemikler cinsiyet, lokasyon ve yapısal olarak sınıflandırlmıştır. Analizleri yapılan elementler, kemiğin korunma durumu hakkında

bilgi verenler (Ca ve P), beslenme modelini yansıtanlar (Sr, Ba, Zn ve Mg) ve diyagenez hakında bilgi verenler (Mn, Fe, K, Pb, Al, U, Zr, ve Y) olmak üzere üç grupta değerlendirilmiştir. Kemiğin toprak altında kaldığı süre boyunca maruz kaldığı kirlenme miktarının tespiti için Ca/P oranları hesaplanmıştır.

Bunların yanısıra, gömülerin bulunduğu toprağın kemikler üzerindeki diyagenez etkisinin belirlenmesi amacı ile, toprağın pH değeri, kil miktarı ve elektrik geçirgenliği analizleri yapılmıştır. Ayrıca, kemiğin toprak altındaki değişimleri, porozite miktarı ve Fourier dönüşümlü kızılötesi (FTIR) spektroskopi yöntemi ile yeniden kristallenmesi analiz edilmiştir. Son olarak, XLSTAT program kullanılarak, elementlerin istatistiki analizleri yapılmıştır.

Anahtar Kelimeler: Diyagenez, Eser element, Femur, Hidroksiapatit, Beslenme, Kızılötesi

To my daughter Gece: May you never forget that I will always love you.

ACKNOWLEDGEMENTS

I would like to express my sincere gratitude to Prof. Dr. Şahinde Demirci for her guidance, continuous support, and immense knowledge.

I am deeply grateful to Prof. Ay Melek Özer for providing a wonderful interdisciplinary area to study.

I would like to thank to Assoc. Prof. Dr. Kaan Sayıt for his support and guidance.

I owe special thanks to Assoc. Prof. Dr. Kameray Özdemir for his valuable guidance.

I would like to thank Prof. Dr. Selim Yılmaz Erdal for providing the samples and his valuable support.

I am grateful to Assoc. Prof. Dr. Ali Akın Akyol for his guidance, generosity, and suggestions.

Very special thanks to Gülşen Albuz Geren, Kaan Kirde and Orcan Kolankaya for their assistance and supports during sample analysis.

And finally, my very special thanks to my wife Dr. Elif Başak Aksoy for her support and encouragement.

TABLE OF CONTENTS

ABSTRACT v

ÖZ vii

ACKNOWLEDGEMENTS x

TABLE OF CONTENTS xi

LIST OF TABLES xiv

LIST OF FIGURES xv

LIST OF ABBREVIATIONS xvii

1. INTRODUCTION 1

1.1. Introduction 1

1.2. Aims and Objectives 3

2. WHAT IS A BONe? 7

2.1. Defining Bones 7

2.1.1. Functions of bones 7

2.1.2. Anatomy of bones 8

2.1.3. Classification of bones 9

2.1.3.1. Structural classification of bones 9

2.1.3.2. Morphological classification of bones 12

2.2. Chemistry of Bones 16

2.2.1. The organic phase of bone 16

2.2.2. The inorganic phase of bone 17

2.3. Elements in bones 19

2.3.1. Essential Elements 20
2.3.2. Minor Elements 22
2.3.3. Adsorption and absorption of ions 26
2.3.3.1. Adsorption on the surface of the solids 31
2.3.3.2. Adsorption of ions 37
2.4. Degradation of Bones (Diagenesis) 38
2.4.1. Microbial Attack 39
2.4.2. Porosity 40
2.4.3. Crystallinity 41
2.4.4. Soil Properties and Groundwater 42
3. MATERIALS AND METHODS 45
3.1. İznik (Nicaea) 45
3.1.1. History of İznik 46
3.1.2. The Excavations at İznik 48
3.1.3. Burial typology 49
3.1.4. Architectural properties of the theatre 52
3.2. Sampling and Methodology 53
3.2.1. Selection of Samples 53
3.2.2. Sample Preparation 56
3.2.3. Porosity measurements 60
3.2.4. Soil analysis 61
3.2.4.1. Acidity of soil 61
3.2.4.2. Soil type analysis 61
3.2.4.3. Electrical conductivity of soil (salinity) 62

3.3. Instrumental Analysis 63
3.3.1. XRF (X-ray Fluorescence) 63
3.3.1.1. Optical emission and mass spectroscopy 64
3.3.2. FTIR (Fourier Transform Infrared Spectroscopy) 67
3.4. Statistical Analysis 69
4. RESULTS AND DISCUSSION 71
4.1. Description and Measurement of Diagenetic Parameters 71
4.1.1. Chemical and physical analysis of soil 71
4.1.1.1. Hydrogen-ion activity (pH of soil) 71
4.1.1.2. Salt analysis 73
4.1.1.3. Soil type analysis 74
4.1.1.4. Elemental analysis of soil 75
4.1.2. Chemical and physical analysis of the bones 77
4.1.2.1. Crystallinity 77
4.1.2.2. Porosity 83
4.1.2.3. Elemental analysis 84
4.2. Statistical Analysis of Elemental Compositions 94
4.2.1. Princible Component Analysis (PCA) 96
5. Conclusion 103
REFERENCES 107
A. Bone Samples 117
B. TGA ANALYSIS 129
CURRICULUM VITAE 141

LIST OF TABLES

TABLES

Table 2.1. Ionic exchange between apatite and soil 18
Table 2.2. The elemental composition of different environments 19
Table 2.3. Concentration of elements found in adult human cortical bone mineral .. 20
Table 2.4. Relationship between CN, radius ratio, and geometrical identification ... 28
Table 3.1. The studied samples of the Roman Theatre 54
Table 3.2. Sex patterns in the samples 55
Table 3.3. Age at death patterns in the samples 55
Table 3.4. Soil type according to grain size 61
Table 4.1. The pH of the soil samples 72
Table 4.2. Electrical conductivity analysis 73
Table 4.3. Soil type analysis 75
Table 4.4. XRF analysis of soil samples 76
Table 4.5. FTIR crystallinity results 77
Table 4.6. Porosity and the water absorption capacity of bones 83
Table 4.7. Raw data of the XRF and ICP-OES analyses 85
Table 4.8. XRF fesults for the sampled bones 86
Table 4.9. ICP-OES results for the sampled bones 86
Table 4.10. Ca/P ratio of the sampled bones 89
Table 4.11. t-test values for XRF vs ICP analysis of elements 95
Table 4.12. Squared cosines of the variables 99
Table 4.13. Correlation matrix of the XRF results 100
Table 4.14. Squared cosines of the variables for ICP-OES 100
Table 4.15. Correlation matrix of ICP-OES 101

LIST OF FIGURES

FIGURES

Figure 2.1. Example of a long bone (REF) 11
Figure 2.2. Types of bone 12
Figure 2.3. The human (adult) skeletal system 15
Figure 2.4. Chemical formula of an amino acid 16
Figure 2.5. Polyhedron examples 29
Figure 3.1. Location of İznik 45
Figure 3.2. The Roman Theatre 48
Figure 3.3. The layout of the Roman Theatre 50
Figure 3.4. Burial forms of the skeletons 51
Figure 3.5. Removing visible contamination 56
Figure 3.6. Gibertini Crystal 200 SMI magnetic compensation analytical balance ... 57
Figure 3.7. Ultrasonic Bath 57
Figure 3.8. Mipro Etüv Dryer 58
Figure 3.9. High heat oven 59
Figure 3.10. Grounding the samples 59
Figure 4.1. FTIR pattern of sample ITK 90 57/3 78
Figure 4.2. FTIR pattern of sample ITK 90 58/5 79
Figure 4.3. FTIR pattern of sample ITK 90 57/3 B 80
Figure 4.4. FTIR pattern of sample ITK 90 58/5 B 81
Figure 4.5. The overall comparison of trace elements according to instrumentation 87
Figure 4.6. Ca and P values of samples with each utilised method 88
Figure 4.7. The Ca/P ratio comparison of XRF and ICP-OES inside of the cavea ... 90
Figure 4.8. The Ca/P ratio comparison of XRF and ICP outside of cavea 91
Figure 4.9. The Ca/P ratio comparison of XRF and ICP of male individuals 92
Figure 4.10. The Ca/P ratio comparison of XRF and ICP of female individuals 93

Figure 4.11. XRF analyzed element correlation chart for functions F1 and F2 97
Figure 4.12. ICP-OES analyzed elements correlation chart for functions F1 and F298
Figure 0.1. ITK 88 43/10 117
Figure 0.2. ITK 88 41-43/6 117
Figure 0.3. ITK 41-43/1 118
Figure 0.4. ITK 89 53/9 118
Figure 0.5. ITK 89 53/26 119
Figure 0.6. ITK 89 53/30 119
Figure 0.7. ITK 90 57/3A 120
Figure 0.8. ITK 90 57/3B 120
Figure 0.9. ITK 89 51/24 121
Figure 0.10. ITK 90 58/7 121
Figure 0.11. ITK 90 58/3 122
Figure 0.12. ITK 90 57/11 122
Figure 0.13. ITK 90 57/8 123
Figure 0.14. ITK 88 43/21 123
Figure 0.15. ITK 88 43/13 124
Figure 0.16. ITK 88 43/3 124
Figure 0.17. ITK 89 41/2 125
Figure 0.18. ITK 89 53/3 125
Figure 0.19. ITK 89 53/6 126
Figure 0.20. ITK 90 58/5A 126
Figure 0.21. ITK 90 58/5B 127

LIST OF ABBREVIATIONS

ABBREVIATIONS

Al: Aluminium

As: Arsenic

ATP: Adenosine Triphosphate

Ba: Barium

C: Carbon

Ca: Calcium

Cd: Cadmium

Cu: Copper

DNA: Deoxyribonucleic acid

F: Fluorine

Fe: Iron

H: Hydrogen

HA: Hydroxyapatite

ICP-OES: Inductively Coupled Plasma Optical Emission Spectroscopy

K: Potassium

Log: Logarithm

Mg: Magnesium

Mn: Manganese

N: Nitrogen

Na: Sodium

O: Oxygen

OH: Hydroxide

pH: Hydrogen ion concentration

P: Phosphorus

Pb: Lead

PCA: Principal Component Analysis

Ppm: Particle per mass

Sr: Strontium

U: Uranium

XRF: X-Ray Fluorescence

Y: Yttrium

Zn: Zinc

Zr: Zirconium

CHAPTER 1

INTRODUCTION

1.1. Introduction

In archaeology, the settlement forms, architectural features, works of art, and everyday materials obtained from the archaeological sites provide indirect information about a settlement and its people. Written sources such as books, tablets, inscriptions etc., however, provide more direct information for determining the life-style of a society. For reconstructing the demographic and biological structure of societies, the skeletal remains are a key component for developing our understanding. Archaeological bones can provide us with the basic information about the socioeconomic structure of an ancient community, in other words they can help us to understand their subsistence patterns. (Erdal, 1996; Özdemir, 2008).

Bone is one of the hardest structures of the human body. It is a complex tissue consisting of inorganic calcium phosphates precipitated in an organic collagen matrix (Pate, 1994). Calcium and phosphorus (calcium-phosphate salt called apatite) are the main elements of the mineral matrix (Sillan et al., 1989). The ion calcium is necessary for a number of essential physiologic processes. Calcium is abundant in seawater, where life is assumed to have originated. However, calcium is not as abundant as sodium outside of a marine environment and so, once out of the sea, animals evolved mechanisms to conserve calcium. One of these key mechanisms is the endoskeleton, which also doubles as a support structure for the body and its essential organs, as well as providing a store of calcium. Phosphorus is the fuel supply of the body as well as an intimate part of its structure. It is abundant and physiologically tolerable. Calcium, in conjunction with phosphate, provides the hardness of bone tissue, and its ability to remain rigid (Jowsey, 1977).

Since bone is one of the hardest parts of the body (after enamel), after death it can, in the right conditions, more easily resist post-mortem degradation factors to a greater extent than other parts of the body. This is especially true for the mineral phase of bone, with it being able to endure time even more than many other materials. This provides one of the key reasons why skeletal remains have provided an invaluable source of information for archaeologists in many fields, such as relative and chronometric dating, paleodiet reconstruction, palaeohydrology studies, and paleoclimatic reconstruction. However, post-mortem chemical contamination from the surrounding soil matrix complicates the results and interpretation for most of these applications.

The composition of buried bones is the result of changes that happened before and after inhumation, more commonly known as pre-mortem and post-mortem degradations, respectively (Costas et al., 2016). The term "diagenesis", originates from its use in geology, meaning across generations, but has become common terminology in archaeology and anthropology as a way of referring to the changes and alterations that affect skeletal material. Diagenesis is the cumulative physical and chemical alteration of bones, and diagenetic processes are highly heterogeneous due to factors such as post-depositional time, taphonomy, and the physical and chemical properties of the burial environment (Hedges, 2002).

Alteration occurs at all scales, from molecular loss and substitution, through crystallite reorganization, porosity and microstructural changes, and in many cases, to disintegration of the complete unit (Pate, 1994). The pathway of diagenesis for bones are as follows; crystallization of amorphous calcium phosphate, dehydration, chemical deterioration of organic material and proteins, chemical deterioration of the mineral phase, and microbial attack of the composite. The dissolution of organic material depends on time, temperature, and soil pH. Acidity of the environment causes accelerated hydrolysis. Due to the increase in porosity of bone through collagen loss,

the bone becomes susceptible to hydrolytic infiltration (Demirci and Kayatürk, 1989). In order to remove post-mortem contamination, protocols for the physical and chemical preparation of samples have been continuously developed and improved (Zapata et al., 2006).

In this study, archaeometric examination was performed on 21 bones belonging to 19 individuals with different sex, age, and burial locations excavated from the İznik Roman theatre, and five soil samples taken from different parts of the site were also analysed. The sampled osteological and soil material was analyzed for their chemical and physical compositions using a number of analytical methods. The elemental composition of the bones from İznik were measured using both XRF (x-ray fluorescence spectrometry) and ICP-OES (inductively coupled plasma optical emission spectrometry) methods. For the accreditation of the methods used for the analysis, five of these samples were sent to ALS Global labs and analysed by ICP-MS (inductively coupled plasma mass spectrometry) method. Cortical bones (femora) and trabecular bones (costa) were analysed separately. The elemental analyses focused on the matrix elements Ca and P, diagenesis related elements Fe, K, Pb, Al, As and Cu, and dietary elements Zn, Ba, and Sr. To identify uncontaminated bone matrix, the Ca/P mass ratio in the crystal structure of bone hydroxyapatite was calculated. The results were evaluated by principal component analysis (PCA). To obtain diagenetic implications from the soil surrounding the burial, electrical conductivity, hydrogen-ion activity, and soil type analyses were employed. Furthermore, diagenetic alteration of bone apatite was physically tested, due to the changes of porosity and recrystallization by using FTIR (Fourier Transform Infrared) spectroscopy and porosity measurements.

1.2. Aims and Objectives

The main objective of the study is to apply and improve archaeometric methods to develop a set of criteria for archaeological and anthropological material analysis.

1- In this study elements were selected to provide afocus on the highest potential for providing information on archaeometric bases. The elements related to diagenesis, dietary reconstruction, identifying toxicity, as well as the matrix elements were prioritized. With this study, a comparison of the elemental composition of İznik bones, with other concurrent studies in the literature, will provide a data criterion for Anatolian archaeology.

2-One of the most complicated problems when monitoring past lives from skeletal remains is the post-mortem chemical contamination of bone from the surrounding soil matrix. In this study, the diagenesis of İznik bones was tested using the quantitative analysis adapted from protocols described in the literature. The results will evaluate the factors of degradation and create a pathway to distinguish biogenetic and diagenetic alteration.

3-Diet is an essential concern for establishing the adaptive strategies of ancient population and their paleo-ecological relationship with their environments. The amount of minor and trace elements deposited in bone is also dependent on dietary intake. The elemental composition, especially the values of diet related elements, coucan potentially provide clues about these adaptive strategies.

4-Elements can be classified as nutritionally essential (e.g. Cu and Zn), or toxic (e.g. Pb, As and Cd) in living organisms (Jurkiewicz et al., 2004). The pathways for metallic elements to enter the living body include consumption of food, ingestion of drinking water, inhalation of air containing metals as impurities, and use or during manufacturing processes of utensils or tools made of metal(s). An increase in the elemental content of metals, even for those essential to organisms, may cause major health problems (Özdemir et al., 2009). Lead toxicity, for example, is one of the major issues in environmental health, since it has been used for at least 5000 years. Blood lead levels higher than 70 μg/dl can cause severe neurological symptoms and even

death (Millard, 2006). Exposure to a sufficiently high concentration of arsenic can also lead to intoxication in living organisms (Nriagu et al., 2007).

Another primary interest of this study was to determine the toxic element accumulation in the apatite (inorganic) part of the bone samples. Most of the absorbed metals in organisms accumulate in bones, as well as in nails, hair, and the kidneys (Jurkiewicz et al., 2004). The detection of known toxic element concentrations in the İznik bones would be significant, since İznik was characterized by its unique and highly qualified ceramic production center, which had its origins in the Byzantine period (Kırmızı, 2004). Toxic metals such as lead, cadmium, and copper were heavily used in the production process of these ceramics as glaze stabilizers and coloring agents that may have resulted in the population (particularly those working in the ceramic industry) being affected by toxic metal poisoning.

5- Although the advantages and disadvantages are clear, according to the literature, another goal of this study is to compare the precision between the results of two quantitative analyses; XRF and ICP. Determination of the most efficient method can provide a guide for further research.

To understand the past lives of ancient populations, archaeometric studies are inevitably mandatory, and in the end like all other sciences, data is one of the most important tools of archaeometry. Before drawing any conclusion about any concept of science, in our case a metric approach to archaeology and anthropology, the data needs to be established. Although elemental analysis in fossilised bones has been conducted for over half a century in the world, these types of studies are not currently extensive and common in Turkey. Hopefully, this study will provide an important set of data for archaeology and will stimulate greater interest in archaeometric studies in Turkey.

CHAPTER 2

WHAT IS A BONE?

2.1. Defining Bones

A ‘bone’ is an organ comprised of several different tissues working together: bone (osseous) tissue, cartilage, dense connective tissue, epithelium, adipose tissue, and nervous tissue (Fig. 2.1). “The entire framework of bones and their cartilages constitute the skeletal system. Bone tissue accounts for about 18 percent of the total mass of the human body. Bone refers to a family of materials, each with a somewhat different structural motif, but all having a common basic building block, the mineralized collagen fibril. The mineralized collagen fibril is composed of the fibrous protein collagen in a structural form that is also present in skin, tendons, and a variety of other soft tissues (Weiner, Wagner, 1998: 271-279).” There are 206 bones in an adult skeleton (Fig. 2.3), which allow the human body to stand its own weight with little or no muscular effort involved to stay upright and aligned (Berlin, Adams, 2017). They range in size from the small ear bones in the skull to the nearly two-foot-long femur (thigh bone) of an adult. (Tortora, Nielsen, 2012). Ossification of the bony skeleton begins in about the fifth week of fetal life, and skeletal growth is completed by about 25 years of age.

2.1.1. Functions of bones

The most important functions of the skeletal system include the following:

• To serve as a rigid structure of mechanical stability, to support soft tissues, and serve as attachment points for muscles

• To protect vital organs (brain, heart, lungs, spinal cord) and nerves

• To break down and regenerate (bone cells continually do this)

• To produce blood cells (in the red bone marrow)

• To assist in movement (skeletal muscles move bones) by allowing for efficient transfer of force and torque

• To store minerals (particularly calcium phosphate)

• To store chemical energy (triglycerides, in the yellow bone marrow)

"The way the skeleton is designed (Fig. 1), with an upright spinal column and long extremities with different bone widths and lengths, is the result of evolutionary requirements for human survival and development, in terms of structural strength, mobility, and flexibility (Berlin, Adams, 2017)."

2.1.2. Anatomy of bones

In terms of gross structure, there are two different types of bone tissue: cortical and trabecular bone. "Cortical (compact) and trabecular (cancellous) bone are distinguished by the degree to which each is calcified, and by their general functions. Only 15-25%, by volume, of trabecular bone is calcified, compared to 80-90% of cortical bone (Ezzo, 1994b)". Cortical bone is the solid, dense part that forms the outer layer of the bones; it is thickest in the diaphysis (shafts) of the long-bones. It forms a thin layer around the ends of the long bones, and the flat and irregular bones. "Trabecular bone is less dense than cortical bone and has a honeycomb structure. Trabecular bone is located within the ends of long-bones and in the interior of the flat and irregular bones. In living bone, most of the outer surface is surrounded by a thin membrane, the periosteum. The internal walls of the medullary cavities of long bones are lined with another membrane, the endosteum, which also lines the network of tiny cavities in trabecular bone (Mays, 1998)."

“There are three main types of bone cells. Osteoblasts are responsible for the formation of new bone, osteocytes are involved with the maintenance of bone as a living tissue, and osteoclasts are responsible for desorption (removal) of bone. Osteoblasts are often concentrated on bone surfaces (for example, beneath the periosteum), and are responsible for producing the organic matrix, osteoid, which is then mineralized to form bone (Mays, 1998).”

2.1.3. Classification of bones

Bones are classified under two groups according to their structural and morphological properties.

2.1.3.1. Structural classification of bones

A typical long bone (Fig. 2.1) consists of the following parts:

“1. The diaphysis is the bone’s shaft, or body—the long, cylindrical, main portion of the bone.

2. The epiphyses or extremities are the proximal and distal ends of the bone.

3. The metaphysis is the region between the diaphysis and the epiphyses. In a growing bone, each metaphysis contains an epiphyseal (growth) plate, a layer of hyaline cartilage that allows the diaphysis of the bone to grow in length (a process described later in this chapter). When bone growth in length stops somewhere between the ages of 18 and 21, the cartilage in the epiphyseal plate is replaced by bone and the resulting bony structure is known as the epiphyseal line.

4. The articular cartilage is a thin layer of hyaline cartilage covering the part of the epiphysis where the bone forms an articulation (joint) with another bone. Articular cartilage reduces friction and absorbs shock at freely movable joints. Because articular cartilage lacks a perichondrium and blood vessels, the ability to repair damage is limited.

5. The periosteum is a tough connective tissue sheath with its own associated blood supply that surrounds the bone surface, wherever it is not covered by articular cartilage. It is composed of an outer fibrous layer of dense and irregular connective tissue, and an inner osteogenic layer that consists of cells. Some of the cells enable bone to grow in thickness, but not in length. The periosteum also protects the bone, assists in fracture repair, helps nourish bone tissue, and serves as an attachment point for ligaments and tendons. The periosteum is attached to the underlying bone by perforating (Sharpey's) fibers, thick bundles of collagen that extend from the periosteum into the extracellular matrix of the bone.

6. The medullary cavity, or marrow cavity, is a hollow, cylindrical space within the diaphysis that contains fatty yellow bone marrow and numerous blood vessels in adults. This cavity minimizes the weight of the bone by reducing the dense bony material where it is least needed. The long bones' tubular design provides maximum strength with minimum weight.

7. The endosteum is a thin membrane that lines the medullary cavity. It contains a single layer of bone-forming cells and a small amount of connective tissue (Tortora, Nielsen, 2012)."

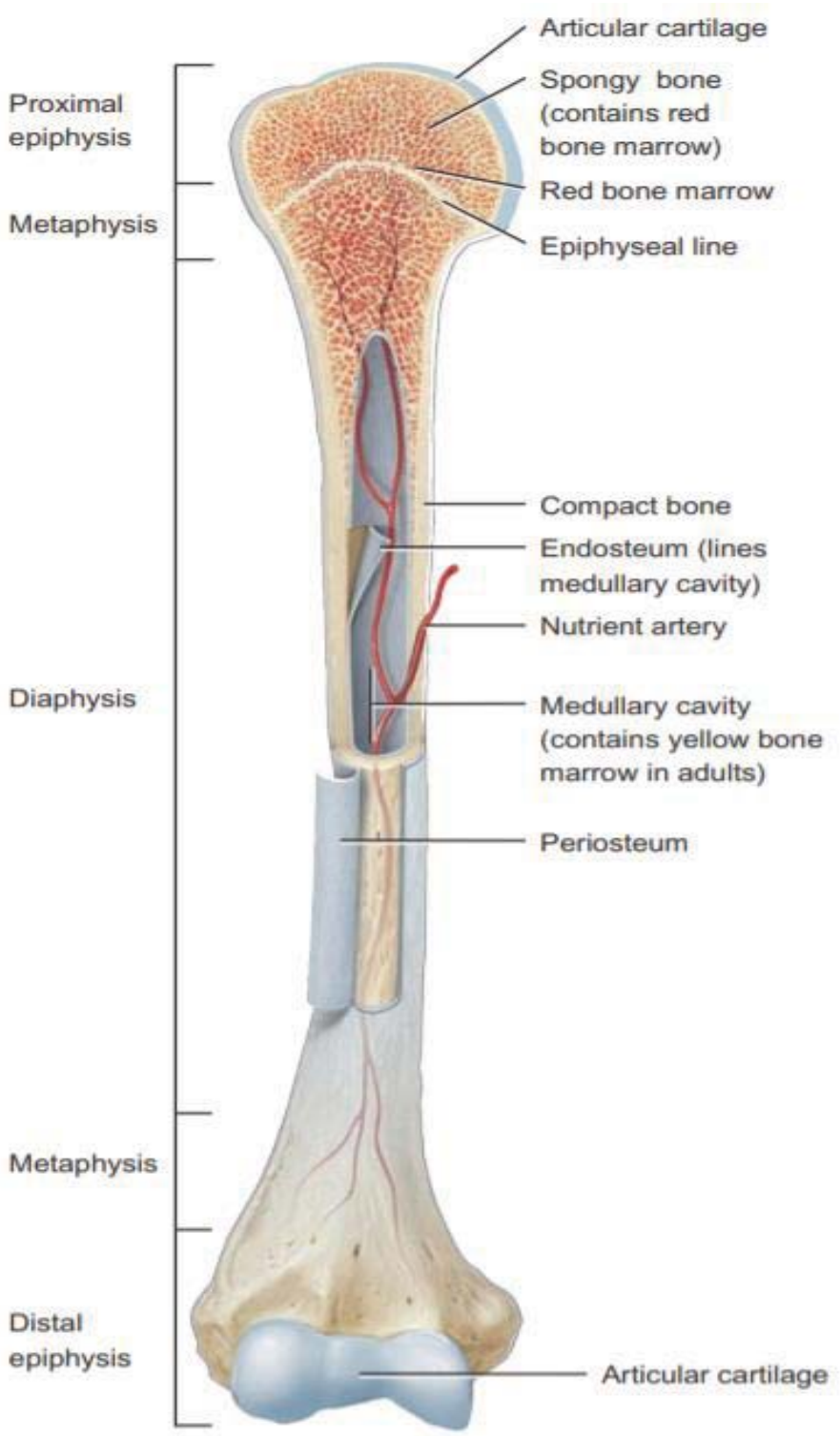

Figure 2.1. A typical long bone (adapted from Steele, Bramlett, 1998)

2.1.3.2. Morphological classification of bones

Anatomists recognize five types of bones (Fig 2.2) in the skeleton on the basis of shape.

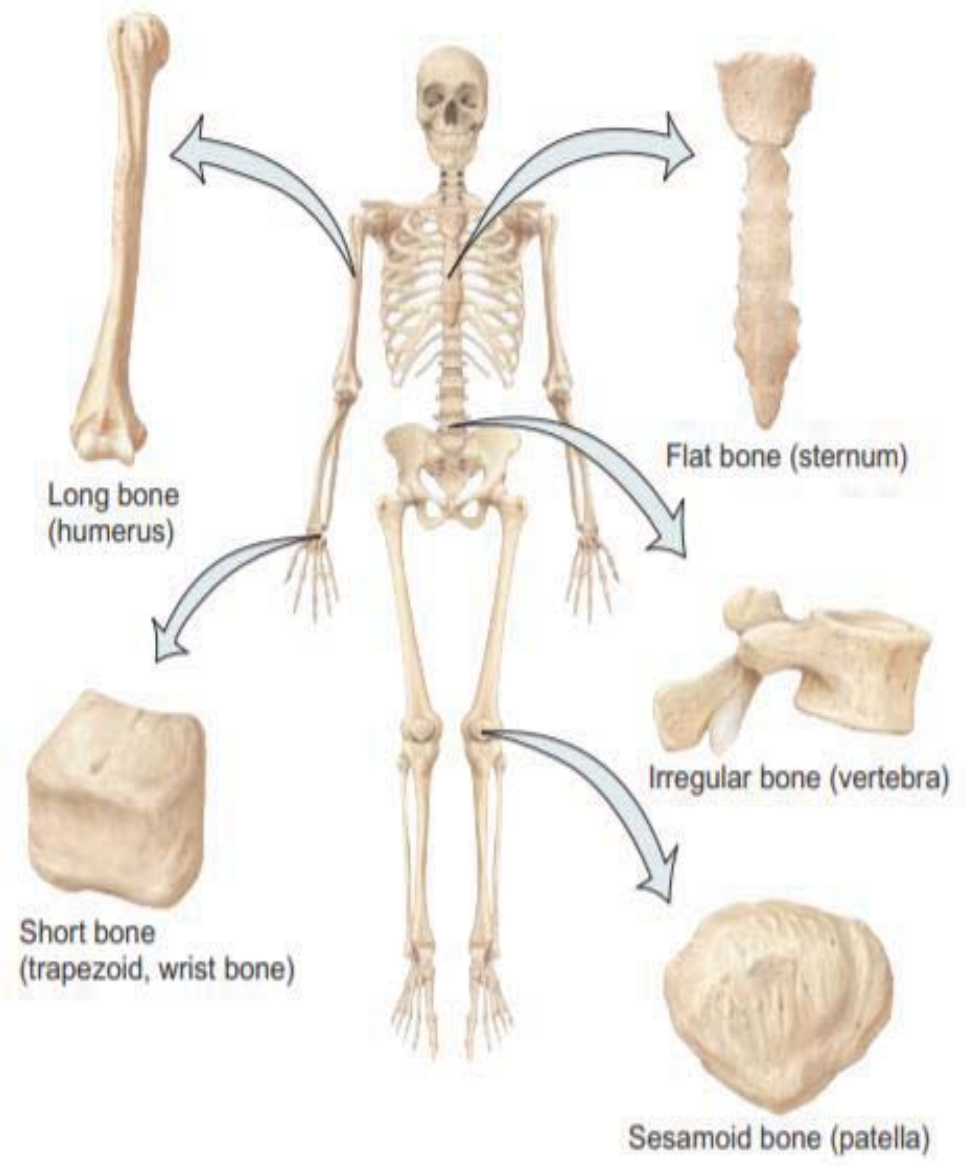

Figure 2.2. Types of bone (adapted from Steele, Bramlett, 1998)

“1. Long bones have a greater length than width and consist of a diaphysis (shaft) and a variable number of epiphyses or extremities (ends). They are slightly curved for strength. A curved bone absorbs the stress of the body’s weight at several different points so that it is evenly distributed. If such bones were straight, the weight of the body would be unevenly distributed and the bone would fracture easily. Long bones consist mostly of compact bone tissue, which is dense and has smaller spaces, but they also contain considerable amounts of spongy bone tissue, which has larger spaces. Long bones include the humerus (arm bone), ulna and radius (forearm bones), femur (thigh bone), tibia and fibula (lower leg bones), metacarpals (hand bones), metatarsals (foot bones), and phalanges (finger and toe bones).

2. Short bones are somewhat cube-shaped and nearly equal in length, width, and depth. They consist of spongy bone except at the surface, where there is a thin layer of compact bone. Examples of short bones include most carpal (wrist) bones, and most tarsal (ankle) bones.

3. Flat bones are generally thin and composed of two nearly parallel plates of compact bone enclosing a layer of spongy bone. The layers of compact bone are called the external and internal tables. Flat bones afford considerable protection and provide extensive areas for muscle attachment. They include the cranial (skull) bones, which protect the brain; the sternum (breastbone) and ribs, which protect the organs of the thorax; and the scapulae (shoulder blades).

4. Irregular bones have complex shapes and cannot be grouped into any of the three categories previously described. They also vary in the amounts of spongy and compact bone they contain. Such bones include the vertebrae (bones of the spinal column), certain facial bones, and the calcaneus (heel bone).

5. Sesamoid bones (shaped like a sesame seed) develop in certain tendons where there is considerable friction, compression, and physical stress. They are not always completely ossified and measure only a few millimeters to centimeters in diameter, except for the two patellae (kneecaps) which are the largest of the sesamoid bones. Sesamoid bones vary in number from person to person except for the patellae, which are located in the quadriceps femoris tendon and are normally present in all individuals. Functionally, sesamoid bones protect tendons from excessive wear and tear, and they often change the direction of pull of a tendon, which improves the mechanical advantage at a joint (Tortora, Nielsen, 2012:151-152).”

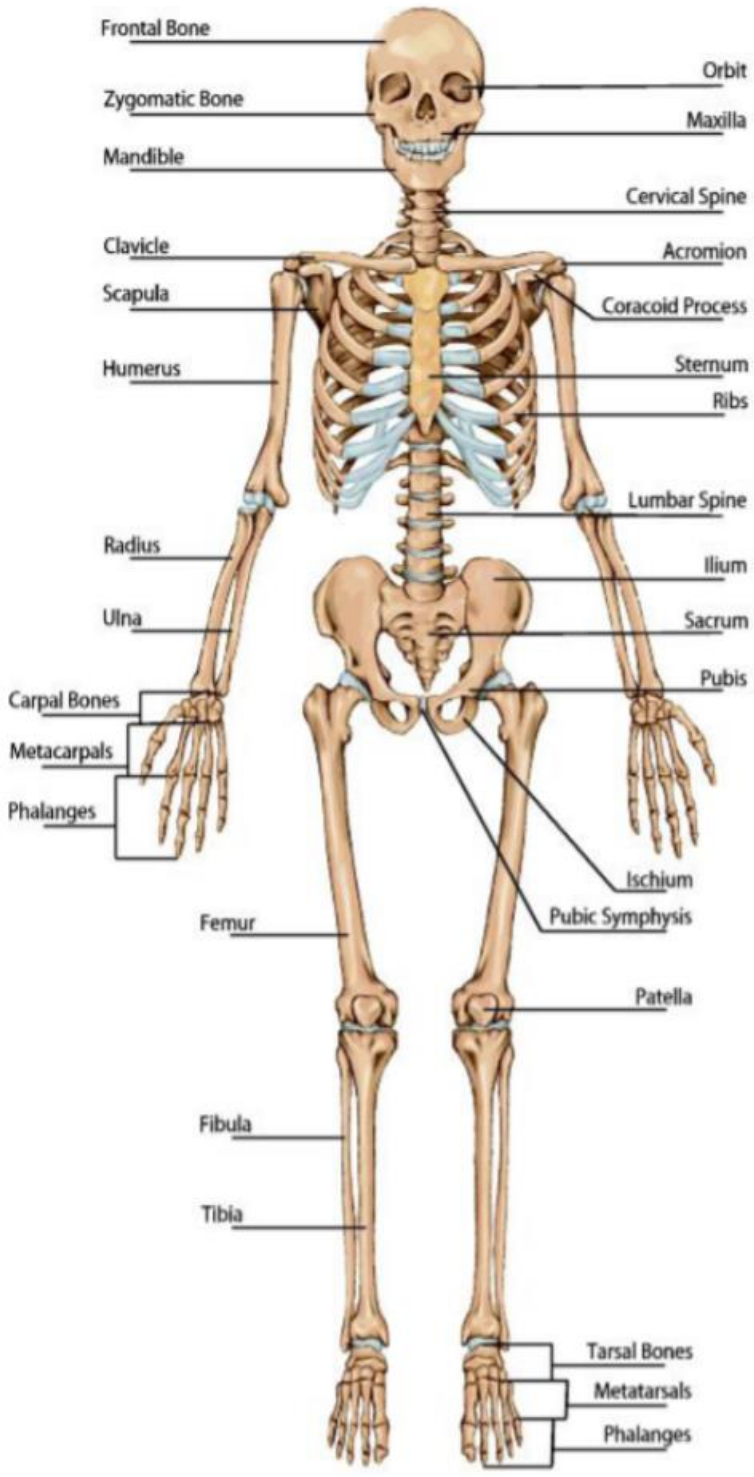

Figure 2.3. The human (adult) skeletal system (adapted from Steele, Bramlett, 1998)

2.2. Chemistry of Bones

In general, bone is a rigid tissue with a matrix composed of organic (collagen) and inorganic (mineral) material.

2.2.1. The organic phase of bone

According to Miller (1985) there are 11 different types of collagen currently known, with bone collagen being Type 1 which is derived from the molecular protein tropocollagen (Ezzo, 1994b). Type I collagen molecules are highly organized, comprised of three stretched helical amino acid chains, which are themselves twisted into a triple helix. "Collagen is characterized by a high glycine content, which makes up every third amino acid (33%), with high levels of proline and hydroxyproline, which together account for a further 20%. Each triplet is approximately 300 nm in length and 1.5 nm in diameter (Turner-Walker, 2008)." The protein collagen comprises approximately 90% of the organic portion of the whole cortical bone. The remaining 10% consists of non-collagenous proteins (phosphoproteins, glycoproteins, GLA proteins, proteoglycans), lipids, carbohydrates, enzymes, and hormones. "The collagen molecule consists of three polypeptide chains coiled about one another in a triple helix. Amino acids are the basic structural components of the fibrils (Turner-Walker, 2008)." Amino acids are represented by the chemical formula $NH_2CHRCOOH$ (Fig. 2.4).

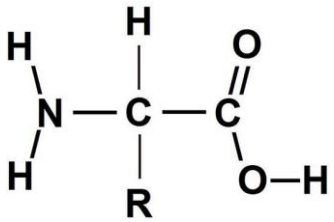

In this chemical formula R represents an alkyl radical such as methyl or isopropyl, or a carbon chain. Ingested dietary proteins are broken down into their constituent amino acids, and new proteins are synthesized from these amino acids (Pate, 1994). Due to the slow remodeling processes, the chemical composition of normal adult human bone will reflect long-term dietary averages.

Bone renews itself by replacing the damaged bone with a new one (calcium renewal). Bone turnover associated with skeletal development, referred to as modeling, proceeds rapidly in infants, declines during growth, and approaches zero at skeletal maturity. After the age 20 years remodeling accounts for over 95% of human bone tissue turnover. This remodeling continues until the time of death. In contrast, small and short-lived vertebrates lack appreciable remodeling. Remodeling occurs in microscopic packets referred to as bone structural units (BSU). The average BSU lifetimes in humans ranges from 3 to 20 years depending on the local bone turnover rate. The annual turnover rate for compact bone is ca. 2.5%, and 10% for trabecular bone. The mean annual cortical replacement percentage for adult bones is 8.3% for vertebrae, 4.7% for ribs, 2.9% for femora, and 1.8% for the skull (Pate, 1994).

2.2.2. The inorganic phase of bone

The mineral phase of bone consists of apatite, a calcium phosphate mineral (Parker, Toots, 1970). Bone apatite has a large reactive specific surface, and is characterized by its crystal imperfection and nonstoichiometric structure (Posner, 1969). The mineral phase is characterized by exceptionally small crystals with lengths averaging about 500 A^{o}, widths 250A^{o}, and thicknesses of 20-30A^{o} (Ezzo, 1994b).

The highly insoluble hydroxyapatite, $Ca_5(P0_4)_3OH$, is the dominant calcium phosphate phase in bone mineral. The more soluble, immature phases occur only at the endosteal, subperiosteal, cortical, and Haversian surfaces. The composition of each of these calcium phosphate phases varies due to ionic substitution by carbonate, citrate, and numerous minor and trace elements supplied by ingested food and water (Table 2.1) (Pate, 1994). In other words, biologically, formed apatite always contains a significant amount of several minor elements in addition to the essential elements of the apatite structure. The amount of these elements differs between different species and also between individuals and population of the same species. These variations are caused by various biological and environmental factors (Parker, Toots, 1980).

As a result, bone mineral acts (1) as a reservoir to provide the body fluids with these ions to maintain the biologically required levels, and (2) as a detoxifying depository to store unwanted ions from the body fluid such as lead, strontium etc. Therefore, bone mineral is involved in both the biomechanical and metabolic functions of osseous tissue (Posner, 1969).

Table 2.1. *Ionic exchange between apatite and soil*

Ca^{2-}	PO_4^{3-}	OH^-
Li, Zr, Hg, Na, V, Al, Fe, Pb,	CO_3^{2-}	F^-
K, Nb, Ga, Be, Cr, Si, Sn, Ba,	$C_6H_8O_7$	Cl^-
Mg, Mn, Y, Zn, U, Th, Cd, Ac	Amino acids	
	Piro-phosphates	

2.3. Elements in bones

In general, six elements - carbon, hydrogen, nitrogen, oxygen, phosphorus, and sulfur - contribute to making the molecular building blocks of living matter: amino acids, sugar, fatty acids, purins, pyrimidines, and nucleotides (Table 2.3). These elements not only have independent biochemical roles, but are also the respective constituents of the following large molecules: proteins, glycogen, lipids, starch, and nucleic acids. Furthermore, the electrochemical properties of living matter depend critically on elements, or combinations of elements, that either gain or lose electrons when they are dissolved in water, thus forming ions. "The principal cations (electron-deficient, or positively charged, ions) are provided by four metals: sodium, potassium, calcium, and magnesium. The principal anions (ions with a negative charge because they have surplus electrons) are provided by the chloride ion, and by sulfur and phosphorus in the form of sulfate ions (SO_4^{2-}) and phosphate (PO_4^{3-}) ions. These seven ions maintain the electrical neutrality of body fluids and cells and also play a part in maintaining the proper liquid volume of the blood and other fluid systems (Frieden, 1972 :52-57)."

Table 2.2. *The elemental composition of different environments (Frieden,1972)*

Universe		Earth's Crust		Seawater		Human Body	
Percent of total number of atoms							
H	91	O	47	H	66	H	33
He	9.1	Si	28	O	33	O	25.5
O	0.057	Al	7.5	Cl	0.3	C	9.5
N	0.042	Fe	4.5	Na	0.28	N	1.4
C	0.021	Ca	3.5	Mg	0.033	Ca	0.31
Si	0.003	Na	2.5	S	0.017	P	0.22
Ne	0.003	K	2.5	Ca	0.006	Cl	0.03
Mg	0.002	Mg	2.2	K	0.006	K	0.06
Fe	0.002	Ti	0.46	C	0.0014	S	0.05
S	0.001	H	0.22	Br	0.0005	Na	0.03
		C	0.19			Mg	0.01
Others <0.01		Others <0.1		Others <0.1		Others <0.01	

Table 2.3. *Concentration of elements found in adult human cortical bone mineral (Pate, 1994)*

Elements	Approximate levels (ppm)
Calcium	380.000
Phosphorus	180.000
Sodium	15.000
Magnesium	1.000-10.000
Strontium, barium, iron, potassium,	
Zinc, fluorine	<1.000
Lead, Aluminum	1-100
Manganese, copper, chromium	<10
Nickel, silver etc.	Trace amounts

2.3.1. Essential Elements

"The ion calcium (Ca) is necessary for a number of essential physiological processes. Calcium Phosphate, accounts for the hardness of the bone tissue and its ability to remain rigid. However, the extra skeletal role of calcium is more vital; calcium plays an essential role in blood coagulation as a cofactor in the conversion of prothrombin to thrombin. (Jowsey, 1977)." Although all calcium enters the body via the gastrointestinal system and kidneys, the overwhelming majority (99%) of the body's calcium is stored in the skeleton and the remaining 1% is in the extracellular fluid. As with the absorption of all other essential minerals, calcium absorption is a controlled biological mechanism influenced by the blood and extracellular fluid's calcium levels. This balance reflects calcium added by bone desorption, intestinal absorption, and

reabsorption from the kidneys as well as by the calcium lost through skeletal formation (accretion) (Ezzo, 1994b).

Phosphorus (P) is the fuel supply of the body, which means that it plays an important role in the nucleotides, such as adenosine triphosphate (ATP). This is the center of energy for the cell, as well as an intimate part of body structure, and it is abundant. In a normal dietary intake, over 80-85% of phosphorus resides in the bones and teeth and functions in the structural support of the body (Ezzo, 1994b; Jowsey, 1977). Phosphorus is absorbed as free inorganic phosphate (PO_4) and exists in three forms: ionic, bound to other compounds, or complexed to other compounds (Ezzo, 1994b). The level of phosphorus in the blood has a great impact on mineral metabolism. The most severe bone diseases are related with a lack of phosphorus. Calcium and phosphate must be abundantly present in the blood, otherwise a failure of mineralization may occur (Jowsey, 1977).

Magnesium (Mg) is an alkaline earth element and is a major essential element for humans, like calcium and phosphorus. A standard human body contains 20-28 grams of magnesium. Magnesium is widely found in foods; it is the central atom in the chlorophyll molecule, and that is why green vegetables are rich sources of magnesium. Legumes, animal products, and cereal grains are also good sources (Ezzo, 1994b). Obviously, magnesium enters the body by dietary intake and the average absorption of magnesium is 35-40%. Magnesium has many critical physiological roles, often in association with phosphorus, calcium, and carbonate. Transportation of phosphate, all reactions involving ATP, and duplication of DNA are the main functions of magnesium in human physiological processes (Frieden, 1972). Magnesium also plays a critical role in bone metabolism, particularly in bone mineralization. Inadequate dietary intake of magnesium results in decreased bone mineralization, or even cessation of the mineralization process in remodeling (Ezzo, 1994). Although as much as two thirds of magnesium absorbed by the body is stored in bones, very little of it becomes incorporated into the apatite lattice. Since most bone magnesium is surface

bound, or in a separate phase and has a high ionic mobility in a geochemical environment, it makes it not an ideal indicator for paleodietary reconstruction (Ezzo, 1994b).

Sodium (Na) and potassium (K) are primary cations in extracellular and intracellular fluids, respectively. These two electrolytes are important for maintaining the water and acid-base balance. They also create 'pumps' that permit movement of ions in and out of the cells, and they also play a role in carbohydrate and protein metabolism as well as nerve impulse conduction and muscle contraction. Sodium and potassium are widely distributed in foods, to the extent that it is extremely difficult to eliminate either from the diet. Only a very small proportion of total body sodium and potassium resides in the bones. A trace amount of sodium and potassium do become trapped into the hydroxyapatite lattice, but this has no correlation to dietary intake (Ezzo, 1994b).

2.3.2. Minor Elements

Minor elements occur in a variety of, and comparative abundance in most fossil bones and teeth. it is important to distinguish the two modes of occurrence of these minor elements. A minor element can become incorporated through substitution into the apatite crystal structure, or it can occur as a separate mineral phase, filling minute voids and fractures in the bone (Parker, Toots, 1970)

In vertebrate life forms, iron (Fe) functions primarily to transport oxygen and electrons by the help of hemoglobin. Iron is found in food sources as two forms: Heme ($C_{34}H_{32}FeN_4O_4$) produced by hemoglobin in meat sources, and non-heme, found in both plant and animal sources. Very little iron is incorporated into bone. Bone does not act as an ion reservoir for iron, and with the exception of bone marrow, iron does not contribute to any known physiological function in bone (Ezzo, 1994). In general, it can be said that iron concentration is much higher in soil than in bone, and even

small physical fractions on the bone sample can elevate iron levels. In fossil bones, iron occurs by filling voids in/on the bone, especially larger ones such as the haversian canals (Fig 2,1) (Parker, Toots, 1970).

Manganese (Mn) has been recognized as an essential, ultra-trace mineral. The primary physiological function is as an enzyme cofactor. The body stores 12 to 20 mg of manganese, and 25% of it is stored in bones (Ezzo, 1994b). Manganese is found exclusively as void and fracture fillings in fossil bones, showing a strong tendency to fill very tiny openings, such as voids formerly occupied by single cells (lacunae). Manganese does not appear to replace calcium in the apatite of any previously analysed specimens (Parker, Toots, 1970).

Human populations acquire broadly varying quantities of fluorine (F) from their food, and water supply. An remarkably high proportion of the total body content of fluorine exists in the skeleton, with a positive correlation between higher intake and a higher amounts and proportions present in the bones. The F concentrations of normal teeth parallel those of the long bones, but usually at lower levels (Underwood, 1977). The content of fluorine in fossil bones was initially studied more than a century ago by Middleton (1844), who proposed that the fluorine amount increased with increasing antiquity of the fossil. Fluorine isassumed to replace hydroxyl ions in the apatite structure (Parker, Toots, 1970).

Zinc (Zn) occurs in relatively high concentrations throughout the body (Underwood, 1977), and functions primarily as a metalloenzyme cofactor (Ezzo, 1994b). Zinc occur in its highest amounts in the prostate, liver, kidney, and skeleton. The body's concentration of zinc increases during the suckling period, becoming increased compared to the levels found in newborns. Under deficient status , the growth of organs can be so hindered that the total amount of zinc is highly lowered, whereas the concentrations may not be considerably lowered (Underwood, 1977). Zinc has also been depicted as being related to the organic phase of the bone, possibly as a

cofactor in collagen crosslinks. Zinc can be used as a paleodietary indicator having assumed a trophic-level difference between herbivores and carnivores. In human groups, higher levels of zinc are found in individuals with a greater percentage of meat contributing to their dietary intake (Ezzo, 1994b).

Strontium and barium are considered to be bone-seeking elements. Strontium is restricted to the apatite portion of the bone where it replaces calcium (Parker, Toots, 1970). There occurs no decisive evidence that Sr is critical for living organisms. However, previous studies argue that the omission of this element from the mineral supplements fed to rats and guinea pigs consuming a purified diet led to growth depression, an impairment of the calcification of bones and teeth, and a higher incidence of carious teeth (Underwood, 1977). Absorbed Sr is transported in the blood to the tissues, where it is preferably deposited in the bones and teeth by two distinct processes: (A) a rapid incorporation phase attributed to the blood Sr deposited by ion exchange, surface absorption, and/or protein binding, and (B) slow incorporation of Sr into the lattice structure of the bone crystals during their formation. Usually, plant-derived foods are richer sources of Sr than animal products (Underwood, 1977).

According to Sillen and colleagues (1989) strontium and barium are trophic markers . The trophic reduction in the strontium-calcium ratio (Sr/Ca) relies on the following principles. Calcium is a ubiquitous element that is also an essential nutrient for plant and animal life. Chemically, strontium, is akin to calcium (and may replace it in metabolic processes). However, it occurs far less common, and is not an essential nutrient. In a given ecosystem plants usually possess the highest Sr/Ca as they do not distinguish between the two elements. In contrast , mammals commonly absorb between 40 and 80% of ingested Ca, but only 20-40% of ingested Sr. “This discrimination against Sr (also referred to as the bio purification of Ca) results in lower Sr/Ca in the bone than in the diet. In theory, herbivore bones have a lower Sr/Ca than the plants that the animals consume, and since carnivores also discriminate, their bones should have an even lower Sr/Ca (Sillen et al., 1989).”

Barium, like strontium is an alkaline earth and bone-seeking mineral. Since, according to Underwood (1977), there is no decisive evidence that barium realizes any essential function in living organism, it has received less attention in paleodietary studies. Barium is poorly absorbed from ordinary diets with little retention in the tissues or excretion in the urine (Underwood, 1977). However, barium behaves similarly to strontium in biological systems. It is non-toxic and has similar chemical properties as calcium. Again, herbivores have a lower barium-calcium ratio than the plants they consume, with carnivores having an even lower Ba/Ca (Özdemir, 2008). Recent studies on material from archaeological contexts have shown that, as a paleodietary indicator, barium is more sensitive than strontium not only in separating on the basis of trophic level, but also in the identification of marine versus terrestrial diets. The ratio of barium to strontium has allowed us to define three distinctive diets: marine with a low Ba/Sr (>-1 on a log scale), a terrestrial diet with a high Ba/Sr (approaching zero on a log scale), and a desert diet (high Sr low Ba). Also, there is a strong separation in the ratio between marine and freshwater resources (Ezzo, 1992b).

Lead toxicity is a significant r issue in environmental health, and has been used and exploited by humans for at least 5000 years. Lead, a bone-seeking element, is similar to some extent calcium in the body. About 95% of lead body burden resides in the bones. Lead uptake and fixation into bone is a defensive mechanism to restrict its dangerous effects on more sensitive organs and tissues (Lachowicz et al., 2016). In contrast to earlier populations, contemporary humans throughout the world are exposed to considerable quantities of lead through multiple environmental pathways. The current pervasiveness of lead makes measurement of a ‘‘natural’’ or “uncontaminated” body concentration impossible in living humans. An area of interest is the identification of skeletal lead concentrations in ancient, relatively uncontaminated, human populations (Fleming, Blom, 2007).

Cadmium (Cd) is practically absent from the human body at birth and accumulates with age up to 50 years. It is another toxic element, having similar properties as calcium. It reduces the absorption of calcium, and, moreover, increases the extraction of calcium by motivating the digestive system. Cadmium has a toxic effect on the kidneys and bones. Cadmium can induce renal tubular dysfunction, decrease bone mineral density, and cause hypercalciuria, all of which can increase the risk of fractures, osteomalacia, and osteoporosis (Underwood, 1977).

Arsenic is extensively distributed across the tissues and fluids of the body in low and greatly variable concentrations. In most tissues, of a healthy adult human, arsenic concentration is between 0.04 – 0.09 ppm. The skin (mean 0.12 ppm), nails (0.36 ppm), and hair (0.65 ppm) are considerably and constantly higher in arsenic content than other tissues. Arsenic absorption and retention, and routes of its excretion, are affected by the level and chemical form in which it is consumed . Arsenic in the forms in which it ordinarily exists in foods, containing the organically bound arsenic of shrimp, is well absorbed and rapidly removed , largely in the urine. Less than 10% of the usual soluble forms of arsenics are presents in the feces. Arsenic trioxide is also well absorbed, but more of it is held in the tissues of humans (Underwood, 1977).

2.3.3. Adsorption and absorption of ions

Ions, held together by ionic bonds, are often spherical and an ionic bond forms when two or more ions touch each other. It is assumed that the radius of an ion remains the same in all its ionic compounds. For example, apatite is an ionic crystal consisting of Ca^{2+} and PO_4^{3-} ions. The atomic structure of ionic crystals can be studied by a set of rules given by Pauling (Czepirski, et al., 2000).

Although this theory is only an approximation, the error involved is about 0.1 ^{0}A and its adoption greatly simplifies the problem of the structure of ionic compounds. An investigation of ionic radius data shows that the radii of anions are considerably larger

than those of cations because the outermost shells of anions are occupied whereas for cations, the outermost shells are vacated. Assuming that ions are spherical and each ion has a radius of its own (Czepirski, et al., 2000). Here the Pauling rules state that;

1) Anions coordinate around each cation forming polyhedra. The cation-anion distance is equal to the sum of the radius of the cation and anion. The number of anions around each cation (the coordination number) is determined by the ratio of the radius of the cation r+ to the radius of the anion r-. The coordination number is abbreviated as CN.

$r=r^{+} + r^{-}$

$CN=f(r^{+}/r^{-})$

In other words, the sizes, or geometry, of the ions determines the chemical structure of the ionic crystals. The CN, geometrical identification of polyhedra can be found in Fig. 2.5 and for r^{+}/r^{-} in Table 2.4.

Table 2.4. Relationship between CN, radius ratio, and geometrical identification

CN	Geometrical Identification	Radius ratio r^+/r^-
1	Linear	0-infinite
2	Linear	0-infinite
3	Triangular (Planar)	0.155
4	Tetrahedral	0.225
6	Octahedral (8 triangular faces)	0.414
8	Dodecahedral (12 pentagonal faces)	0.732
12	Icosahedral (20 triangular faces)	1

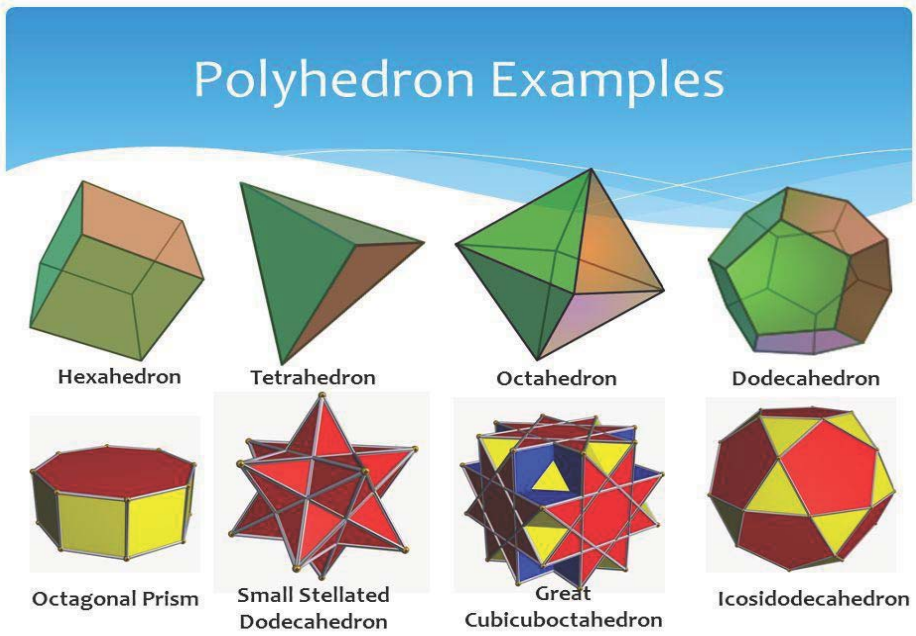

Figure 2.5. Polyhedron examples

(www.slideserve.com/takara/polyhedron-inspired-art)

However, it is not likely that an exact agreement between the actual radius ratios and those given in the table above (Table 2.4) will always occur. In fact, the shape of the polyhedrons (Fig. 2.5) should be considered as the lower limit for the corresponding coordination. For example, 0.225 is the lowest radius ratio for the tetrahedral coordination and a radius ratio of less than 0.225 gives a triangular coordination even though the ratio may be considerably larger than 0.155. The reason for this phenomenon is that a loose ion in a polyhedral hole (the place of the cation) represents an extreme unstable high-energy system. On the other hand, although a tight ion in the polyhedral hole may cause distortion (dipole formation by the action of permanent dipole). The distortion energy is not high enough to cause extreme instability (Adamson et al., 1997).

When the cations are much smaller than anions i.e. the radius ratio is less than required for a given structure, the anions come close enough together so that there is appreciable repulsion between their electron clouds and, thereby, the structure becomes somewhat loosened and has high energy and therefore low stability.

Ionic crystals are constructed by polyhedra links, sharing corners, edges, and faces which are called geometry elements. The following rules of Pauling provide the accepted criteria for polyhedral linkage (Adamson et al. 1997)):

1. In a stable structure of linked polyhedra, the valence of the cation is equally divided among the neighboring anions. The fraction of valence reaching an anion is called bond strength. The total strength of the valency bond which reaches an anion from all neighboring cations is equal to the charge of the anion.

B.S. (bond strength) = V^+ (valency of cation)/CN

And

V^- (valency of the anion) =$B.S._1+B.S._2+B.S._3$.....

2. The existence of edge, and particularly face, linkage decreases the stability of the structure. This effect is more pronounced for cations with low coordination number and high valency. This rule may be explained on the basis of repulsion between cations. The higher the cation charge and the lower the separation, the higher the repulsion between cations. The separation distance is highest when the corners are shared, and lowest when faces are shared. Also, small polyhedra which are characterized by a low coordination number permits smaller cation separation than in large polyhedra. Thus, for example, silicon polyhedra can only share corners, whereas aluminum polyhedra can share edges.

3. In a crystal containing different cations, those of high valency and small CN can't share a geometry element. This rule is also explained with the same explanation as above.

4. The number of essentially different kinds of constituents in a crystal tends to be small. Essentially, different constituents should be referred to by crystallographic configuration, not by chemical species. For example, Si and Al tetrahedra can be considered as only one constituent.

2.3.3.1. Adsorption on the surface of the solids

Adsorption is the adhesion of atoms, ions, or molecules from a gas, liquid, or dissolved solid to a surface. Typical adsorption processes such as purification of gases and vapors, the extraction of valuable substances, heterogeneous catalysis, and chromatographic analysis of mixtures are used in practice. So, it is one of the important subjects to study. A solid on whose surface accumulation (adsorption) occurs is called an adsorbent. While the adsorbed substance is called an adsorbate (Adamson et al., 1997).

Rules for adsorption

It is difficult to find simple relationships for adsorption. It is affected by various factors such as temperature, pressure, concentration of the material to be adsorbed, the physical surface area, chemical and physical properties of the adsorbent, and so on. A general equation based on Thermodynamic consideration for the adsorption of a gas at the solution-gas interface was given by Gibbs (Demirci, *Lecture Notes*). This equation can be written as follows:

$$X=-f(C,T.....)(\partial G/\partial C)w$$

where x is the amount of substance adsorbed.

This equation can be simplified as follows:

$$X=-C/RT\ \partial G/\partial C.$$

Gibbs' eq. can be applied to all phase interfaces. The presence of a strong force field on a surface of a solid introduces complications into our treatment in comparison with that of a liquid-gas interface. Adsorption of gases on solid surfaces is given in terms of the amount of gas or vapor in moles adsorbed by a unit mass of adsorbent (mol/g), or in terms of volume reduced to standard conditions.

$$V(volume)=X.22400cm^3/g.$$

These amounts can be measured experimentally (unlike the adsorption on the surface of a liquid) because the surface is large enough in most cases.

The difficulties limiting the Gibbs eq. are also associated with the difficulty in the direct measurement of γ (surface tension), but it is possible experimentally to determine a different energy characteristic, which is the heat of adsorption Q_a (Adamson et al. 1997).

The adsorption process can be expressed by three curves.

1) an isotherm, where T is constant

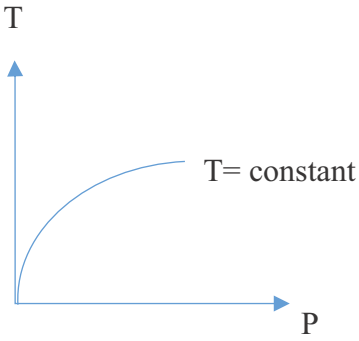

2) an isobar, where P is constant

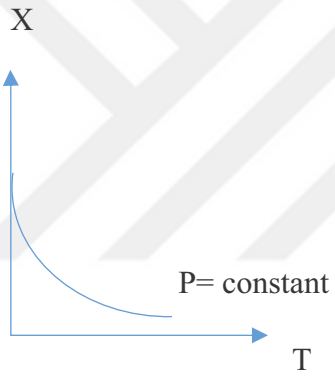

3) an isostere, where x is constant

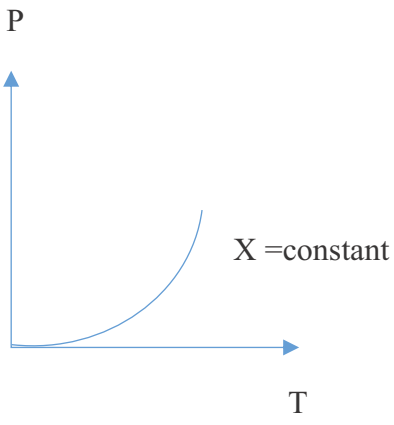

Depending on the nature of the acting forces, we can distinguish physical and chemical adsorption. In the latter case, the chemical reaction occurs on the surface layer. For example, oxygen reacts with iron, and Ag reacts with Cl_2

$3O_{2(g)} + 2Fe^{-} > Fe_2O_{3(S)}$

$2Ag_{(s)} + Cl^{2-} > 2AgCl_{(S)}$

In these cases, the reaction products form a film that is impermeable to the reacting gas. Physical and chemical reactions are thermodynamically indistinguishable. In practice, they are characterized by the different values of the differential molar heat of adsorption (qa).

$qa = dQa/dx$

The values of qa range from 4 to 40 kj/mol (1 to 10 kcal/mol) for physical adsorption (characteristic of the heat of condensation) and from 40 to 400 kj/mol (10-100 kcal/mol) for chemical adsorption (characteristics of the heat of chemical reaction).

In addition to adsorption, which is a typical surface process, a gas or a vapor may be absorbed by the entire volume of the solid, for example the absorption of hydrogen by the palladium. This phenomenon is called absorption. When observing the adsorption of a gas in experiments it is difficult in most cases to identify the two processes, whether it is a physical or chemical adsorption. When the mechanism of the process is unknown, or when various processes occur simultaneously, the more general term “sorption” is used (Czepirski et al., 2000).

In 1915 Irving Langmuir and Michael Polanyi developed two different theories for the adsorption of gases on solids. Langmuir was the first to propose a scientifically based adsorption isotherm with respect to statistical thermodynamics, and based his theory on four assumptions, as follows:

a) The atoms or molecules of a gas are bound at active centers of the solid, which means that the adsorption occurs not on the entire free surface, but on separate points where unsaturated bonds are uncovered.

b) Each active center holds only one atom or molecule by adsorptive forces, similar in nature to chemical forces.

c) The adsorptive forces are of short range. So, this means that they are independent of whether adjacent points are free or occupied.

d) At the maximum adsorption, only a monolayer is formed. Adsorption only occurs on localized sites on the surface.

Langmuir suggested that adsorption takes place through this mechanism: $A + S \leftrightarrow AS$, where A is a gas molecule, and S is an adsorption site. The direct and inverse rate constants are k and $k{-}1$. If we define surface coverage, Θ, as the fraction of the adsorption sites occupied, in the equilibrium we have:

$K=k/k\text{-}1= \Theta/(1- \Theta)P$

or

$\Theta=KP/1+KP$

Where P is the partial pressure of the gas, or the molar concentration of the solution. For very low pressures $\Theta \approx KP$, and for high pressures $\Theta \approx 1$.

The value of Θ is difficult to measure experimentally; usually, the adsorbate is a gas and the quantity adsorbed is given in moles, grams, or gas volumes at standard temperature and pressure (STP) per gram of adsorbent. If we call ν_{mon} the STP volume of adsorbate required to form a monolayer on the adsorbent (per gram of adsorbent), then $\Theta=\nu/ \nu_{mon}$, and we obtain an expression for a straight line:

$1/\nu=(1/K\nu_{mon})(1/P)+(1/ \nu_{mon})$

Often molecules form multilayers, that is, some are adsorbed on already adsorbed molecules, and the Langmuir isotherm is not valid. In 1938 Stephen Brunauer, Paul Emmett, and Edward Teller developed a model isotherm that takes that possibility into account. Their theory is called BET theory, after the initials in their last names (Czepirski et al.,2000). They modified the Langmuir mechanism as follows:

$A+ S \leftrightarrow AS$

$A+ AS \leftrightarrow A_2S$

$A+ A_2S \leftrightarrow A_3S$ and so on

2.3.3.2. Adsorption of ions

Adsorption of molecules on a solid surface is referred to as apolar or nonpolar adsorption. Strong electrolytes are also adsorbed, generally in equal amount with respect to anion and cation. So, no net charge is observed and it is also regarded as a polar process. In the case of polar adsorption one kind of ion is preferentially adsorbed, and in this case the adsorbent may or may not be charged. There is no charge if the polar adsorption is simply an exchange adsorption, meaning that one ion is adsorbed preferentially, displacing the ion of the same sign from the surface of the adsorbent while the other ion with the opposite sign is adsorbed very little, or not at all.

Adsorption of ions by ionic crystals may be predicted on the basis of some adsorption rules; the Fajans-Phaneth rules. The rules can be summarised as follows;

1- Of two ions present at equal concentration, the ion of a higher charge, lower size, and higher polarizability (deformability) is adsorbed preferentially.

2- Of two ions of equal charge, the ion with the higher concentration is adsorbed preferentially.

3- An ion is strongly adsorbed if there is possibility of forming a difficult soluble, or weakly ionized compound with the ions of opposite charge of the lattice. For example, Ra^{2+} ions are easily adsorbed by $BaSO_4$, but are not adsorbed by AgCl. Because Ra^{2+} and SO_4^{2-} form, with difficulty, the substance $RaSO_4$. But Ra^{2+} and Cl^- cannot form a least soluble substance where $RaCl_2$ is a soluble substance. Similarly, radioactive cations like Sr^{2+} and Ra^{2+} are easily adsorbed by bone structure because of the formation of low soluble phosphate salts of Sr and Ra.

4- As the surface of ionic crystals are preferentially covered by the same kind of ions, they show increasing attractive or repulsive forces. Related to this there are two more Fajans-Phaneth rules; the adsorption of anions is increased by adsorbed cations, and

is lowered by adsorbed anions. The adsorption of cations is increased by adsorbed anions, and is lowered by adsorbed cations (Adamson, et al.,1997).

2.4. Degradation of Bones (Diagenesis)

Diagenesis is a geological term and is described as the process by which sediment is converted to sedimentary rock under low temperature and pressure conditions . Recently , this term has been adopted to explain the changes undergone by skeletal tissues in the burial environment. These changes may include dissolution of bone tissue or its cementation by exogenic minerals, and recrystallization of bone mineral or its replacement by other mineral species. Frequently, these alterations to bone tissue are commonly known as fossilization (Behrensmeyer, Hills, 1980), and a combination of taphonomy and diagenetic processes specify whether a bone decays, and finally diminishes , or endure throughout the course of archaeological or geological time (Turner-Walker, 2008).

To draw a conclusion about the biology of a fossil vertebrate from the composition of bones and teeth, then it is critical to separate the original life time (antemortem) biological factors that affect the content of the structure from the physical and chemical changes of the bones and teeth after burial (post mortem) - diagenesis (Parker, Toots, 1980). Bones obtained from archaeological sites have been altered over time. Alteration takes place at all scales, from molecular loss and substitution, to crystallite re-organization, porosity and microstructural changes, and in many cases, to complete disintegration of the entire bone (Nielsen-Marsh, et al, 2000). The uptake of cations and circulating organics, the exchange of ions, the breakdown and leaching of collagen, microbiological attack, alteration and leaching of the mineral matrix, and infilling with mineral deposits etc. are the main diagenetic parameters (Hedges, 2002).

2.4.1. Microbial Attack

During the decomposition of a corpse, microorganisms play a dominant role, and the loss of soft tissues is largely mediated by bacteria and fungi - although autolysis also plays an important role in the early stages of decay of the body. When a cell dies, a cocktail of enzymes is released which quickly break down the surrounding cell components and tissues. The onset of this autolysis is very rapid, but it is short-lived. Thereafter, bacterially mediated tissue destruction takes over with large numbers of microorganisms being released from the gut into the abdominal cavity (Turner-Walker, 2008). The sequence of autolytic decomposition follows that of tissues with the highest rates of synthesis of adenosine triphosphate (ATP), the fuel that drives the body's metabolism. Thus, the intestines, stomach, liver and organs related to digestion are the first to deteriorate, together with the heart, and the blood and circulatory systems. These are followed by the lungs, kidneys and bladder, the brain and nervous tissues, and later the skeletal muscles. Connective tissues, which are predominantly collagen, are highly resistant to autolysis (Gill-King, 1997). The autolysis phase ends when an anaerobic environment is created which is favorable to local soil bacteria.

After burial, vertebrate skeletons undergo a variety of chemical changes. This is predominantly due to the chemical environment of the burial site and the properties of the surrounding sediment, as well as the properties of the hard tissue itself. Rates of diagenetic change differ enormously from place to place, and from tissue type to tissue type (Parker, Toots, 1970).

Much of the weight loss (20%) and porosity increase (50%) in bone can be ascribed to the loss of collagen, and most of the collagen loss in bone is correlated with microbial attack (Hedges, 2002). Once reduced to a skeleton, the diagenesis of bones is mediated almost entirely by microorganisms, the presence of which has a profound influence on their preservation potential. Of course, local groundwater, oxygen availability, pH, and temperature will not only influence what kinds of

microorganisms are present, but also how quickly they multiply. From the earliest histological investigations of ancient bones, fungi were implicated in the post-mortem destruction of bone tissues. Certainly, fungi can readily be found on excavated bones, which are frequently washed in contaminated water, and often kept in low priority storage facilities where damp and poor air circulation encourage mold growth (Turner-Walker, 2008).

2.4.2. Porosity

The distribution of porosity can provide a large amount of descriptive information regarding the diagenetic alteration of bone. Water sorption measurements have been complemented by alternative approaches using nitrogen and/or mercury intrusion which are able to exhibit the diagenetic developments of new pore structures. Many of these can be matched with the structures noticed and scored during histological examination, and therefore can quantify the effects of microbial attack. The smallest porosity (less than 5 nm) is responsible for most of the surface area of bone, and therefore its reactivity. However, the situation is further perplexed by the presence of collagen, which itself possesses a hydrophilic surface and porosity of similar magnitude. When collagen is lost, so the finest porosity of bone, as measured by water retention, decreases (Hedges, 2002).

Dry, fresh bone contains about 8% water that is loosely bound and can be removed by heating in air at 105^0C. However, for materials like bone with a high microporosity, the total amount of bound water held by a sample depends strongly on both the temperature and local relative humidity. For very small pores, quite high temperatures are required to remove all of the liquid water held in small capillaries, and even higher temperatures are necessary for chemically bound water. The determination of total bound water in fresh bone is further complicated because, in thermogravimetric measurements, weight losses at elevated temperatures are compounded by thermal

decomposition of organic matter and a loss of bound carbonates from the bone mineral (Turner-Walker, 2008).

2.4.3. Crystallinity

"One diagenetic phenomenon which has received increasing attention in recent years is bone mineral crystallinity. During post mortem diagenesis, bioapatite dissolves and recrystallizes into bigger and more stable crystals (known as Ostwald ripening) (Pollard et al., 2007 :87-92)." Crystallinity is a broad term, which, in apatite, is a function of crystal size, structural defects, and strain. To a certain degree , these qualities tend to be inversely correlated; large crystals tend to possess somewhat few structural defects and minimal strain (Sillen, Parkington, 1995). Chemical changes, particularly the uptake of fluorine or carbonate as well as actual crystallite size, strain etc. also influence crystallinity (Hedges, 2002).

IR crystallinity measurements rely on the "splitting factor" (SF), introduced by Termine and Posner in 1966, an index on the basis of the splitting of PO_4 anti-symmetric bending mode peak at wave numbers 550-600 nm (Posner, 1966). The occurrence of collagen provides the stability of the mineral matrix and the SF increases with the chemical removal of collagen. Greater increases are found in buried bone, sometimes after relatively short burial times. On thermodynamic grounds the crystallinity is supposed to increase once substantial collagen has been lost. The process can remain at a rate that is perhaps internally buffered and not responsive to most ambient environmental conditions. Still, its evaluation is perplexed by the chemical changes of hydroxyapatite and the microbial reconstitution of the micromorphology (Hedges, 2002).

2.4.4. Soil Properties and Groundwater

The availability and movement of water within the soil, and thus through and around archaeological bones, has an enormous influence on their potential for survival. Water is the medium of almost all chemical reactions that happen in the soil, and the occurrence of water also assists microbial metabolism. While in the body, bone mineral occurs within a somewhat closed system and is surrounded by fluids that have a strictly controlled pH and are approximately saturated with respect to hydroxyapatite (HAP). Dissolution and recrystallization of bone mineral is mediated by bone cells, which are themselves stimulated by a complex web of systemic and local chemical signals, including physical stimuli, growth factors, parathyroid hormone, and calcitriol - the active form of vitamin D. On the contrary, the soil characterizes an open system that is far from saturated in calcium and phosphate ions (except probably in the case of deeply cut charnel pits containing many hundreds of tightly jumbled bones). Hence, bone mineral, therefore, is prone to dissolution in soil water, which can also deliver exogenous ions that may bind to the surface of the HAP or substitute for Ca^{2+}, PO_4^{3-} or CO_3^{2-} ions within the crystal lattice (Turner-Walker, 2008).

The testing of geochemical models dealing with the elemental composition of these post-mortem phases in bone is based on accurate data regarding the ionic composition of the soil solution under various field conditions. Critical variables are soil pH, organic matter content, mineralogy and texture, temperature regime, abundance and distribution of precipitation, and local groundwater movement (Pate, Hutton, 1988). Basic knowledge of the colloidal (mixture of fine suspended solids and liquids) properties of soils is essential to the understanding of soil solution chemistry. Soil particle surfaces usually have a net negative charge that attracts cations and repels anions. This charge originates from the negative charges on layer silicates and organic matter. Therefore, anions are more easily leached from soils than cations. These electrostatic relations are most simply characterized by Coulomb's law. Based on Coulomb's law, the strength of ionic retention or repulsion increases with (1)

increasing ionic charge, and (2) decreasing ionic radius or distance between the charge and soil particle surface. Therefore, trivalent cations are retained more firmly by the soil surface than divalent or monovalent cations owing to their greater charge. Cations with the same valence but smaller radius are retained more firmly due to the reduced distances between the positive and negative charges. Thus, degradation is expected from high cation concentrations near soil particle surfaces to significantly lower concentrations in the surrounding solution (Pate, Hutton, 1988).

These changes can be summarized thusly; (1) precipitation of separate mineral phases, e.g. calcite, in small voids and fractures, (2) ionic exchanges between the soil solution and calcium phosphate lattice positions, and (3) recrystallization and crystal maturation involving the conversion of microcrystalline biogenic hydroxyapatite to a larger, well-crystallized geological apatite.

CHAPTER 3

MATERIALS AND METHODS

3.1. İznik (Nicaea)

İznik is a small district in the province of Bursa, in the southern part of the Marmara region, 85 km northeast of Bursa city center. It was located along the eastern shore of lake İznik, the fifth biggest lake of Turkey, bounded by ranges of hills to the north and south (Fig. 3.1). Since the city lies in a fertile basin and lake İznik is a freshwater source, the area has promoted sedentary occupation since the prehistoric period. İznik was historically known as Nicaea, from which its modern name was derived. Evidence for prehistoric occupation at İznik comes from the abundance of mounds like Çakırca, Çiçekli, Hüyücek Karadin, Karacakaya, and Çonga which are dated to 5000 BC (Kılıçkaya, 1981; Kayan, 1988; Eyice, 1991).

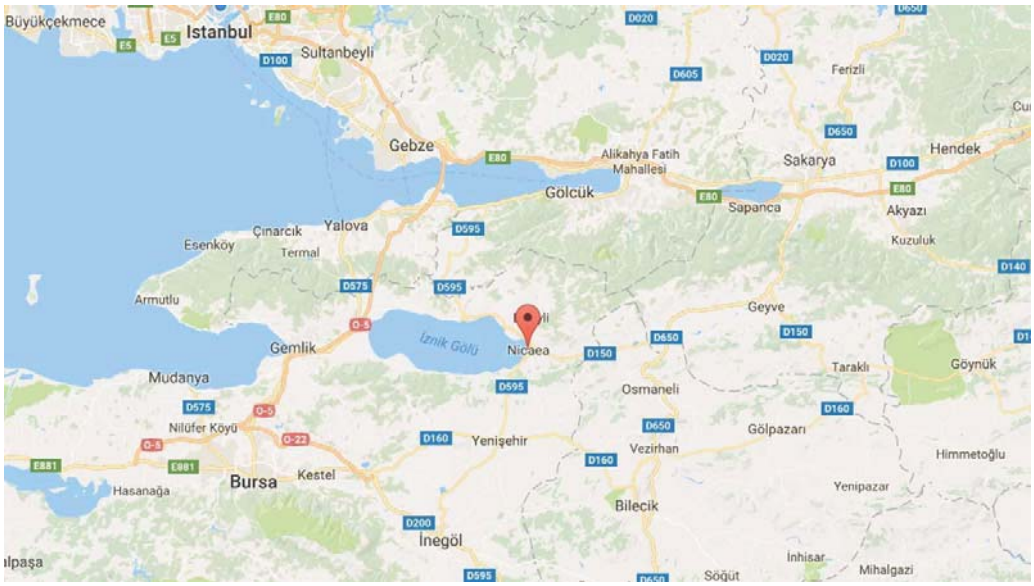

Figure 3.1. Location of İznik (source: Google maps)

3.1.1. History of İznik

According to Strabon, Nicaea became an important city during the time of Alexander the Great, the king of Macedonia. After his death, his empire was split into smaller kingdoms by his commanders. Antigonos, one of the leading commanders, claimed control of the city in 316 BC. However, the Byzantine historian Stephanos mentions Helikore, a colonial city in the same location that was named by the Macedonians and then destroyed by the Mysians, but it was Antigonos who rebuilt it (Erdal, 1996). Within a few years, however, Antigonus was killed in the war with Lysimachus. The new king Lysimachus named the city as Nicaea as a dedication to his wife, Nike, in 301 BC (Eyice, 1991; Kılıçkaya,1981).

In 293 BC İznik was assigned as the capital city of Bithynia. Soon after the death of King Nicomedes the third, İznik became a Roman province. During this period the city gained increased importance, former borders were enlarged and many buildings and city walls were built. At the beginning of the second century the Proconsul Plinius built a great Roman Theatre with the help of emperor Trajanus within the city (Yalman, 1989).

In 325 A.D. during the spread of Christianity throughout the Roman Empire, emperor Constantine gathered more than 300 religious leaders to discuss and settle the matters of doctrine and the Christian Faith in the senate of İznik. This meeting is also known as the First Oecumenical (Ecumenical) Council, aiming to reunite the empire, regain its power and repel the potential Arab attacks. Eventually, spread of Christianity and the Ecumenical Council did nothing but accelerate the disintegration of the Empire (Eyice, 1991). This weakness had led to invasions of the city including by the Goths, and İznik also suffered with many epidemic diseases like plague (Erdal, 1996).

within the eighth century A.D. Arab intruders increased their attempts to spread Islam, and also conquer İznik. In 718 and 727 A.D. two unsuccessful sieges greatly weakened the defenses of the city. Seljuk Turks, following victory at Malazgirt in 1071 A.D., moved on to İznik, capturing it in 1075 A.D.. The Turks settled in İznik, although the Byzantine administration was still in charge. Soon, though, the Seljuk Turks took control of the whole of Bithynia and İznik was declared as the capital of the Seljuk State by the ruler Süleyman Şah. The Seljuks retained control of İznik for 22 years, but with difficulty following many battles and sieges, leading to the eventual loss of the city (Kırmızı, 2004).

After the fall of Constantinople to the fourth crusade in 1204 A.D., and the establishment of the Latin Empire, Nicaea escaped Latin occupation and maintained an autonomous stance. From 1206 A.D., it became the base of Theodore Laskaris, who in 1208 A.D. was crowned emperor there and founded the Empire of Nicaea. In 1331 A.D., Orhan captured the city from the Byzantines and for a short period the town became the first capital of the expanding Ottoman Empire (Eyice, 1991).

During the sixteenth century A.D., İznik was an important staging post and settlement on the military and trade route from İstanbul to Central Anatolia. At the same time, it was a cultural center producing a great deal of poets and scholars. Beside these important features, İznik is characterized by its fine pottery and tile art in the 16th and 17th centuries A.D. It was very famous in Europe, with its unique and highly qualified ceramic production marking the peak of Ottoman art. The beautiful tiles adorning the interiors and exteriors of the Ottoman monuments were all manufactured here, using advanced techniques. This ceramic industry, however, can undoubtedly find its roots in the Byzantine period (Kırmızı, 2004).

3.1.2. The Excavations at İznik

The first excavation at İznik was performed by Oktay Aslanapa in 1963, with a focus on the mosque of Orhan İmaret. Several ceramic pieces and kiln tools associated with four kilns were revealed. The destroyed and burnt pieces with tripods provided clues about İznik's potential as a past ceramic production center. In 1984, a ceramic workshop was revealed to the east of the Hamza Bey Hamamı (Eyice, 1991).

Without a doubt, the most important excavations and discoveries in İznik were at the Roman theatre (Fig. 3.2). The theatre is situated in the Selçuk district, Saraybahçe area in the southwest of the city center and 400m. away from the lakeshore. The skeletal remains examined in this study were obtained from the Roman Theatre, where excavations were begun by Dr. Bedri Yalman in 1980. The excavations and the preservation studies at the theatre continue to the present day, in the name of Ministry of Culture, but with a break during the 1996-97 seasons.

Figure 3.2. The Roman Theatre

https://archaeologynewsnetwork.blogspot.com/2016/07/restoration-works-at-roman-theatre-in.html

The theatre was built on a flat field, as is often a characteristic of Roman theatres, and it sits at 7 m above sea level (Yalman, 1986). It lays 72 m along the east-west axis, and 67 m along its north-south axis (Yalman, 1993). In the early 8th century, stones from the theatre were removed to repair and enforce the city walls as a result of Arab raids in the 14th and 15th centuries A.D. After that, a deposit of earth and rubbish, including animal bones, ceramic pieces, and kiln tools, filled the cavea of the theatre to a depth of 3-4 meters and the rendered the theatre unusable, for its original function (Yalman, 1989).

In the 13th century A.D. the area was used as a cemetery, including a church that was built during this time. During work to maintain the substructure of the theatre, human skeletal remains were excavated. According to the contextual finds, such as coins and ceramic pieces found with the bodies, the skeletons can mostly be dated to the 13th century A.D. (Yalman, 1983- 1996; Erdal, 1996).

3.1.3. Burial typology

When the burial types, demography, and pathology are considered the skeletal remains excavated from the theatre can be classified into three groups by means of the location; (1) Within the cavea, a 20x50 m area occupying where the seats of the theatre and the scene (the stage) originally were, (2) outside of the cavea, and (3) the area around the church (Fig. 3.3).

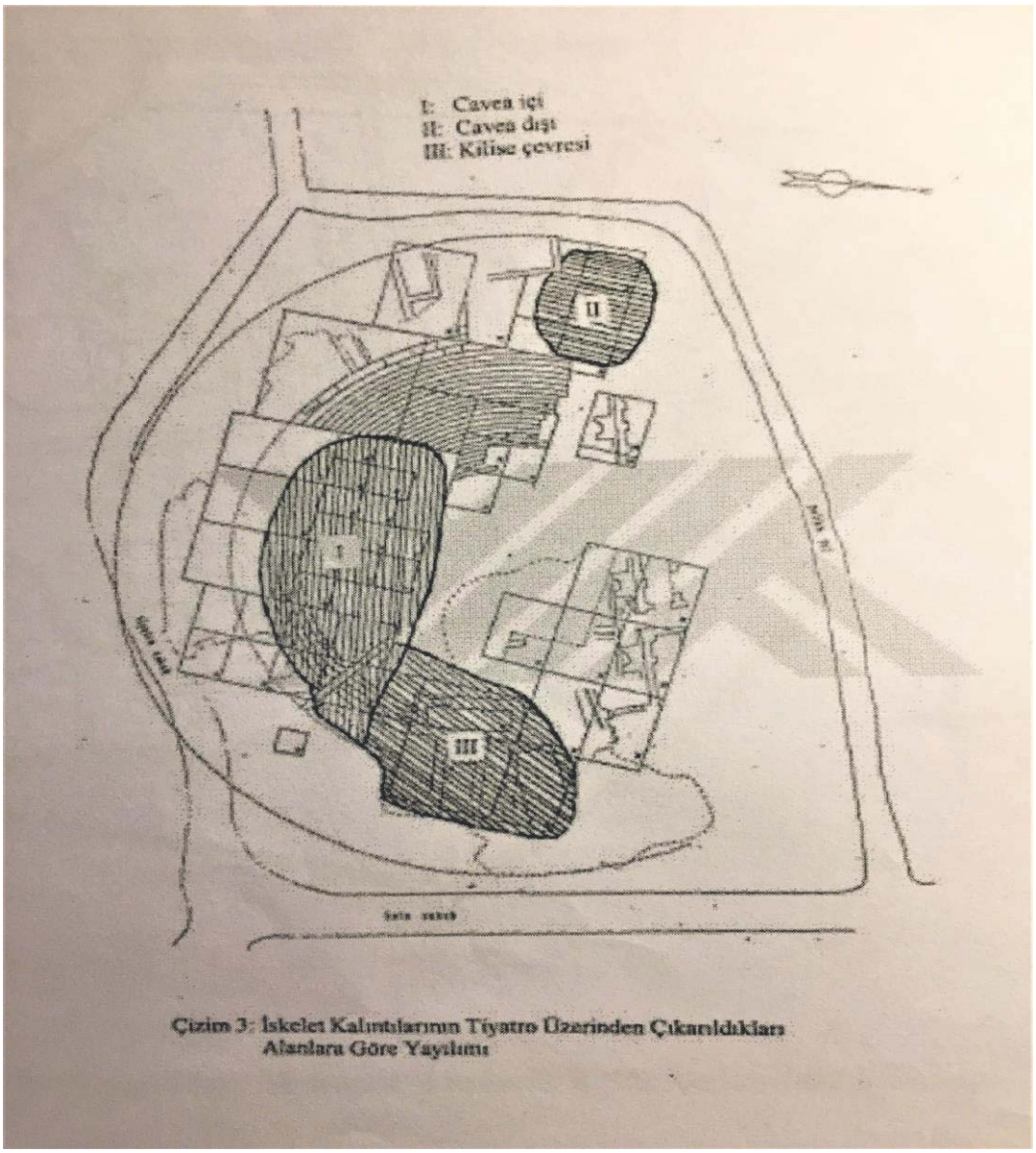

Figure 3.3. The layout of the Roman Theatre, with the three areas where the skeletons were found (adapted from Erdal, 1996)

Within the cavea, most of the skeletons are orientated in a west-east direction (Atlas-Sacrum), and are face up with the arms laid/crossed over the chest and stomach areas (Fig. 3.4). During the excavations some isolated bone parts that could not be correlated with the other individuals were also excavated. The laboratory results showed that almost all of the skeletons belong to men aged between 20-40 years old at death. It is also important that most of the skeletons had traumatic skeletal injuries which may suggest that the bodies are those of soldiers. Some of the bodies were covered with wood attached with iron cast nails and some of them were covered with flat tiles and brick (Erdal, 1996; Özbek, 1989; Yalman, 1983-1996).

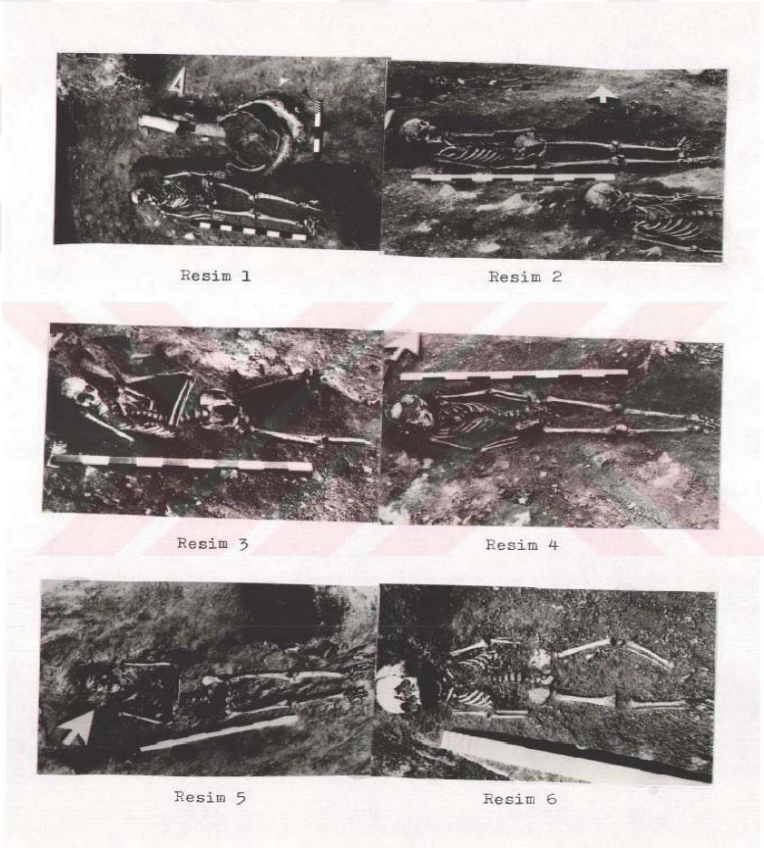

Figure 3.4. Burial types of the skeletons (adapted from Erdal, 1996)

Outside of the cavea, the skeletons were mostly located near or under the west wall of the city, called the analemma. Almost all of the skeletons were orientated in a west-east direction and the arms were parallel to the body. There was a relatively homogeneous distribution between the sex and age at death of the skeletons unlike those inside the cavea, and almost no traumatic skeletal injuries were detected, which may suggest that these burials belonged to the common people of the city. Faces were facing up or towards the south, and the depth of the burials were from half a meter for babies, and one meter for an adult male, to one and a half meters for female, which is an indication of the Islamic tradition of burial (Erdal, 1996; Özbek,1989; Yalman, 1983-1996).

And finally, around the church area, similar to the burials within the cavea, most of the skeletons were orientated in an west-east direction, with face facing up and the arms folded/crossed over the chest and stomach. As with outside of the cavea, there was a homogeneous distribution between sex and age at death, and no traumatic skeletal injuries were detected. the skeletons from the church area are demographically similar to outside of the cavea, but are more similar to those inside the cavea in terms of the burial typology. All of the skeletons buried in these three locations have morphologically similar properties (Erdal, 1996; Özbek,1989; Yalman, 1983-1996).

3.1.4. Architectural properties of the theatre

The construction of the theater was based on a barrel vault system; an arched building element that supports the structure of the ceiling or the roof. The whole structure was raised by means of 12, high barrel vault spaces carrying the upper seats of the theatre, and another 12 barrel vault spaces at their back, and a trapezoidal vault space carrying the lower seats. There are two barrel vault galleries extending in a north-south direction, two long barrel vault galleries extending in an east-west direction, and two

other narrow and short barrel vault galleries in an east-west direction - for the entrance of the actors. In addition, two other systems in a north-south directions and two in an east-west direction, also function as entrances for the audience (Yalman, 1996).

3.2. Sampling and Methodology

3.2.1. Selection of Samples

During the excavations at İznik (1980-1996) more than 1000 skeletons were recovered (Erdal, 1996). The 21 samples in this study were selected from 170 skeletal remains belonging to individuals of different age, sex, and ethnicity, extracted during the excavations in 1988-1990 under the leadership of Dr. Bedri Yalman. The preservation and categorization of these 170 skeletons were provided by Hacettepe University's Anthropology Laboratory.

The tibia and femora are highly recommended bones for the analysis of minor elements for the reconstruction of dietary habits owing to the advantages of their turnover rate, diagenetic properties, and (low-)risk factors for contamination (Lambert, 1984; Hedges, 1999; Turner-Walker, 2008). The bones were sampled according to their structure, preservation condition, abrasion and erosion conditions, resistance, porosity, and turnover rate. Samples were chosen to exclude those displaying pathological conditions and modern modifications such as glue or varnish. However, since the methods used for the analysis are destructive, to avoid damaging the structural integrities of the skeletons, and to prevent restrictions in further studies, the samples were chosen mostly from rib bones. Also, five representative soil types were chosen from inside the site area. The pH values, electrical conductivity, soil type, and elemental configuration were determined.

All of the 21 samples, belonging to 19 individuals, were provided by Hacettepe University's Anthropology laboratory under the leadership of Prof. Dr. Yılmaz Selim Erdal and on the authority of Assoc. Prof. Dr. Kameray Özdemir. The documentation, photography, and the preparation of the samples for analysis were performed at "Ankara Hacı Bayram Veli University Material Research and Conservation Laboratory" under the authority of Assoc. Prof. Dr. Ali Akın Akyol. The bone type, location, sex and age at death of the samples are given in Table 3.1.

Table 3.1. *Studied Samples of Roman Theatre*

Sample No	Sample Code	Gender	Age	Bone Type	Region
1	ITK 88 43/10	FEMALE	26	COSTA	Inside Cavea
2	ITK 88 41-43/6	MALE	20.5	COSTA	Inside Cavea
3	ITK 88 41-43/1	MALE	32.5	COSTA	Inside Cavea
4	ITK 89 53/9	FEMALE	35.5	COSTA	Outside Cavea
5	ITK 89 53/26	MALE	39.5	COSTA	Outside Cavea
6	ITK 89 53/30	FEMALE	21.5	COSTA	Outside Cavea
7A	ITK 90 57/3 A	MALE	22.5	COSTA	Inside Cavea
7B	ITK 90 57/3 B	MALE	22.5	FEMUR	Inside Cavea
8	ITK 89 51/24	MALE	35	COSTA	Outside Cavea
9	ITK 90 58/7	MALE	37	COSTA	Outside Cavea
10	ITK 90 58/3	MALE	22.5	COSTA	Outside Cavea
11	ITK 57/11	FEMALE	39.5	COSTA	Inside Cavea
12	ITK 90 57/8	MALE	38.5	COSTA	Inside Cavea
13	ITK 88 43/21	MALE	20	COSTA	Inside Cavea
14	ITK 88 43/13	MALE	21.5	COSTA	Inside Cavea
15	ITK 88 43/3	MALE	27.5	COSTA	Inside Cavea
16	ITK 89 41/2	MALE	30.5	COSTA	Inside Cavea
17	ITK 89 53/3	MALE	24	COSTA	Outside Cavea
18	ITK 89 53/6	MALE	33.5	COSTA	Outside Cavea
19A	ITK 90 58/5 A	MALE	27.5	COSTA	Outside Cavea
19B	ITK 90 58/5 B	MALE	27.5	FEMUR	Outside Cavea

In this study, 21 bone samples of 19 individuals were examined. Accumulation of elements in the bone, by either biogenic or diagenic alteration, will differ according to sex and age of the individuals, so it is very important to consider these demographic factors. In this study four females and 15 males between the ages of 20 and 39.5 were examined. The results are given in Table 3.2 and 3.3.

Table 3.2. *Sex patterns in the samples*

Gender	Number of Samples(N)	Percentage (%)
Male	15	78.95
Female	4	21.05
Total	19	100

Table 3.3. *Age at death patterns in the samples*

Age Group	Number of Samples (N)	Percentage (%)
Infant (0-2.5)	0	0
Child (2.5-15)	0	0
Young Adult (15-30)	10	52.63
Middle Adult (30-45)	9	47.37
Old Adult (+45)	0	0
Total	19	100

3.2.2. Sample Preparation

After documentation, the visible and external contaminants on each specimen were removed with a lancet. Each sample was cleaned with a different lancet to prevent inter specimen contamination (Fig. 3.3). The same procedure was applied with the same individual having two different types of bones.

Figure 3.5. Removing visible contaminants

The bones were weighed and documented to obtain their dry weight using a Gibertini Crystal 200 SMI magnetic compensation analytical balance (Fig. 3.6). For the physical tests the samples were kept in ionized water for 24 hours. This process was a necessity to calculate unit mass, water absorption capacity and porosity. Wet weights and Archimedes weights were also documented.

Figure 3.6. The Gibertini Crystal 200 SMI magnetic compensation analytical balance used in this study

All of the samples were cleaned for approximately 10 minutes in an ultrasonic bath (Fig. 3.7) in warm deionized water to get rid of unseen contaminants. For each sample, the container of the ultrasonic bath was cleaned by deionized water to ensure an unaltered condition. After the cleaning process, the samples were dried at 105^0C in a Mipro Etüv (Fig. 3.8) for 24 hours and then weighed again.

Figure 3.7. *Ultrasonic Bath used in this study*

Figure 3.8. Mipro Etüv Dryer used in this study

During fossilization, organic matter reduces. Ancient bones contain less organic material than fresh bones. The loss of organic matter depends on environmental conditions and also the type of bone. Spongy bones are more susceptible to deterioration than compact ones. CO_2 is an indicator of carbonate, and carbonate is an indicator of calcination, and that means changes in the structure of bone. The differences between the weights of samples between the temperatures 900 and 600^0C, indicates the amount of CO_2 released from the carbonate minerals (Eissenstat, 1994).

In order to remove the organic phase of bone, the samples were heated to 600^0C for at least three hours and then re-weighed. To calculate loss from heating of the samples a thermo-gravimetric analysis (TGA) was applied to the samples, and then they were reheated to 887^0C for at least for one hour, and then weighed again (Appendix B).

Figure 3.9. High heat oven used in this study

Finally, the samples were ground in an agate mortar (Fig. 3.10), and to prevent contamination the mortar was sterilized with distilled water several times in-between each sample. Later, the samples were given to Ankara University for XRF analysis and the Middle East Technical University's Central Lab for ICP-OES analysis.

Figure 3.10. Grinding the samples

Measurements described up to now were based on the water content of the bones and have been adapted from the protocols described by "İstanbul Büyükşehir Belediyesi İmar ve Şehircilik Daire Başkanlığı Koruma Uygulama ve Denetim Müdürlüğü (KUDEB)" Restoration and Conservation Lab Manual.

3.2.3. Porosity measurements

The porosity and water absorption capacity of the samples was determined by measurement of their dry, wet, and Archimedes masses. To obtain the wet mass of the samples, the samples were entirely submerged in distilled water for 48 hours and then placed in a vacuum (100 torr pressure) for one hour in order to remove the remaining air inside the pores. After being saturated with water, the samples were weighed (in normal air conditions), and the measurements were recorded as saturated mass "M_{sat}". To measure the Archimedes mass of the samples, each water-saturated piece was weighed whilst in distilled water and this was recorded as the Archimedes mass "M_{arc}". In order to obtain the dry weight of the samples, they were dried in an oven at 60°C for at least 24 hours, then they were weighed on the analytical balance and the results were recorded as the dry mass of the samples, "M_{dry}".

All masses were measured with a balance having a sensitivity of 0.0001 g and the bulk density (d), porosity (P), and water absorption capacity (WAC) were calculated with the following formulas:

$d\ (g/cm3) = (M_{dry})/ (M_{sat}-M_{arc})$

$P\ (\%\ volume) = [(M_{sat}-M_{dry}) / (M_{sat}-M_{arc})] \times 100$

$WAC\ (\%weight) = 100 \times (M_{sat}-M_{dry}) / M_{dry}$

3.2.4. Soil analysis

3.2.4.1. Acidity of soil

The pH measurements of the soil samples taken from inside the cavea, outside of the cavea, and from outside of the city walls were analyzed using a Neukum Serie 3001 conductometer/pH meter.

3.2.4.2. Soil type analysis

Clastic sediments are either rock or solid mineral grains. Sand is a term to describe the clastic particle size. In soil science, the term clay, is often used to describe a soil fraction with an equivalent Stokes diameter of less than 2 micron. The clay fraction of the soil also comprises other minerals such as quartz in particle sizes less than 2 microns, clastic particles which are smaller than 0.02 mm in diameter (Van Olphen 1966). The classification of soil particles according to their particle size as established by the US Department of Agriculture is given in Table 3.4.

Table 3.4. *Soil type according to grain size*

Size Class	Range (mm)	Fraction	Range (mm)
Very Coarse Sand	2.0-1.0		
Coarse Sand	1.0-0.5	I	2.0-0.2
Medium Sand	0.5-0.25		
Fine Sand	0.25-0.1	II	0.2-0.02
Very Fine Sand	0.1-0.05		
Silt	0.05-0.02	III	0.02-0.002
Clay	<0.02	IV	<0.002

Fractionation of soil to obtain clay is achieved by removing the sand and silt particles from the mixture of soil and water. The removal of the particles from the mixture was achieved by allowing different size of particles to settle in the mixture at different times, and the clay particles take the longest time to settle.

Ten grams of each sample was accurately weighed and mixed with 1000ml of water. The mixture in the glass container was shaken for about 1 minute and then 5 cm in height volume of the mixture was removed from the top most layer after resting for 4 hours. The mixture then was centrifuged and dried at 600^0C to remove water and weighed.

3.2.4.3. Electrical conductivity of soil (salinity)

The determination of electrical conductivity is achieved by measuring the electrical resistance between parallel electrodes. Resistivity, R=rL/A, where r is electrical resistivity constant, L is the length between the electrodes, and A is the cross-sectional area of the conductor. Here, a potassium chloride solution (KCl) in distilled water is the standard reference solution with an electrical conductivity 0.0014118 mho per cm at 25^0C. The electrical conductivity of 0.01 M of KCl dissolved in 25 ml of distilled water is 0.0014118 mho per cm. Electrical conductivity is calculated by the equation

$E.C.=0.0014118*R_{std}/R_{ext}$.

The positive correlation between the electrical conductivity and the total concentration of cations or anions of soil water sample gives the percentage of salt in the soil sample. The salt concentration (A) is calculated by the formula

A= EC x 640 x 1000 mmho/cm

where 640 is the coefficient which expresses electrical conductivity in mmho/cm to salt concentration in mg/L. The electrical conductivity was measured by using a Neukum Serie 3001 conductometer/pH meter.

3.3. Instrumental Analysis

3.3.1. XRF (X-ray Fluorescence)

XRF is an analytical method using the properties of X-Rays to identify the composition of any sample. X-rays are electromagnetic radiation of very short wavelengths (10^{-8}-10^{-12}m) and characterized by high energy. X-rays are produced by the transitions of electrons of heavier elements between suitable energy levels. The most common method of producing X-Rays is by the use of high-energy electrons with solid targets. Two distinct phenomena occur, the production of X-rays characteristic of the target element and the production of a continuum of X-rays (Pollard et al., 2007).

XRF spectrometry is based on the principle that primary X-rays are incident upon a sample and create inner shell vacancies in the atoms of the surface layers. These vacancies de-excite by the production of a secondary X-ray whose energy is characteristic of the elements present in the sample. Some of these characteristic X-rays escape from the sample, these are then counted and their energies are measured. A comparison of these energies with known values for each element allow the elements present in the sample to be identified and quantified (Pollard et al., 2007).

In this study, multi-element concentrations were determined by using PED-XRF. The sample was placed on the detector in 32 mm disk shapes, formed after the grounding procedure. The instrument used was a Spectro XLAB 2000 PED-XRF spectrometer which was equipped with a Rh anode X-Ray tube, and a 0.5 mm Be side window. The detector of spectrometer Si (Li) by liquid N_2 cooled with a resolution of <150 eV at

Mn K_α 5000 cps. In this analysis 50 elements were detected with the exception of lithium and boron because of the lost-on ignition (LOI) factor at 950^0C. The standards of the analysis were GEOL, GBW-7109, and GBW-7309, determined by United States Geological Survey (USGS).

3.3.1.1. Optical emission and mass spectroscopy

ICP-OES

Optical emission spectroscopy, originally carried out with a spark source and photographic recording, due to the replacement of the source with an ICP torch and better detection methods has given way to a new generation of emission spectrometers. The original OES instruments, dating from the 1930s but used consistently from the 1950s, used a spark source to excite the emission spectrum, which usually consisted of a graphite cup as one electrode, and a graphite rod as the other. The sample (solid or liquid) is placed inside the cup and the graphite rod lowered until it was close to the cup. The sample is then vaporized by applying a high voltage across the two electrodes, which caused a spark to "jump" across the gap. The energy of the spark is sufficient to promote some outer electrons of the sample atoms into excited states, which then relaxed back to the ground state and emitted light of a wavelength characteristic of that particular atom. The resultant emitted light is resolved into its different wavelength components using a large quartz prism or, in later models, a diffraction grating, and recorded on a single photographic plate. Later instruments use a number of fixed photomultiplier tubes sited at the correct angle from the diffraction grating for a particular emission line of one element, thus giving simultaneous information about a fixed number of elements. Quantitative information is obtained from the photographic plate using a scanning densitometer, which measured the intensity of each emission line (Pollard et al. 2007).

ICP-MS

Inductively coupled plasma-mass spectrometry was first commercialized in 1983, and since then it has gradually replaced techniques such as AAS and NAA as the method of choice for fast, trace elemental analysis in a wide range of materials. It offers multi element detection limit below parts per billion, sometimes down to parts per trillion, and can give a rapid throughput of samples. Most elements, except for some of the light elements (H, He, C, N, O, F, Ne, Cl, Ar), can be analyzed. Unlike ICP-OES, each elemental measurement in ICP-MS is made on one or more selected isotopes of that element, and so potentially even a quadrupole instrument can provide isotopic ratio measurements for elements of interest to archaeology, such as Pb and Sr (Pollard et al., 2007).

ICP-MS uses torch plasma, and is a solution-based analysis. The liquid is taken up through a thin tube via a peristaltic pump. This feeds directly into the instrument nebulizer, where argon gas is introduced into the liquid and a fine mist of droplets is expelled from the tip of the nebulizer. This aerosol is sprayed into the condenser to reduce the size of the droplets, ensuring an even sample loading and preventing cooling of the plasma. About 1% of the sample solution uptake is transported to the plasma torch. The plasma is maintained at a temperature of 10000^{0}C by an external radio frequency. At this temperature, many molecular species are broken down and approximately 50% of the atoms are ionized. So far this is identical to ICP-OES, but for ICP-MS the emission of electromagnetic radiation is concerned with the creation of positive ions. To transfer a representative sample of this plasma ion population to the mass spectrometer there is a special interface between the plasma and the mass spectrometer. This consists of two sequential cones with narrow apertures. The cones are made from pure nickel, which is resistant to acids, is physically robust, and has good thermal conductivity. The position of the plasma relative to the cone apertures is critical to the quality of the analysis (Pollard et al., 2007).

The ICP-OES analyses were performed in the METU Central Lab. The protocol for dissolution of each sample starts with weighing 0.17 g of each sample and then mixing them with 8 ml of distilled HNO_3. To dissolve the samples an Anton Paar Multiwave 3000 Microwave Digestion System with a rotor type 8SXF100 was used. Firstly, the samples were ramped for 10 minutes and held for 5 minutes under a 200w microwave. Secondly under a 500w they were ramped for 5 minutes, held for 5 minutes, and then finally ramped under a 800w for 5 minutes and held for 10 minutes. The samples were integrated with 50 ml of deionized water. Analyses were made by a Perkin Elmer Optima 4300 DV ICP-OES.

Parameters:

Wavelengths: P: 213.617nm, Al: 396.153nm, Fe: 238.204nm, K: 766.490nm, Ca 317.933nm, Zn: 213.857nm, Sr:407.771nm, Ba 233.527nm.

RF power: 1300 W

Plasma gas flow rate: 15 L/min.

Auxiliary gas flow rate: 0,2 L/min.

Nebulizer gas flow rate: 0,8 L/min.

Sample uptake rate: 1.50 ml/min.

Number of replicates: 3

Spray chamber: Ryton Double Pass (Scott Type)

Nebulizer: Gem Tip Cross-Flow

For ICP- MS analyses, one soil sample and four bone samples were sent to ALS GLOBAL Laboratories, which meets all of the requirements of the International Standards ISO/IEC 17025:2017 and ISO 9001:2015. All ALS geochemical hub laboratories are accredited to ISO/IEC 17025:2017 for specific analytical procedures.

3.3.2. FTIR (Fourier Transform Infrared Spectroscopy)

Like any other absorption spectroscopy, the aims are to measure the amount of light absorbed by the sample at different wavelengths. The most common form of infrared spectroscopy methods is the FTIR, based on the Michelson interferometer. In this device, a single beam of IR radiation is split into two, and recombined in such a way that the relative intensities of the two beams can be recorded as a function of the path difference between them (Pollard et al., 2007).

In chemistry, infrared spectroscopy is usually the first method of choice for the identification of organic functional groups, and inorganic species such as carbonate in a wide range of material. It can easily identify the hydroxyl group in any material. Many IR spectrometers can be modified with an attachment which allows multiple reflections to be collected from the surface of a solid sample.

Infrared spectroscopy has been used in archaeological bone studies to quantify the degree of degradation of the biological hydroxyapatite mineral. In vivo, human bone is characterized by very small crystal size distribution. This gives bone mineral a massive surface area upon which physiological processes can occur. During post-mortem diagenesis, the bioapatite dissolves and recrystallizes into bigger and, thermodynamically, more stable crystals. This is usually referred to as increasing the crystallinity. In fact, crystallinity is related not only to crystal size, but also to the frequency of structural defects and the presence of strain in the structure (Pollard et al., 2007).

IR crystallinity measurements are based on the “splitting factor” (SF), which is an index based on the splitting of PO_4 anti-symmetric bending mode peak at wave numbers 550-600 nm. Hedges and colleagues measured crystallinity increases using

XRD. Nielsen and Marsh in 1999 used the index based upon the splitting of the IR phosphate doublet at 567 and 603 cm^{-1}, the SF which corresponds to the generalized degree of crystallinity of bioapatite.

The splitting factor is calculated by the formula

$$SF = \frac{a+b}{c}$$

where a and b are the height of the absorption peaks of amorphous calcium phosphate in the 550-600 cm^{-1} band, and c is the lowest point between the two peaks. The SF reported by Weiner and Bar-Yosef (1990) is 2.8 for modern fresh bone, and can be as high as 7 for archaeological bones (Pollard et al., 2007).

In this study two femur fragments and two rib bones belonging to two individuals were examined by FTIR. Relative to XRD, FTIR has an advantage in that a very small amount of sample is required, as well as providing more accurate results and the sample preparation is easier. The FTIR analysis were performed ar TÜBİTAK SAGE (defense industries research and development institute) FTIR Lab. A Perkin Elmer Spectrum 100 with a diamond ATR was used in the analysis. A general standard scan was applied without any calibration. The results were given in percentage of transmittance, and they are converted into absorbance (A) by the formula given below:

A= 2-log(%T).

3.4. Statistical Analysis

The elemental configuration of the archaeological bones excavated from the İznik Roman Theatre, and the soil samples obtained from the site were reorganized in Excel to calculate their mean values, standard deviations, and coefficient of variations. The extreme minimum and maximum values for each element, either for fossil bones or soil samples, was also reorganized and visualised in charts. The values of the essential elements were graded with percentages (%), and minor and trace elements with ppm (μg/g). The reference values for elemental configuration of archaeological bone were also added to the charts.

To evaluate elemental variations according to location and sex, ANOVA statistical analysis were performed. For each sample, to determine the relationship with each other, a correlation matrix was used. The values were between -1 and +1, demonstrating negative and positive correlation values, where 0 referred to no correlation.

For the distribution of elemental mean values a Principle Component Analysis (PCA) was made. In addition, a Student t-test was used to analyze the statistical significance of the relationship for each sample group.

CHAPTER 4

RESULTS AND DISCUSSION

4.1. Description and Measurement of Diagenetic Parameters

To describe the diagenetic patterns of the İznik bone samples, it is important to classify the post mortem alteration factors.

4.1.1. Chemical and physical analysis of soil

Changes in porosity relate to changes in the bone's physical structure, which may be due to variations in either the organic or inorganic components (Nielsen-Marsh, 1999). Much of the weight loss (~20%) and porosity increase (~50%) in bone can be ascribed to a loss of collagen. Many bones exhibit additional porosity, and there is a general impression that dissolution is more prevalent in sites where water movement is more active. Internal pore waters tend to be saturated and the rate of bone mineral loss is governed by diffusion into the surrounding soil water. Dissolution depends on the composition of the soil water. Therefore, most dissolution takes place in greatly unsaturated conditions due to the reduction of pH, or recharging with fresh water. Such recharging happens when the object (i.e. bone) is close to the ground surface, or in highly conductive soil (Hedges, 2002).

4.1.1.1. Hydrogen-ion activity (pH of soil)

There are two well-known methods to identify the pH of soil (Kacar, 2009). Colorimetric measurements are based on the changing of colour dyes, which react with the H ion or acidic indicators, and electrometric measurements based on H^+ ion

sensitive glass electrodes to analysis the changing electro motive forces. The results of soil pH testing for this study are given in Table 4.1.

Table 4.1. *The pH of soil samples*

Sample	Location	pH
D1	Inside Cavea	8.27
D2	Inside Cavea	8.28
D3	Outside Cavea	8.29
D4	Outside Cavea	8.28
D5	City Walls	8.27
Av.		8.278

The obtained pH values range between 8.27 and 8.29, with a mean value of 8.28. Values for soil pH over 5.3 are considered to provide good preservation of archaeological bones (Tortora et al., 1994). However, high pH values in the soil may induce the degradation of bone when the hydroxide ion replaces phosphates, producing calcium hydroxides $Ca(OH)_2$, and in neutral or alkaline conditions this can also increase microbial attacks on bone collagen, resulting in increased porosity.

It is important to understand that the acidity of a soil suspension decreases with increasing concentrations of neutral salts in the soil matrix. The pH of soil undergoes periodic variation, being lowest during hot and dry seasons, and highest during cool

and rainy seasons. This seasonal variation is closely related to fluctuations in the amount of soluble salts, which accumulate during dry seasons and lowers the pH of the soil but are subject to leaching during the rainy season when the pH returns to its maximum level. Several factors have to be considered in soil analysis with regards to acidity, such as the salinity of the soil.

4.1.1.2. Salt analysis

Pure water is a very poor conductor of electric current, whereas water containing dissolved salts found in soil conducts current in proportion to the amount of salt present (Van Olphen, 1966; Kacar, 2009). Salt analysis is based on this fact, the measurement of the electrical conductivity of a sample gives an accurate indication of the total concentration of ionized constituent. The results are given in Table 4.2.

Table 4.2. *Electrical Conductivity Analysis*

Samples	Weight (mg)	*RS (x2000 **µS)	V (ml)	***R_{st} (0.01 M KCl)	Soluble Salt (%)
D1	5.3065	315	25	0,001494	1.01
D2	5.1782	304	25	0,001494	1.07
D3	5.5429	200	25	0,001494	1.52
D4	5.1950	247	25	0,001494	1.32
D5	5.0397	721	25	0,001494	0.46

*Resistivity Sample

**Micro Siemens

***Resistivity Standard

The amount of soluble salt in the İznik soil samples range between 0.46% (sample D5) to 1.52% (sample D3). The lowest percentage in the sample group (0.46%) belongs to sample D5, which was taken from outside of the city walls. The calculated average for inside the cavea is 1.04%, whereas it is 1.42% for outside cavea.

For the İznik soil samples, the measured values show evaluated saline content, according to the US Salinity Lab criteria's (cited in Gartley, 2011). Moreover, Dursun et al. (2008) stated that if the amount of salt in the soil is greater than 0.15%, it can be considered as being high in salinity. As discussed previously (Chapter 2), high salinity of soil increases ion mobility, which can accelerate post mortem alterations of buried bones (Akyol, 2009; Tanrıverdi, 2018; Gartley, 2011).

4.1.1.3. Soil type analysis

Clay, since it is negatively charged (Van Olphen, 1966), is the most chemically active part of the soil matrix, and increases both water absorption capacity and cation mobility of the soil. Depending on temperature and acidity, bone preservation can be good in clayey soil (Van Olphen, 1966). The results show that the clay percentage in the soil is approximately 20% of the mixture, the obtained results are given in Table 4.3.

Table 4.3. *Soil Type Analysis*

Sample	Weight (g)	Water (ml)	Drained Clay(g)	Total Clay (g)
D1	5.3065	500	0.9551	0.9850
D2	5.1782	500	0.9694	0.9985
D3	5.5429	500	0.9702	0.9917
D4	5.1950	500	0.9750	1.0150
D5	5.0397	500	0.9741	1.0230

4.1.1.4. Elemental analysis of soil

The elemental composition of the soil surrounding buried skeletons is the key pathway to understanding bone diagenesis. The XRF results of the elemental composition of the five soil samples taken from the site are given in Table 4.4.

Table 4.4. *XRF analysis of soil samples*

Element	Dimension	ITK-D1	ITK-D2	ITK-D3	ITK-D4	ITK-D5
Na2O	%	0.050	0.046	0.053	0.049	0.049
MgO	%	1.76	0.74	1.61	1.62	1.48
Al2O3	%	6.30	3.33	6.69	6.76	3.99
SiO2	%	40.77	13.83	39.07	38.25	17.46
P2O5	%	1.324	0.239	0.548	0.877	0.368
SO3	%	0.224	0.138	0.110	0.186	0.333
Cl	%	0.023	0.016	0.018	0.012	0.089
K2O	%	1.53	0.72	1.35	1.56	1.16
CaO	%	28.41	42.66	29.68	26.71	36.19
TiO2	%	0.401	0.263	0.425	0.553	0.291
V2O5	%	0.013	0.007	0.013	0.012	0.006
Cr2O3	%	0.024	0.006	0.054	0.067	0.011
MnO	%	0.112	0.062	0.097	0.115	0.068
Fe2O3	%	3.17	2.28	3.34	3.84	2.46
LOI	%	15.53	35.82	15.98	18.99	6.73
Toplam	%	99.64	100.15	99.04	99.60	70.68
Co	ppm	12	12.6	34.1	21.2	26.2
Ni	ppm	45.4	25.6	42.3	45.6	29.2
Cu	ppm	128.7	55.4	187.9	215.2	51.7
Zn	ppm	121	49	69	113.4	64.7
Ga	ppm	8.1	7.5	7.2	8.8	6.5
Ge	ppm	0.5	0.5	0.9	0.5	0.4
As	ppm	59.5	8.9	6.3	13.3	10.7
Se	ppm	0.3	0.3	0.3	0.3	0.3
Br	ppm	6.2	1.8	3.1	4	10.8
Rb	ppm	49.1	29.9	43.4	49.4	36.1
Sr	ppm	290.4	229.3	400.8	221.2	286.3
Y	ppm	14.5	11.2	11.5	14.2	10.9
Zr	ppm	129.9	56.5	114.4	225.9	69.6
Nb	ppm	3.5	5.7	3.8	7.3	9.9
Mo	ppm	3.2	3.4	4.3	3.5	3.5
Cd	ppm	0.8	0.9	0.9	0.9	0.9
In	ppm	0.5	0.9	0.9	0.8	0.8
Sn	ppm	9.9	2.7	25.5	23.3	4.7
Sb	ppm	1	1	13.5	2.3	0.9
Te	ppm	1.1	1.3	1.2	0.7	1.2
I	ppm	2.1	2.1	2.2	2.2	4.1
Cs	ppm	3.6	5.5	3.7	4.8	3.5
Ba	ppm	258.5	235.9	246.5	248.4	180.2
La	ppm	22.5	18.8	22.6	27.9	23.6
Ce	ppm	41.6	25.4	18.2	41	16.2
Hf	ppm	9.6	4.1	6.3	12.2	3.8
Ta	ppm	6.4	4.7	7.5	7.9	4.4
W	ppm	3.1	2.7	2.9	3.1	2.8
Hg	ppm	0.8	0.9	0.9	0.9	0.9
Tl	ppm	0.6	1	1.2	0.8	0.9
Pb	ppm	114.5	47.3	198.8	269	37.4
Bi	ppm	0.9	0.8	0.4	1.5	0.7
Th	ppm	4.8	5.6	6	7.5	3.8
U	ppm	8.7	10	8	8.9	8.6

4.1.2. Chemical and physical analysis of the bones

4.1.2.1. Crystallinity

SF and Absorption bands are given in Table 4.5.

Table 4.5. *FTIR Crystallinity Results*

Sample No.	Bone Type	Absorption Band	Splitting Factor
ITK 90 57/3 A	Costa	563.13-599.62 cm^{-1}	5.55
ITK 90 57/3 B	Femur	562.48-599.77 cm^{-1}	5.62
ITK 90 58/5 A	Costa	562.70-599.93cm^{-1}	5.03
ITK 90 58/5 B	Femur	562.67-600.03cm^{-1}	5.59

The SF results of the two rib bones are 5.55 and 5.03. These amounts are smaller, respectively, than the femurs which are 5.62 and 5.59. The FTIR chart diagrams of the samples obtained by SAGE are given below (Fig. 4.1, 4.2, 4.3, 4.4).

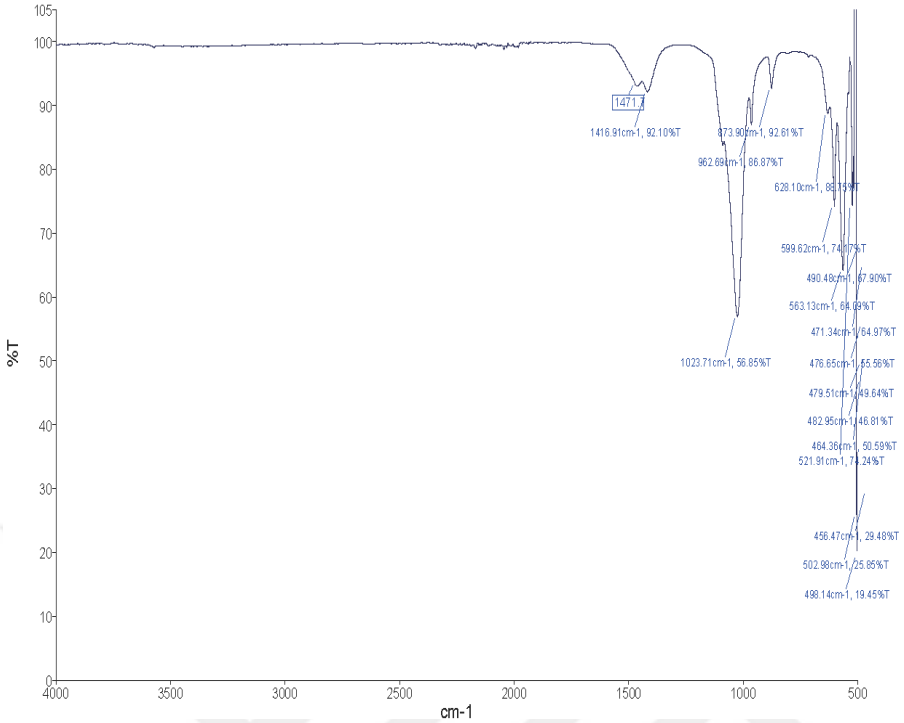

Figure 4.1. FTIR pattern of sample ITK 90 57/3

For the sample ITK 90 57/3 A, the rib bone of a male excavated from inside the cavea, the wave numbers are 599.62cm^{-1} representing 74.17% and 563.13cm^{-1} for 64.09% transmittance.

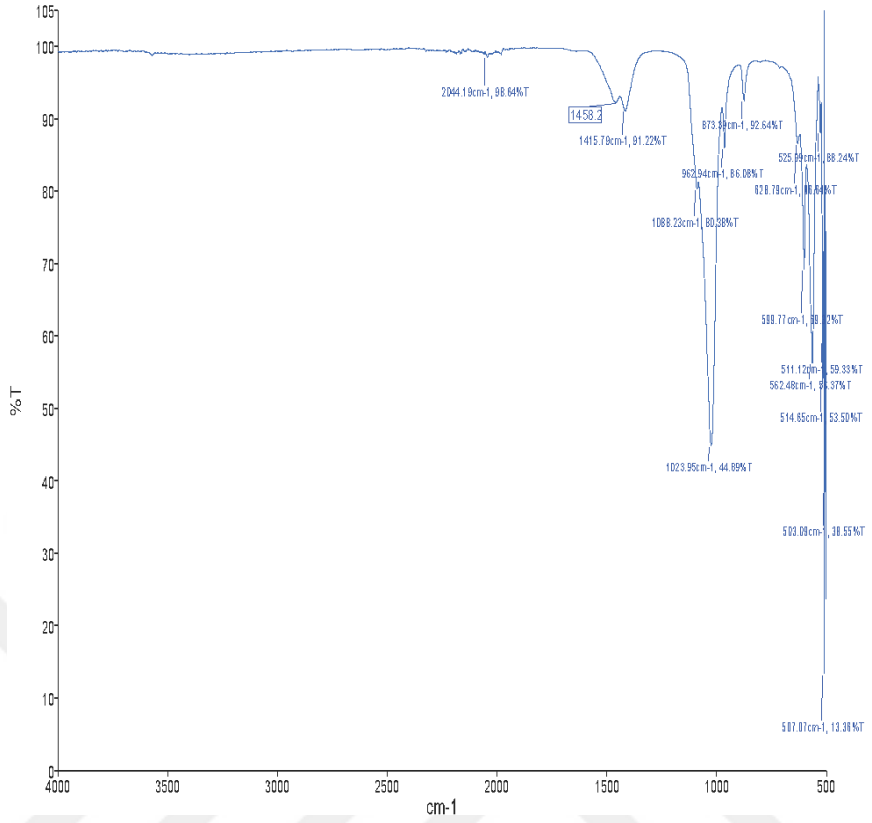

Figure 4.2. FTIR pattern of sample ITK 90 58/5

For sample ITK 90 58/5 A, which is a rib bone from a male individual excavated from inside of cavea, the wave numbers are 599.77 for 69.32% and 562.48cm^{-1} for 56.37% transmittance.

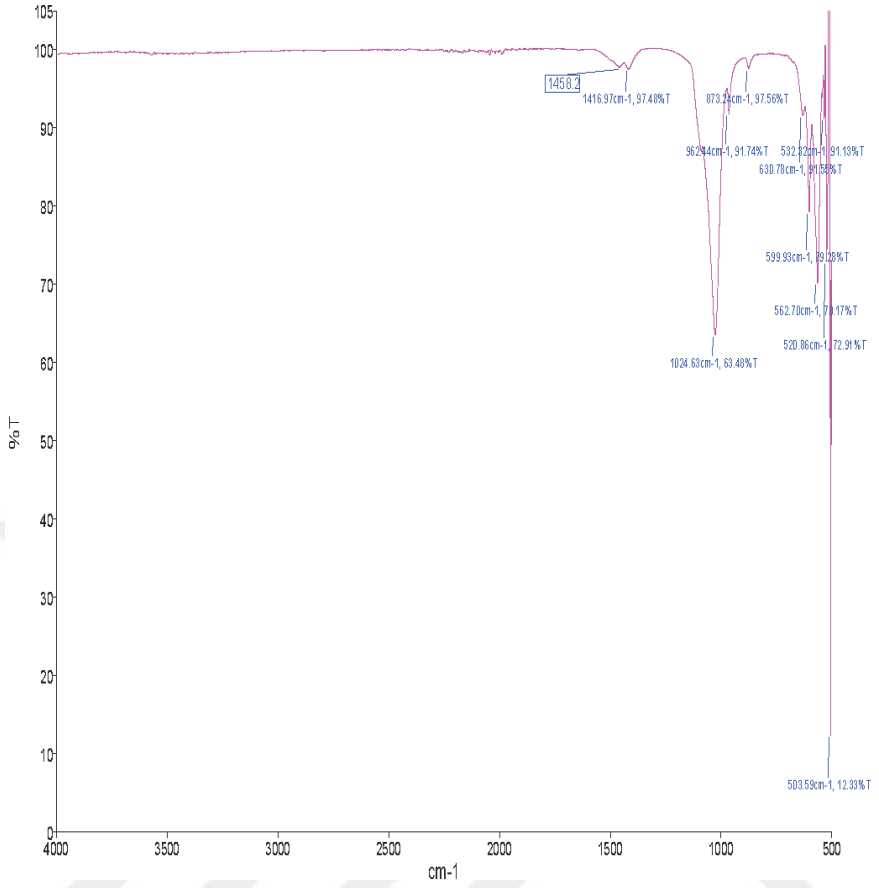

Figure 4.3. FTIR pattern of sample ITK 90 57/3 B

For sample ITK 90 57/3 B, the femur bone of a male individual excavated from inside the cavea, the wave numbers are 599.93cm^{-1} for 79.28% and 562.70cm^{-1} for 70.17% transmittance.

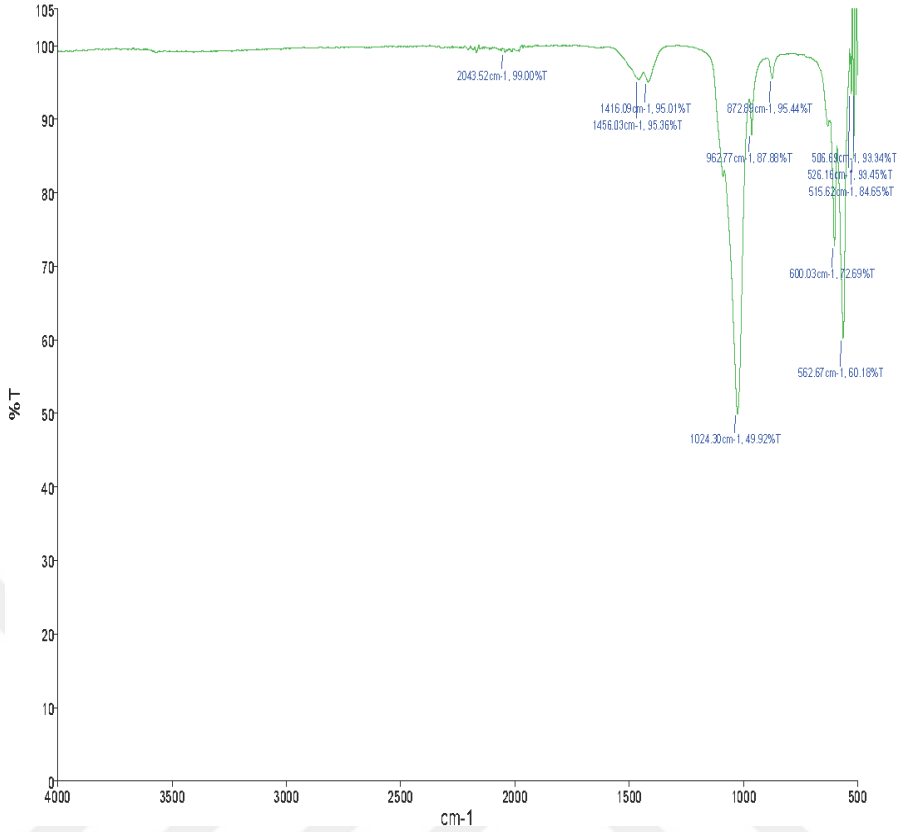

Figure 4.4. FTIR pattern of sample ITK 90 58/5 B

For sample ITK 90 58/5 B, a femur bone belonging to the same individual excavated from outside the cavea, the wave numbers are 600.03 cm-1 for 72.69% and 562,67cm^{-1} 60.18% transmittance.

In general, increases in crystallinity are a fundamental part of the diagenetic process. The major contribution to increases in the Splitting Factor measured in archaeological bone was due to recrystallization and dissolution of the smallest crystallites in the apatite. Although Bar-Yosef (1990) reported the Splitting Factor values of archaeological bone increase from a base line of approximately 2.8 up to 7, the results from 5.03 to 5.62 are relatively high with respect to previous studies and indicate a crystallinity increase in the apatite. The analysed samples can, therefore, be considered to have undergone post mortem alteration. Sillen and Parkington (1995), Nielsen-Marsh and Hedges (1999), and Baltazar (2001) reported SF with a mean value of between 2.8 and 4. The discrepancies in these results may be the result of the samples analyzed by FTIR being oven dried at 600^0C to remove the organic phase of bone. The presence of collagen ensures the stability of the mineral matrix; the IRSF increases with the simple chemical removal of collagen (Hedges, 2002).

Here, it is important to mention Ca/P measurements, since in archaeological bone the carbonate peak observed in IR spectra often includes additional carbonate. In a calcite environment, carbonate is usually deposited as calcium carbonate on the surface and within crack and pores of the bone, but can also be present via adsorption on the surface of bioapatite. It may also enter into the crystal lattice by replacing biogenic carbonate or phosphate. Bone containing calcite often possess much higher Ca/P values than those where carbonate is adsorbed, and such calcite can be distinguished by the presence of the 713cm^{-1} peak in the IR spectrum. Low values of Ca/P indicate the diagenetic loss of carbonate (Hedges, 2002). In further studies, as well as SF factors, Ca/P measurements must be considered as a screening technique for identifying the bones which have been altered by post-mortem processes.

4.1.2.2. Porosity

The percentage of porosity (%P), wet and dry unit volumes, and water absorption (%WAC) capacities of the İznik bones are given in Table 4.6.

Table 4.6. *Porosity and water absorption capacity of the sampled İznik bones*

Samples	WET (g/cm^3)	DRY (g/cm^3)	WAC (%)	P (%)
İTK-K1	2.21	1.32	30.31	40.07
İTK-K2	2.12	1.29	30.57	39.33
İTK-K3	1.98	1.39	21.72	30.10
İTK-K4	1.86	1.28	24.27	31.06
İTK-K5	2.02	1.55	15.16	23.44
İTK-K6	1.51	1.11	24.04	26.59
İTK-K7	1.86	1.15	33.50	38.40
İTK-K7b	2.28	1.44	25.38	36.63
İTK-K8	1.69	1.23	22.07	27.20
İTK-K9	1.87	1.20	29.48	35.51
İTK-K10	1.90	0.96	51.08	49.24
İTK-K11	1.95	1.27	27.49	34.85
İTK-K12	2.23	1.29	32.47	41.99
İTK-K13	2.52	1.37	33.27	45.60
İTK-K14	2.03	0.93	57.81	54.05
İTK-K15	1.95	1.85	2.97	5.49
İTK-K16	2.05	1.41	22.24	31.26
İTK-K17	1.80	1.29	21.76	28.15
İTK-K18	1.90	1.31	23.87	31.22
İTK-K19a	1.89	1.36	20.66	28.03
İTK-K19b	2.20	1.53	19.68	30.19

Total porosity is defined as the volume of water uptake per gram of bone sample. As seen in Table 4.6, the porosity percentage distribution varies from 5.49% (sample İTK-K15) to 54.05% (sample İTK- K14). Many bones exhibit additional porosity and, according to Hedges (2002), during diagenetic alteration, micro porosity decreases and macro porosity increases with respect to modern bone. Since the procedure of calculating the percentage of micro porosity is complicated and a very long and hard procedure, for this study an increase of total porosity may be presumed. The porosity must be explained not only by protein loss, but also the relationship between the splitting factor, the histological index, as well as the Ca/P measurements, and all of these factors must be considered in detail.

4.1.2.3. Elemental analysis

Bones, due to their significant renewal rate, are considered good life-long monitors for some trace elements. Nonetheless, their open morphological structure with inner channels makes them susceptible to post-mortem alteration (Lachowicz et al., 2016). To be able to draw conclusions about the İznik population, it is very important to understand and interpret the elemental composition of the skeletal remains.

The elemental compositions of the bones excavated from the İznik Roman Theatre were examined by two different analytical methods (XRF and ICP-OES). Although the advantages and disadvantages, of each method, were discussed in detail in Chapter 3, it is very important to observe the actual differences from this study in order to make a salutary comparison with the existing literature.

The raw data from the XRF and ICP-OES analysis are given in Table 4.7. The results of the descriptive statistical analysis of both methods concerning the location and gender subgroups are given in Tables 4.8 and 4.9.

Table 4.7. *Raw data of XRF and ICP-OES analyses*

Sample No	Methods	Ca%	P%	Al%	K%	Fe%	Mn%	Zn%	Sr%	Ba%	As%	Pb%	Cu%	U
		35-40%	*18%*	*≤0.0020%*	*≤0.06%*	*≤0.02%*	*≤0.001%*	*≤0.02%*	*<0.1%*	*<0.1%*	*≤0.0001%*	*1-100ppm*	*<0.003*	*≤1ppm*
1	ICP-MS	31.8	15.6	0.032	0.024	0.032	0.0036	0.026	0.043	0.06	0.0189	0.00127	0.0059	1.59
	XRF	33.27	11.5	0.068	0.137	0.038	0.0031	0.0218	0.0446	0.0353	0.0163	0.00172	0.00507	9.5
2	ICP-MS	33.3	16.7	0.043	0.032	0.042	0.0027	0.036	0.046	0.0345	0.0116	0.00195	0.0085	0.66
	XRF	34.85	15.21	0.1	0.007	0.041	0.0038	0.0303	0.0498	0.0179	0.0098	0.00234	0.00837	12.4
3	ICP-MS	31.8	15.2	0.145	0.069	0.137	0.0087	0.027	0.047	0.062	0.0119	0.0042	0.0068	1.05
	XRF	31.93	10.78	0.154	0.171	0.1	0.0077	0.0205	0.0446	0.0311	0.009	0.0042	0.00506	19.3
4	ICP-MS	34.2	17.7	0.019	0.0129	0.021	0.0026	0.022	0.037	0.0115	0.017	0.00109	0.0029	2.1
	XRF	33.68	11.94	0.058	0.126	0.031	0.0054	0.0102	0.0418	0.0187	0.0038	0.00104	0.00151	16.1
5	ICP-MS	33.3	15.5	0.056	0.027	0.055	0.011	0.022	0.034	0.0114	0.0069	0.0025	0.0062	1.51
	XRF	37.3	12.49	0.109	0.0074	0.063	0.014	0.0149	0.039	0.0159	0.0057	0.00197	0.00238	9.4
6	ICP-MS	34.7	16.3	0.024	0.0179	0.02	0.0059	0.0171	0.041	0.0139	0.0046	0.00118	0.0021	0.91
	XRF	33.31	11.67	0.07	0.123	0.031	0.002	0.0138	0.038	0.0126	0.0142	0.00114	0.00195	19.8
7A	ICP-MS	34.5	15.9	0.041	0.029	0.03	0.0015	0.026	0.048	0.098	0.0177	0.0039	0.0056	1.82
	XRF	27.12	8.04	0.24	0.205	0.029	0.00077	0.0215	0.0433	0.0438	0.0123	0.00405	0.00493	26
7B	ICP-MS	36.4	16.4	0.021	0.0197	0.0055	0.0009	0.0197	0.031	0.0115	0.0085	0.00138	0.00174	0.72
	XRF	36.74	13.12	0.005	0.129	0.018	0.0023	0.0134	0.0344	0.0108	0.0067	0.00136	0.00153	19
8	ICP-MS	34.7	17.2	0.033	0.0137	0.022	0.042	0.025	0.034	0.0118	0.0054	0.00152	0.0036	1.12
	XRF	35.54	12.4	0.046	0.126	0.035	0.036	0.0181	0.035	0.0128	0.0043	0.00182	0.00315	13.1
9	ICP-MS	35.2	18.2	0.04	0.036	0.019	0.0021	0.02	0.05	0.0148	0.0069	0.00118	0.0035	3.53
	XRF	34.18	12.02	0.059	0.006	0.037	0.0031	0.0123	0.501	0.0172	0.0057	0.0013	0.00296	15.3
10	ICP-MS	35.3	16.1	0.086	0.045	0.091	0.0043	0.026	0.045	0.012	0.0137	0.0026	0.0051	1.69
	XRF	31.99	10.59	0.12	0.159	0.056	0.0031	0.0186	0.0453	0.0169	0.0111	0.00145	0.00391	15.8
11	ICP-MS	35.9	16.7	0.011	0.024	0.03	0.0026	0.035	0.044	0.0245	0.0116	0.003	0.0045	1.34
	XRF	38.84	14.36	0.0084	0.007	0.044	0.0038	0.0309	0.0499	0.0204	0.011	0.0028	0.00439	10
12	ICP-MS	35	17.3	0.038	0.021	0.026	0.0136	0.028	0.034	0.065	0.0046	0.0022	0.0091	2.5
	XRF	35.65	11.57	0.22	0.241	0.038	0.015	0.0249	0.0384	0.0209	0.0044	0.00229	0.00928	11
13	ICP-MS	35.5	17.1	0.042	0.041	0.055	0.0132	0.038	0.053	0.0119	0.0089	0.0035	0.0066	1.24
	XRF	33.55	11.94	0.074	0.148	0.059	0.011	0.0291	0.0546	0.0122	0.0077	0.003	0.00585	9.5
14	ICP-MS	35.3		0.029	0.021	0.024	0.0015	0.025	0.038	0.0177	0.0147	0.00179	0.0044	1.93
	XRF	34.79	11.87	0.046	0.007	0.035	0.0023	0.0199	0.0394	0.0157	0.0122	0.00169	0.00427	20.2
15	ICP-MS	35.6	16.8	0.048	0.027	0.052	0.0144	0.055	0.039	0.005	0.0121	0.0026	0.0056	0.92
	XRF	36.08	13.22	0.061	0.007	0.062	0.014	0.0472	0.0424	0.0058	0.0096	0.00222	0.00511	18.3
16	ICP-MS	35.6	15.9	0.029	0.02	0.025	0.0029	0.041	0.042	0.057	0.0041	0.0032	0.0071	0.62
	XRF	33.47	11.43	0.122	0.158	0.035	0.038	0.0353	0.0422	0.0271	0.0035	0.00285	0.00604	10
17	ICP-MS	36.3	17.2	0.042	0.021	0.037	0.002	0.027	0.036	0.017	0.0092	0.00151	0.004	3.7
	XRF	34.26	11.42	0.067	0.154	0.044	0.003	0.0196	0.0367	0.0198	0.0078	0.00132	0.0035	19.4
18	ICP-MS	37.2	16.5	0.037	0.0178	0.042	0.0134	0.026	0.041	0.0151	0.0144	0.0022	0.0032	4.3
	XRF	37.3	12.85	0.01	0.007	0.051	0.013	0.0191	0.0445	0.0182	0.0124	0.0017	0.00235	11
19A	ICP-MS	36.1	19.1	0.059	0.045	0.076	0.007	0.027	0.041	0.014	0.0202	0.0032	0.007	1.8
	XRF	35.01	11.03	0.28	0.275	0.075	0.0077	0.0225	0.0434	0.0158	0.0186	0.00235	0.0069	23.6
19B	ICP-MS	36.4	16.4	0.015	0.07	0.008	0.0011	0.02	0.038	0.0046	0.0152	0.00113	0.00193	0.71
	XRF	38.88	14.68	0.005	0.17	0.016	0.0007	0.0136	0.0433	0.0063	0.0091	0.00083	0.00122	9.7

According to the Tables 4.8 and 4.9, the mean values for P, Zn, Ba, As, and Cu are significantly higher from the ICP-OES analysis than from the XRF analysis. Opposingly, Al, K, Mn, and U have higher values in XRF analysis compared to those from ICP analysis. The results of Ca, Fe, and Sr are similar for both types of analysis method(Fig. 4.5).

Table 4.8. *XRF Results of the İznik Bone Samples*

Bones/Elements XRF		Ca%	P(%)	Ca/P(%)	Zn ppm	Sr ppm	Ba ppm	Cu ppm	Fe %	Mn %	K %	Al %	As ppm	U ppm	Pb ppm	Zr ppm	Y ppm
References		35-40%	18%	2.16	<200	<1000	<0.01	<30	<0.02	<0.001	<600	<20	<1	<1	1-100	<1	<1
Inside Cavea (n=11)	Mean	34.21	12.09	2.86	268	440	220	54.55	0.0454	0.0092	0.1106	0.0999	93	15.02	25.93	11.45	0.52
	SD	3.02	1.91	0.27	92	58	11	20.67	0.022	0.01	0.09	0.08	37	5.72	9.15	4.27	0.04
	Min.	27.12	8.04	2.29	134	344	58	15.00	0.018	0.001	0.01	0.01	35	9.50	13.60	7.50	0.50
	Max.	38.84	15.21	3.37	472	546	440	93.00	0.100	0.04	0.24	0.24	163	26.00	42.00	22.00	0.60
	CV (%)	8.84	15.79	9.26	34.33	13.12	52.14	37.90	48.34	116.22	79.40	78.19	39.68	38.06	35.29	37.26	7.81
Outside Cavea (n=10)	Mean(X)	35.54	12.19	2.92	163.08	417.26	154.64	29.91	0.0439	0.0088	0.1153	0.0824	93.22	15.32	14.92	9.57	0.53
	SD	2.12	1.13	0.14	38.65	45.87	39.72	16.23	0.02	0.01	0.09	0.08	47.80	4.67	4.65	2.25	0.09
	Min.	31.99	10.59	2.65	102.20	349.90	63.30	12.20	0.02	0.00	0.01	0.01	38.80	9.40	8.30	7.10	0.50
	Max.	38.88	14.68	3.17	225.20	501.80	197.90	69.00	0.08	0.04	0.28	0.28	186.40	23.60	23.50	13.20	0.80
	CV	5.95	9.25	4.87	23.70	10.99	25.68	54.25	39.94	120.25	75.09	95.09	51.28	30.49	31.20	23.56	17.90
Male (n=17)	Mean(X)	34.63	12.04	2.90	224.21	427.38	181.51	45.23	0.0467	0.0103	0.1163	0.1011	88.42	15.47	21.61	10.75	0.53
	SD	2.67	1.63	0.23	89.10	54.23	91.65	22.75	0.02	0.01	0.09	0.08	38.19	5.25	9.34	3.74	0.08
	Min.	27.12	8.04	2.29	123.60	344.00	58.00	12.20	0.02	0.00	0.01	0.01	35.00	9.40	8.30	7.10	0.50
	Max.	38.88	15.21	3.37	472.00	546.00	438.00	92.80	0.10	0.04	0.28	0.28	186.40	26.00	42.00	22.00	0.80
	CV	7.72	13.50	7.96	39.74	12.69	50.50	50.29	45.09	108.63	78.25	81.00	43.19	33.93	43.20	34.76	14.58
Female (n=4)	Mean(X)	35.77	12.57	2.85	191.83	435.78	217.68	32.30	0.03600	0.0036	0.0983	0.05	113.90	13.85	16.75	9.75	0.50
	SD	2.73	1.26	0.12	91.90	50.08	96.29	17.63	0.01	0.00	0.06	0.03	54.34	4.97	8.08	2.58	0.00
	Min.	33.27	11.50	2.70	102.20	380.00	125.90	15.10	0.03	0.00	0.01	0.01	38.80	9.50	10.40	7.50	0.50
	Max.	38.84	14.36	2.99	309.00	499.00	353.00	50.70	0.04	0.01	0.14	0.07	163.00	19.80	28.00	12.50	0.50
	CV	7.64	10.01	4.17	47.91	11.49	44.24	54.59	17.42	39.85	62.22	56.65	47.70	35.91	48.22	26.46	0.00
Total (n=21)	Mean(X)	34.84	12.14	2.89	215.57	428.90	188.19	42.67	0.04	0.01	0.11	0.09	92.95	15.16	20.69	10.56	0.52
	SD	2.66	1.55	0.21	81.84	52.29	91.30	22.20	0.02	0.01	0.09	0.08	41.44	5.12	9.13	3.51	0.07
	Min.	27.12	8.04	2.29	102.00	344	58.00	12.00	0.02	0.001	0.01	0.01	35.00	9.40	8.30	7.10	0.50
	Max.	38.88	15.21	3.37	424.00	546	438.00	93.00	0.10	0.04	0.28	0.28	186.00	26.00	42.00	16.20	1.20
	CV	7.62	12.76	7.36	37.96	12.19	48.51	52.03	43.60	115.06	75.38	83.84	44.59	33.74	44.13	33.25	13.37
Soil (n=5)	Mean(X)	23.60	0.38	78.48	83.42	285.60	233.90	127.78	2.11	0.07	1.05	2.87	19.74	8.84	133.40	119.26	12.46
	SD	5.16	0.18	50.31	31.84	71.78	31.07	74.64	0.44	0.02	0.28	0.86	22.36	0.73	99.56	66.92	1.74
	Min.	19.07	0.16	34.97	49.00	221.20	180.20	51.70	1.60	0.05	0.60	1.76	6.90	8.00	37.40	56.50	10.90
	Max.	31.61	0.58	161.50	121.00	400.80	258.50	215.20	2.67	0.09	1.29	3.58	59.50	10.00	269.00	225.90	14.50
	CV	21.87	48.43	64.10	38.16	25.13	13.28	58.41	21.07	27.43	27.05	30.16	113.27	8.26	74.63	56.11	13.98

Table 4.9. *ICP-OES Results of the İznik Bone Samples*

Bones/Elements ICP		Ca%	P%	Ca/P%	Zn %	Sr %	Ba ppm	Cu ppm	Fe %	Mn ppm	K %	Al %	As ppm	U ppm	Pb ppm	Zr ppm	Y ppm
References		35-40	18	2.160	<0.02	<0.1	<1000	<30	<200	<10	<0.06	<0.002	<1	<1	1-100	<1	<1
Inside Cavea (n=?)	Mean(X)	34.61	16.36	2.11	0.03	0.042	406.45	59.85	0.046	59.65	0.03	0.0466	113.27	1.31	26.35	0.09	0.25
	SD	1.61	0.68	0.08	0.01	0.006	295.84	20.34	0.032	54.00	0.01	0.03	47.09	0.60	10.03	0.20	0.16
	Min.	31.80	15.20	1.99	0.03	0.031	50.00	17.40	0.024	9.30	0.02	0.01	41.00	0.62	12.70	0.00	0.00
	Max.	36.40	17.30	2.24	0.06	0.053	980.00	91.00	0.14	144.00	0.07	0.15	189.00	2.50	42.00	0.59	0.63
	CV	4.64	4.18	3.91	27.78	14.79	72.79	33.98	70.26	90.52	48.72	74.26	41.58	45.94	38.06	214.69	64.82
Outside Cavea	Mean(X)	35.34	17.02	2.08	0.02	0.040	126.10	39.53	0.039	95.05	0.02	0.041	113.50	2.14	18.11	0.57	0.20
	SD	1.17	1.08	0.13	0.00	0.005	33.62	16.73	0.03	123.16	0.01	0.02	54.27	1.26	7.55	N.D	0.09
	Min.	33.30	15.50	1.89	0.02	0.034	46.00	19.30	0.01	11.50	0.01	0.02	46.00	0.70	10.90	0.57	0.07
	Max.	37.20	19.10	2.25	0.03	0.050	170.00	70.00	0.09	420.00	0.05	0.09	202.00	4.30	32.00	0.57	0.35
	CV	3.32	6.37	6.27	15.04	12.68	26.66	42.32	69.66	129.58	55.06	51.96	47.82	59.17	41.70	N.D	45.64
Male	Mean(X)	35.15	16.72	2.11	0.03	0.041	175.12	52.93	0.051	85.85	0.03	0.049	101.71	1.75	23.86	0.10	0.21
	SD	1.34	0.99	0.11	0.01	0.006	218.99	21.33	0.03	101.16	0.02	0.03	45.68	1.13	9.50	0.21	0.16
	Min.	31.80	15.20	1.89	0.02	0.031	46.00	17.43	0.02	9.30	0.01	0.02	41.00	0.62	11.30	0.00	0.00
	Max.	37.20	19.10	2.25	0.06	0.053	980.00	91.00	0.14	420.00	0.07	0.15	202.00	4.30	42.00	0.59	0.63
	CV	3.82	5.90	5.25	31.78	15.50	125.05	40.31	60.38	117.83	50.87	58.98	44.92	64.66	39.80	210.83	77.56
Female	Mean(X)	34.15	16.58	2.06	0.03	0.041	274.75	38.50	0.026	36.75	0.02	0.022	105.00	1.49	16.35	0.00	0.10
	SD	1.72	0.88	0.10	0.01	0.005	224.07	16.92	0.006	15.56	0.01	0.01	63.12	0.50	9.13	0.00	0.11
	Min.	31.80	15.60	1.93	0.02	0.034	115.00	21.00	0.02	26.00	0.01	0.01	46.00	0.91	10.90	0.00	0.00
	Max.	35.90	17.70	2.15	0.04	0.044	600.00	59.00	0.03	59.00	0.02	0.03	189.00	2.10	30.00	0.00	0.24
	CV	5.04	5.29	4.81	30.46	11.13	81.55	43.95	23.81	42.35	26.91	40.99	60.12	33.47	55.84	N.D	108.49
Total	Mean(X)	34.98	16.69	2.14	0.028	0.041	272.95	50.14	0.04	74.76	0.030	0.04	113.38	1.70	22.38	N.D	N.D
	SD	1.43	0.94	0.14	0.009	0.006	254.67	21.05	0.03	91.99	0.016	0.03	49.34	1.04	9.67	N.D	N.D
	Min.	31.80	15.20	1.89	0.017	0.031	46.00	17.00	0.01	9.00	0.013	0.01	41.00	0.62	11.00	N.D	N.D
	Max.	37.20	19.10	2.25	0.055	0.053	980.00	91.00	0.14	420.00	0.070	0.15	202.00	4.30	42.00	N.D	N.D
	CV	4.09	5.66	6.37	31.25	14.15	93.30	41.85	75.37	123.04	53.02	68.00	43.52	60.97	43.18	N.D	N.D
Soil	Mean(X)	23.60	0.38	78.48	83.42	285.60	233.90	127.78	2.11	0.07	1.05	2.87	19.74	8.84	133.40	119.26	12.46
	SD	5.16	0.18	50.31	31.84	71.78	31.07	74.64	0.44	0.02	0.28	0.86	22.36	0.73	99.56	66.92	1.74
	Min.	19.07	0.16	34.97	49.00	221.20	180.20	51.70	1.60	0.05	0.60	1.76	6.90	8.00	37.40	56.50	10.90
	Max.	31.61	0.58	161.50	121.00	400.80	258.50	215.20	2.67	0.09	1.29	3.58	59.50	10.00	269.00	225.90	14.50
	CV	21.87	48.43	64.10	38.16	25.13	13.28	58.41	21.07	27.43	27.05	30.16	113.27	8.26	74.63	56.11	13.98

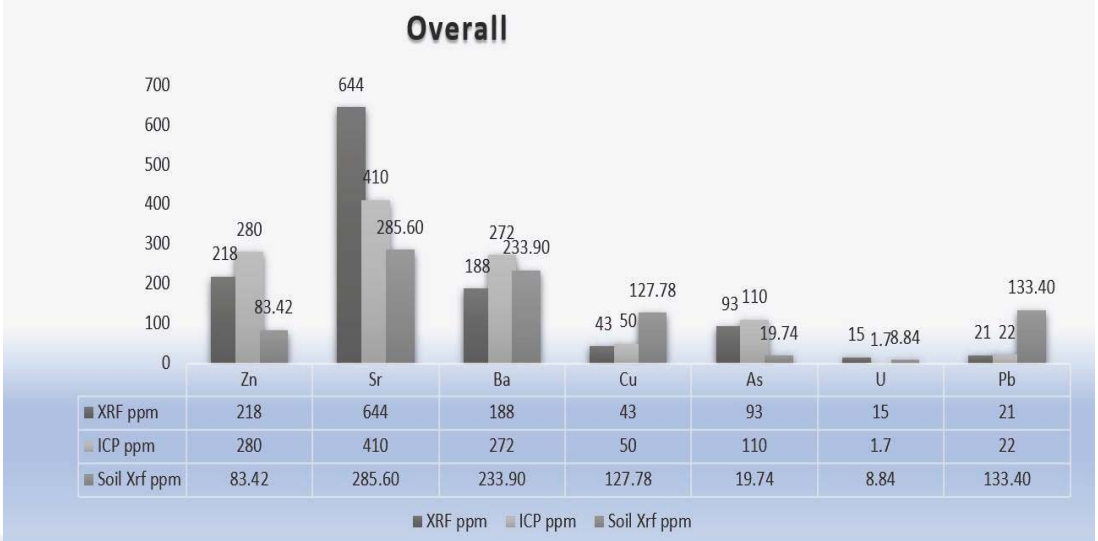

Figure 4.5. Overall comparison of trace elements according to instrumentational method used

The calculated mean value of Ca in the sampled bones analyzed by XRF is 34.69%, and 34.90% for analysis by ICP-OES. The mean value of Ca in the soil samples is 23.6%. The highest standard deviation for all of the samples was found in the soil samples - 5.16%. The average percentages of Ca, by XRF analysis according to the location were: 34.21% for inside the cavea, and 35.54% for outside of the cavea. The ICP-OES results were34.61% for inside the cavea, and 35.34% for outside the cavea. According to the sex of the sample population, female bones have values of 35.77% from XRF analysis, and 35.15% for ICP analysis. The male results were 34.63% for XRF analysis, and 34.15% for ICP analysis. The coefficient variations for XRF analysis are 8.84 from inside the cavea, 5.5 from outside the cavea, 7.72 for males, and 7.64 for females. For ICP analysis, the coefficient results were 4.64 for inside the cavea, 3.32 for outside the cavea, 3.84 for males, and 5.04 for females. The mean value of Ca in the soil samples was 23%.

The mean value for P, as analyzed by XRF, is 12.10% with a standard deviation of 1.54, and a coefficient variation of 11.53. For ICP the mean is 16.69% with a standard deviation of 0.94, and also a coefficient variation of 11.53. The distribution of P according to location and sex is 12.09% XRF values inside the cavea, 12.19% for outside of the cavea, 12.04% for males, and 12.57% for females. For ICP the mean values are16.36% for inside the cavea, 17.02% for outside of the cavea, 16.58% for males, and 16.72% for females. For comparing the amount of of Ca and P values, see Fig. 4.6. The mean value of P in the soil sample was 0.38%.

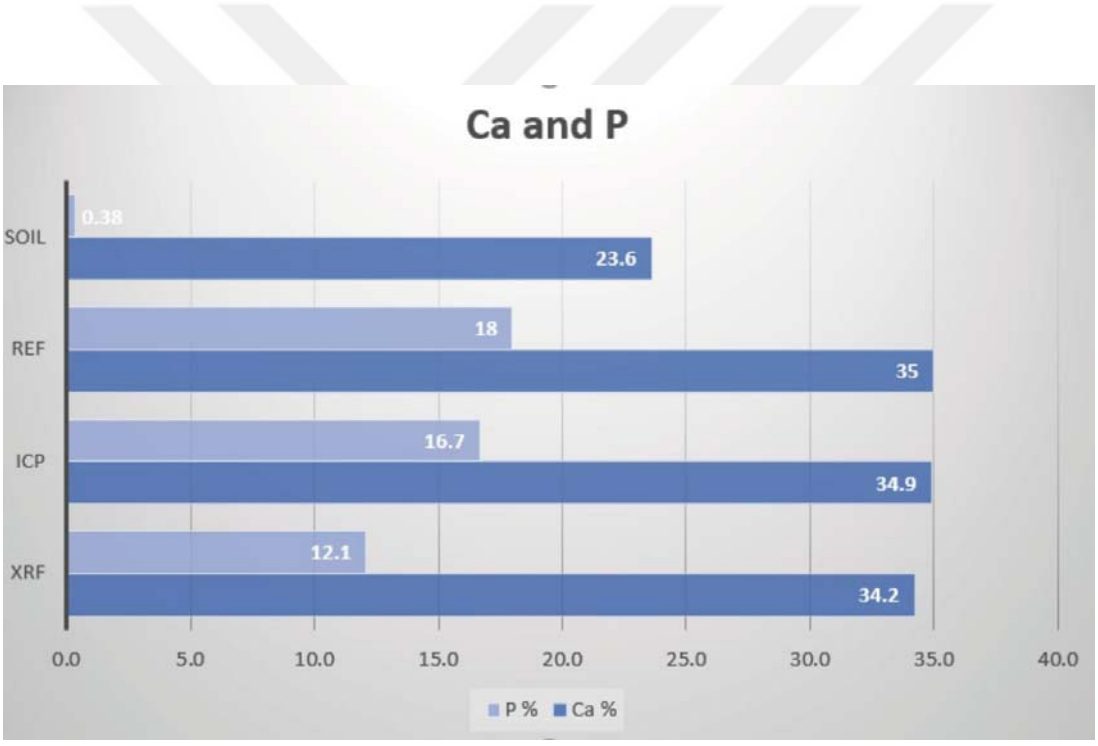

Figure 4.6. Ca and P values of samples, according to each method

In the crystal structure of bone hydroxyapatite, the mass ratio of Ca to P is 2.16. This defines the uncontaminated bone matrix, and it is independent of bone type. Deviation

from this value indicates changes in the bone structure such as calcination and leaching (Demirci and Kayatürk, 1989).

Ratios of Ca/P higher than this value may indicate either a decreasing phosphate content, and/or the presence of calcination in the bone sample. A low Ca/P ratio in the apatite structure may be the result of a deficiency in calcium ions. The Ca/P ratios examined both by XRF and ICP-OES are given in Table 4.10.

Table 4.10. *Ca/P Ratio of the İznik Bone Samples*

Sample No	Ca/P (XRF)	Ca/P (ICP)
İTK 88 43/10	2.89	2.03
İTK 88 41-43/6	2.29	1.99
İTK 88 41-43/1	2.96	2.09
İTK 89 53/9	2.82	1.93
İTK 89 53/26	2.98	2.14
İTK 89 53/30	2.98	2.13
İTK 90 57/3	3.38	2.17
İTK 90 57/3 B	2.8	2.22
İTK 89 51/24	2.78	2.02
İTK 90 58/7	2.84	1.93
İTK 90 58/3	3.02	2.15
İTK 90 57/11	2.7	2.15
İTK 90 57/8	3.08	2.04
İTK 88 43/21	2.8	2.02
İTK 88 43/13	2.93	N.D
İTK 88 43/3	2.73	2.1
İTK 89 41/2	2.92	2.24
İTK 89 53/3	3	2.07
İTK 89 53/6	2.9	2.15
İTK 90 58/5	3.17	1.89
İTK 90 58/5 B	2.64	2.22
Reference	2.16	2.16
Average	2.88	2.14
Standard Deviation	0.21	0.14
Min.	2.29	1.89
Max.	3.38	2.25
CV	7.36	6.37

The ratio of Ca/P differs according to the method. The results from XRF analysisfor the Ca/P ratio was 2.88, and 2.14 for ICP. The standard deviation of the Ca/P ratio from XRF analysis is 0.21, and 0.14 for ICP-OES analysis. The coeficient variationfor XRF is 7.36, and 6.37 for ICP-OES.

The mean values, standard deviations, and coefficient variations of the Ca/P ratio varies by location and sex of the samples. The XRF analysis of the bones inside the cavea produced a mean value of 2.86, with a standard deviation 0.27, and a coefficient variation 9.26. For ICP-OES, the mean values of samples from inside the cavea is 2.11 for the Ca/P ratio, 0.08 for the standard deviation, and 4.18 for the coefficient variation. The comparison of the results of Ca, P, and Ca/P for both methods of analysis given in Fig. 4.7.

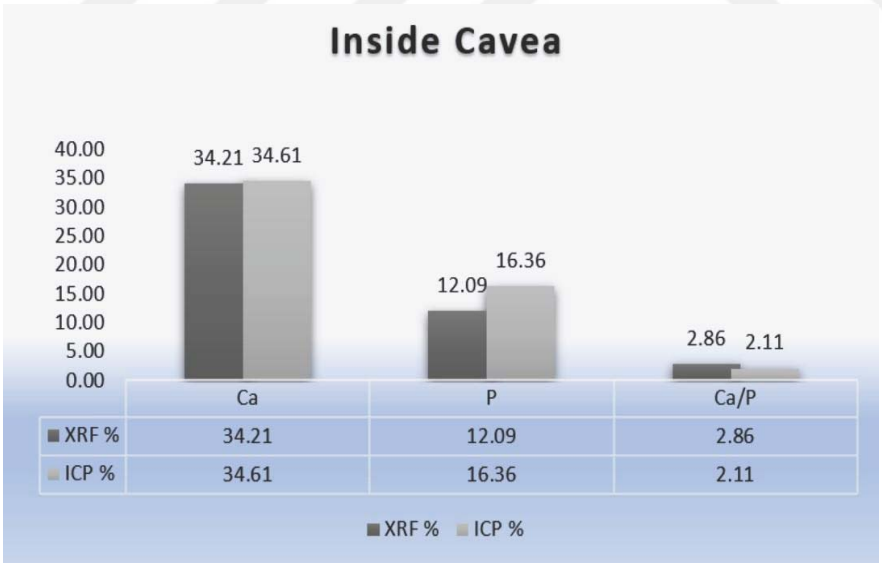

Figure 4.7. The Ca/P ratio comparison of XRF and ICP-OES for samples from inside the cavea

For the samples from outside of the cavea, both XRF and ICP-OES methods indicated approximately a 3% increase in Ca content. The Ca/P ratio, for XRF analysis, is 2.86 with a standard deviation of 0.14, and coefficient variation of 4.87. For ICP-OES, the results show a value of 2.08; with a 0.66 increase in P content outside of the cavea, resulting in a decrease to 2.08 in the Ca/P ratios. The standard deviation and coefficient variation were calculated as 0.13 and 6.27, respectively, for the ICP analysis (Fig. 4.8).

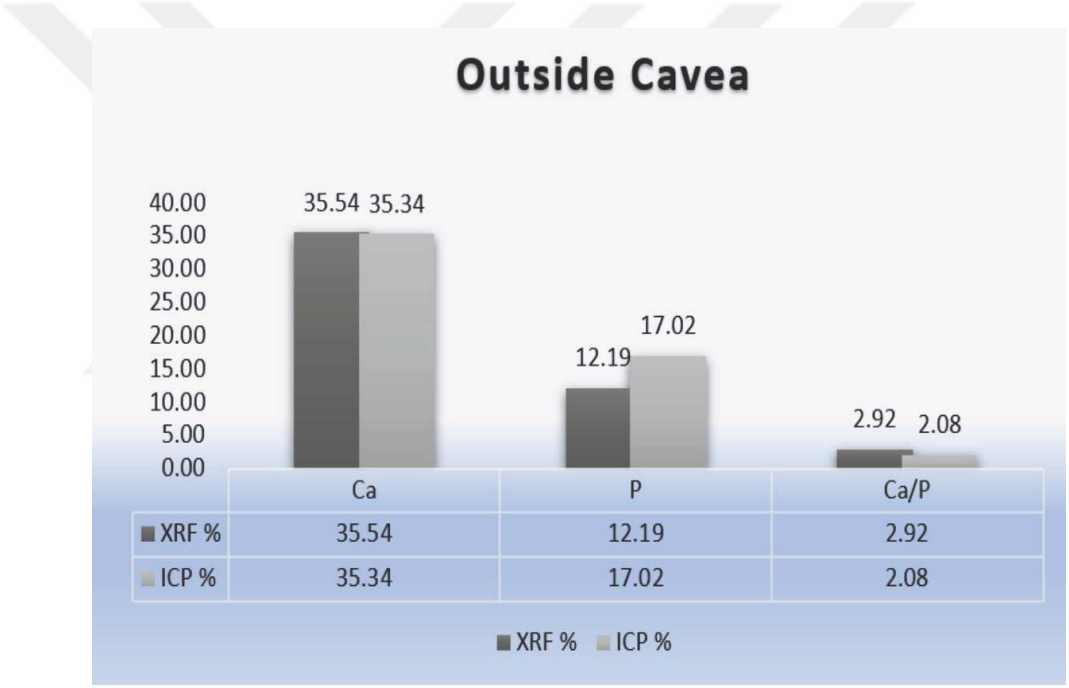

Figure 4.8. The Ca/P ratio comparison of XRF and ICP of samples from outside of the cavea

The Ca/P ratio differs slightly according to the sex of the individual. However, before drawing any conclusions, it is important to discuss the number of samples examined in the study, which were, unfortauntely, too few (15 males and four females) to statistically subgroup the individuals according to their sex.

The mean values of the Ca/P for the male individuals were 2.90 for XRF, and 2.11 for ICP-OES. The standard deviations were 0.23 for XRF with a 7.96 coefficient variation, and 0.11 for ICP-OES with a 5.25 coefficient variation (Fig. 4.9).

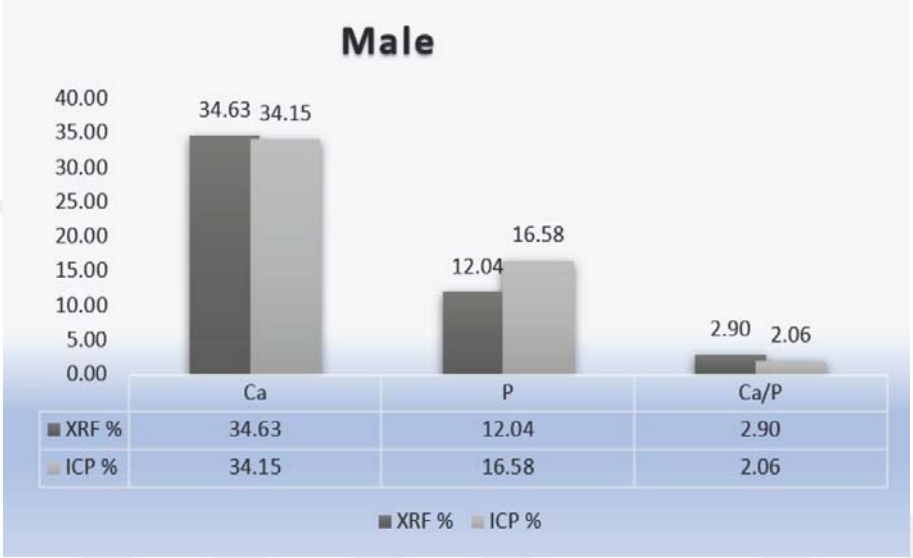

Figure 4.9. The Ca/P ratio comparison of XRF and ICP analyses for sampled male individuals

A significant drop (2.06) in the Ca/P ratio was noticed in the ICP-OES analysis for the female individuals. The standard deviation was 0.12 and the coefficient variation was 4.17. On the contrary, the XRF results were more stable for females, with a mean value of 2.85, and a standard deviation of 0.12, and coefficient variation of 4.17 (Fig.4.10).

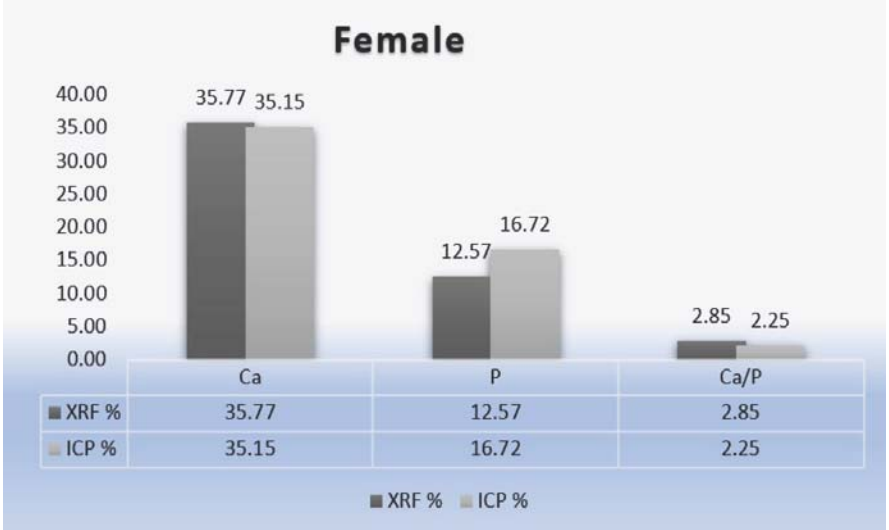

Figure 4.10. The Ca/P ratio comparison of XRF and ICP of female individuals

Soil sample D2, bone samples No. 3 and 19 B (a second rib bone belonging to individual 3, and a femur fragment belonging to individual 19B) were reanalyzed using the ICP-MS method. The comparison of XRF, ICP-OES, and ICP-MS results are given in Table 4.11.

Table 4.11. XRF, ICP-OES, and ICP-MS Results: Comparison of Selected Samples

	Ca%	P%	Mg%	Zn	Sr	Ba	Cu	Fe %	Mn	Na	K %	Al	As	U	Pb	Zr	Y
Soil D2 XRF	31.61	0.55	0.44	49	229.3	235.9	55.4	1.6	0.048	0.034	0.6	1.76	8.3	10	47.3	56.5	11.2
Soil D2 ICP-MS	>25	1.1	0.38	40	142	110	35.6	1.56	0.0352	0.07	0.24	0.96	9.1	0.44	25.6	4.6	6.89
19 B XRF	38.88	14.68		136	433	63	12.2	0.016	7		0.17	0.005	91	9.7	8.3	13.2	0.5
19 B ICP-OES	36.4	16.4		200	380	46	19.3	0.08	11.5		0.07	0.015	152	0.71	11.3	0	0.07
19 B DUST ICP-MS	>25%	>10000ppr	0.47	139	378	40	20.8	0.16	17	0.59	0.12	0.01	121	0.52	7.5	0.5	<.05ppm
19 B RAW ICP-MS	>25%	>10000ppr	0.51	182	448	50	25.6	0.62	42	0.65	0.07	0.02	145.5	0.54	11	1	0.11
			,														
3 XRF	31.93	10.78		205	446	311	51	0.1	77		0.171	0.154	90	19.3	8.3	16.2	0.5
3 ICP-OES	31.8	15.2		270	470	620	68	0.137	87		0.069	0.145	119	1.05	42	N.D	0.07
3 DUST ICP-MS	>25%	>10000ppr	0.23	277	460	380	62.4	0.29	55	0.48	0.05	0.06	108	1	35.3	0.8	0.06
3 RAW ICP-MS	>25%	>10000ppr	0.26	342	539	640	85.1	1.8	146	0.52	0.13	0.19	121	1.29	50.8	2	0.39

The results point demonstrate thar, for the reanalyzed bone samples number 3 and 19b, there are no significant differences between the methods of ICP-MS and ICP-OES, but there are slight differences with the XRF analysis. The results of the rib bone, obtained from a different part of the chest belonging to individual 3, differs in terms of the trace elements. There are also significant differences between the results for the trace elements of soil sample D2. This is especially true for the uranium content of the soil, which is 10 ppm for XRF, and 0.44 ppm for ICP-MS. Also, zirconium has a value of 56.5 ppm for XRF and 4.6 ppm for ICP-MS, and barium 235.9 ppm for XRF and 110 ppm for ICP-MS.

4.2. Statistical Analysis of Elemental Compositions

In this study, the statistical significance between the two elemental analysis methods, XRF and ICP-OES, and the difference between the amount of the elements in the samples were tested using a t-test, performed using the XLSTAT add-on for Excel. A p value of less than 0.05 ($p < 0.05$) was used to determine statistical significance. The first statistical significance test was applied to the analytical methods of element analysis (Table 4.11).

Table 4.11. *t-test values for XRF vs ICP methods of analysis of elements. Statistically significant results are highlighted in bold.*

Elements and Element/Ca ratio	P values
Ca%	0.803446
P%	**6.42E-10**
Ca/P%	**6.39E-12**
Zn %	**0.003905**
Sr %	**0.000164**
Ba ppm	0.190659
Cu ppm	0.380725
Fe %	**1.23E-10**
Mn ppm	**4.97E-20**
K %	**0.040068**
Al %	**0.025501**
As ppm	0.062083
U ppm	**0.000651**
Pb ppm	**1.43E-10**

For both methods the calculated values of Ca in the apatite were nearly the same, and it was expected that (Ca% of XRF: 34.8, of ICP: 34.2) there would not bea statistically significant relationship. On the contrary, the phosphate values were relatively different (P% of XRF:12.1, of ICP-OES:16.7), and statistical significane was determined by the t-test as seen by a *p* value lower than 0.05 (Table 4.11).

The difference between the phosphate values, therefore, would inevitably affect the Ca/P ratio analysed by both methods. Ultimately, the *p* vaue of the Ca/P concludes a statistical significance between the analytical methods of ICP-OES and XRF.

The statistical results are interesting, because whilst the resolution of ICP-OES is higher than that of XRF, it was surprising to see such a significant difference for the same samples analyzed by the two different methods. Theoretically, if we accept, for example, that the XRF results were right, it can be concluded that the phosphate in the crystal apatite will replace soil elements such as Al, K, U, Ba, etc. However, if we accept the restulst from ICP analysis as being right, then we must assume that this replacement of element di not happen, or at negligible rates. PCA analysis was utilised with an aim of clarifying this situation.

4.2.1. Princible Component Analysis (PCA)

To understand the relationship between the elements in more detail, the results were analyzed by PCA. A PCA diagram was created to visualize the data for examining the relationship between the elements tested by XRF analysis (Fig. 4.11).

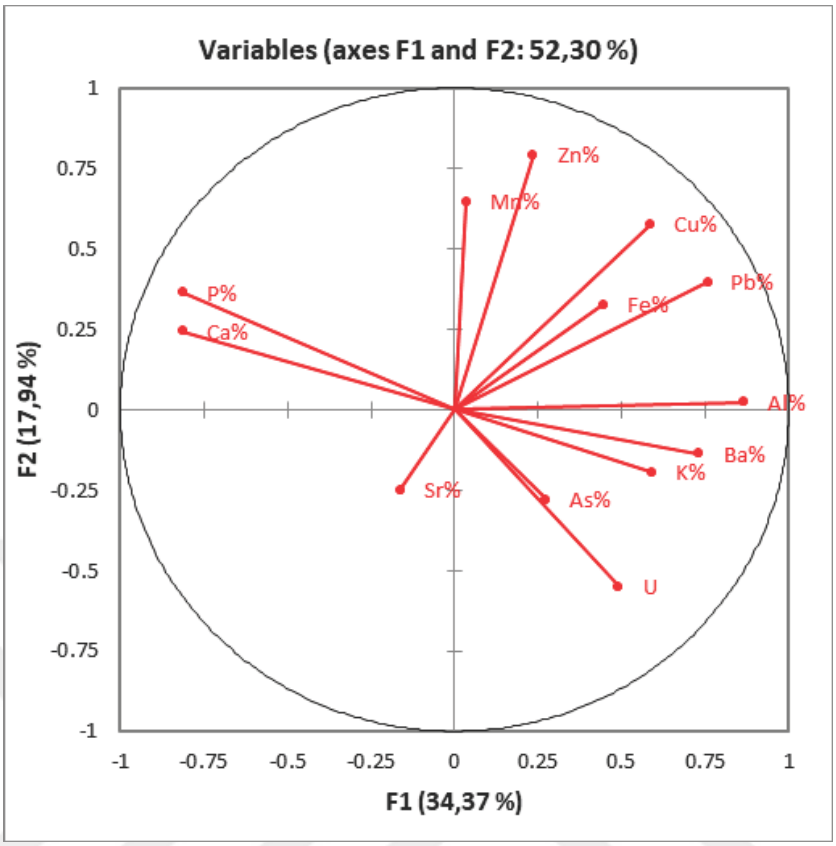

Figure 4.11. PCA for XRF analyzed element correlation; for functions F1 and F2

The PCA variations between the elements analyzed by XRF were explained by five functions (F1, F2, F3, F4, and F5). The PCA analysis for functions F1 and F2, provides the highest percentage of component relation with a value of 52.30% (Fig. 4.11). However, when the same analysis is applied to ICP-OES this number reduces to 45.79% (Fig 4.12).

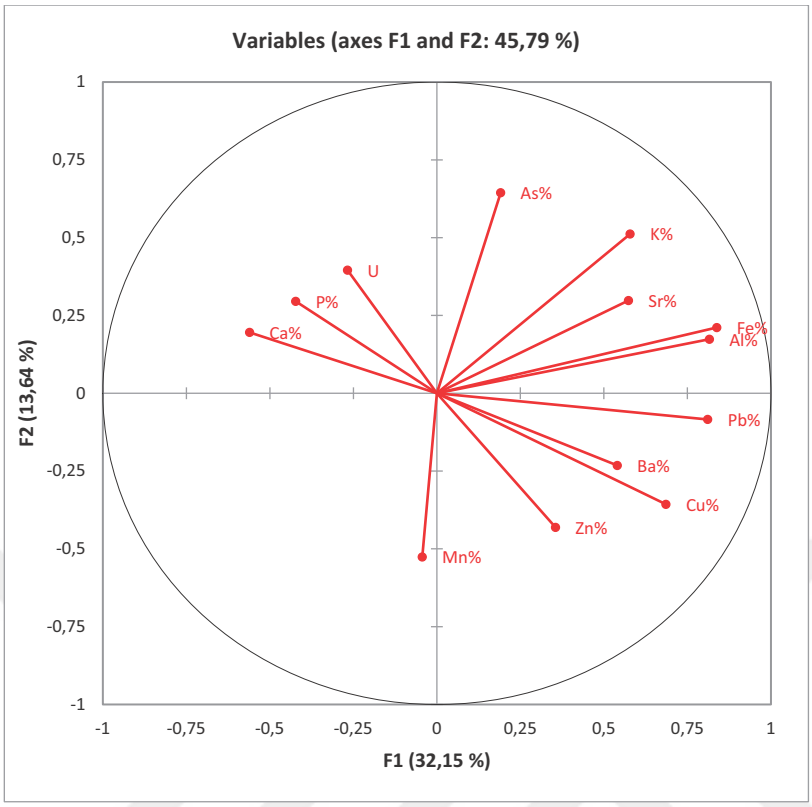

Figure 4.12. PCA for ICP-OES analyzed element correlation; for functions F1 and F2

It is obvious that the percentage of XRF PCA is higher than that for ICP- OES. The differences between these results seems to be the positive loads of Ca, P, Al, Ba, Pb and Cu in F1, which is also visible in the table of squared cosines (Table 4.12).

Table 4.12. Squared cosines of the variables

	F1	F2	F3	F4	F5	F6	F7	F8	F9	F10	F11	F12	F13
Ca%	**0.662**	0.059	0.077	0.045	0.024	0.002	0.021	0.001	0.070	0.001	0.026	0.006	0.007
P%	**0.659**	0.133	0.082	0.000	0.003	0.025	0.002	0.031	0.019	0.001	0.025	0.003	0.018
Al%	**0.749**	0.001	0.000	0.022	0.076	0.064	0.004	0.000	0.020	0.029	0.014	0.007	0.015
K%	0.348	0.038	0.026	**0.404**	0.027	0.044	0.018	0.002	0.004	0.083	0.001	0.005	0.000
Fe%	0.199	0.106	0.120	0.050	**0.239**	0.162	0.097	0.002	0.017	0.001	0.000	0.008	0.000
Mn%	0.001	**0.418**	0.294	0.048	0.024	0.039	0.010	0.138	0.016	0.001	0.010	0.000	0.000
Zn%	0.055	**0.627**	0.069	0.015	0.017	0.005	0.140	0.006	0.022	0.021	0.017	0.003	0.003
Sr%	0.026	0.062	0.081	**0.536**	0.114	0.130	0.001	0.020	0.003	0.026	0.000	0.000	0.000
Ba%	**0.535**	0.019	0.046	0.044	0.246	0.002	0.054	0.004	0.014	0.002	0.001	0.032	0.001
As%	0.075	0.078	**0.638**	0.001	0.024	0.003	0.015	0.153	0.001	0.004	0.004	0.004	0.000
Pb%	**0.574**	0.157	0.001	0.050	0.016	0.046	0.001	0.042	0.056	0.039	0.001	0.016	0.002
Cu%	**0.344**	0.334	0.021	0.001	0.000	0.245	0.000	0.005	0.001	0.023	0.009	0.001	0.015
U	0.240	**0.301**	0.069	0.000	0.051	0.016	0.277	0.003	0.028	0.001	0.003	0.011	0.000

Values in bold correspond for each variable to the factor for which the squared cosine is the largest

Ca and P are the main structural elements of bone apatite. The other elements with the largest factor of squared cosine, Al, Ba, Pb and Cu can be considered as contaminants, since their XRF values in the soil are higher than their presence in the bone. The second function indicates the elementsfor which the squared cosine is the highest, such as U, Zn, and Mn. Many paleodietary studies (Zapata, 2006; Ezzo, 1994; Lambert et al., 1983) consider Zn as an indicator for distinguishing whether the protein source has either an animal or plant basis. However, according to the same studies, Zn also has a diagenetic trajectory. In this study, the percentage of Zn analyzed in the apatite has an amount nearly three times as much as that in the soil. Therefore, it can be concluded that Zn can be considered as a dietary indicator.

The correlation matrix of PCA (Table 4.13) is also an indicator for understanding the relationship between the elements due to factors F1 and F2. The relation between the elements Ca and P is positively correlated with an r^2 value of 0.831. The relationship of Ca with Ba, Al, Pb, and U is inversely correlated with r^2 values and differs inbetween -0.729 and -0.464. In other words, the amount of Ca is decreasing while Al, Ba, Pb , and U are increasing. The other essential element of apatite. P, also has a negative correlation with K, along with the elements also related to Ca. It is also seen in the correlation matrix that Mn has a negative correlation, with an r^2 value of -0.492, whereas Zn is positively correlated with Pb and Cu with values of 0.480 and 0.628.

Table 4.13. *Correlation Matrix for XRF*

Variables	Ca%	P%	Al%	K%	Fe%	Mn%	Zn%	Sr%	Ba%	As%	Pb%	Cu%	U
Ca%	**1**	**0.831**	**-0.565**	-0.391	-0.167	0.055	-0.034	-0.065	**-0.729**	-0.057	**-0.534**	-0.297	**-0.464**
P%	**0.831**	**1**	**-0.652**	**-0.548**	-0.220	-0.024	0.133	-0.011	**-0.661**	-0.128	-0.424	-0.141	**-0.535**
Al%	**-0.565**	**-0.652**	**1**	**0.639**	0.398	0.064	0.137	-0.095	**0.479**	0.220	**0.547**	**0.638**	0.424
K%	-0.391	**-0.548**	**0.639**	**1**	0.048	0.060	-0.145	-0.294	0.288	0.104	0.207	0.265	0.287
Fe%	-0.167	-0.220	0.398	0.048	**1**	0.084	0.286	-0.074	0.100	0.214	**0.522**	0.325	0.119
Mn%	0.055	-0.024	0.064	0.060	0.084	**1**	0.349	-0.140	-0.045	**-0.492**	0.188	0.194	-0.359
Zn%	-0.034	0.133	0.137	-0.145	0.286	0.349	**1**	-0.225	0.007	0.051	**0.480**	**0.628**	-0.129
Sr%	-0.065	-0.011	-0.095	-0.294	-0.074	-0.140	-0.225	**1**	-0.034	-0.186	-0.172	-0.118	-0.010
Ba%	**-0.729**	**-0.661**	**0.479**	0.288	0.100	-0.045	0.007	-0.034	**1**	0.176	**0.604**	0.302	0.182
As%	-0.057	-0.128	0.220	0.104	0.214	**-0.492**	0.051	-0.186	0.176	**1**	0.068	0.110	0.368
Pb%	**-0.534**	-0.424	**0.547**	0.207	**0.522**	0.188	**0.480**	-0.172	**0.604**	0.068	**1**	**0.556**	0.173
Cu%	-0.297	-0.141	**0.638**	0.265	0.325	0.194	**0.628**	-0.118	0.302	0.110	**0.556**	**1**	-0.044
U	**-0.464**	**-0.535**	0.424	0.287	0.119	-0.359	-0.129	-0.010	0.182	0.368	0.173	-0.044	**1**

Values in bold are different from 0 with a significance level alpha=0,05

The PCA variations between the elements analyzed by ICP-OES as explained by functions F1 and F2, gives the highest percentage of component relation with a value of 45.79% . It is surprising that the essential elements Ca and P, although each has relatively high values, they do not indicate the highest squared cosines value due to function F1, as it is for the XRF values (Table 4.14). However, both elements and Zn, have the highest values for the function F3.

Table 4.14. *Squared cosines of the variables for ICP-OES*

	F1	F2	F3	F4	F5	F6	F7	F8	F9	F10	F11	F12	F13
Ca%	0.314	0.038	**0.319**	0.005	0.054	0.122	0.089	0.008	0.033	0.001	0.000	0.016	0.000
P%	0.178	0.087	**0.397**	0.004	0.026	0.102	0.100	0.040	0.026	0.022	0.016	0.001	0.000
Al%	**0.666**	0.030	0.000	0.201	0.043	0.003	0.004	0.009	0.010	0.002	0.022	0.004	0.005
K%	**0.334**	0.262	0.002	0.077	0.128	0.004	0.017	0.024	0.054	0.094	0.000	0.004	0.000
Fe%	**0.702**	0.045	0.030	0.148	0.011	0.001	0.014	0.001	0.026	0.013	0.000	0.003	0.006
Mn%	0.002	0.277	0.098	**0.310**	0.052	0.026	0.001	0.139	0.082	0.012	0.001	0.000	0.000
Zn%	0.126	0.186	**0.326**	0.075	0.122	0.007	0.011	0.011	0.088	0.026	0.021	0.001	0.000
Sr%	**0.329**	0.089	0.025	0.105	0.007	0.077	0.226	0.135	0.001	0.002	0.001	0.003	0.000
Ba%	**0.292**	0.054	0.113	0.286	0.115	0.005	0.009	0.001	0.090	0.004	0.030	0.002	0.001
As%	0.036	**0.415**	0.001	0.084	0.002	0.303	0.088	0.064	0.002	0.001	0.002	0.001	0.000
Pb%	**0.658**	0.007	0.097	0.018	0.003	0.033	0.059	0.001	0.050	0.051	0.006	0.017	0.000
Cu%	**0.470**	0.127	0.068	0.070	0.041	0.044	0.017	0.106	0.000	0.013	0.039	0.004	0.000
U	0.072	0.157	0.081	0.010	**0.541**	0.060	0.010	0.004	0.026	0.033	0.001	0.005	0.000

Values in bold correspond for each variable to the factor for which the squared cosine is the largest

It is obvious that the correlation matrix supports function F3. Ca, with a value of 0.449 is directly correlated with P. as witnessed in Table 4.15. The negative correlation with Al and Ba suggests the replacement of Ca with these elements due to the basis of diagenetic alteration. The correlation matrix also supports the idea of contaminant elements Fe, K and Pb with values of 0.943, 0.579, and 0.573, respectively. These are also directly correlated with Al, which also have also tendencies to be replaced by Ca in the apatite.

Table 4.15. *Correlation matrix for ICP-OES*

Variables	Ca%	P%	Al%	K%	Fe%	Mn%	Zn%	Sr%	Ba%	As%	Pb%	Cu%	U
Ca%	**1**	**0.449**	**-0.459**	-0.144	-0.380	-0.034	0.075	-0.210	**-0.466**	-0.083	-0.121	-0.405	0.303
P%	**0.449**	**1**	-0.289	-0.150	-0.225	0.075	-0.035	-0.062	-0.405	0.127	-0.249	-0.054	0.357
Al%	**-0.459**	-0.289	**1**	**0.579**	**0.943**	0.093	0.065	0.314	0.230	0.083	**0.573**	0.408	-0.022
K%	-0.144	-0.150	**0.579**	**1**	**0.566**	-0.199	-0.042	0.414	0.023	0.282	0.359	0.137	-0.241
Fe%	-0.380	-0.225	**0.943**	**0.566**	**1**	0.079	0.202	0.376	0.130	0.212	**0.664**	**0.457**	-0.050
Mn%	-0.034	0.075	0.093	-0.199	0.079	**1**	0.136	-0.235	-0.161	-0.339	0.031	0.069	-0.042
Zn%	0.075	-0.035	0.065	-0.042	0.202	0.136	**1**	0.240	0.074	-0.044	**0.462**	**0.511**	-0.260
Sr%	-0.210	-0.062	0.314	0.414	0.376	-0.235	0.240	**1**	0.283	0.194	**0.485**	0.285	0.017
Ba%	**-0.466**	-0.405	0.230	0.023	0.130	-0.161	0.074	0.283	**1**	0.097	**0.475**	**0.528**	-0.049
As%	-0.083	0.127	0.083	0.282	0.212	-0.339	-0.044	0.194	0.097	**1**	0.114	-0.032	0.099
Pb%	-0.121	-0.249	**0.573**	0.359	**0.664**	0.031	**0.462**	**0.485**	**0.475**	0.114	**1**	**0.590**	-0.184
Cu%	-0.405	-0.054	0.408	0.137	**0.457**	0.069	**0.511**	0.285	**0.528**	-0.032	**0.590**	**1**	-0.136
U	0.303	0.357	-0.022	-0.241	-0.050	-0.042	-0.260	0.017	-0.049	0.099	-0.184	-0.136	**1**
Values in bold are different from 0 with a significance level alpha=0,05													

Another important detail is that the dietary related elements of Zn, Sr, and Ba are positively correlated with Pb (Table 4.15). Although lead is considered as a contaminant metal in soil, the positive correlation between lead and the dietary related elements (Sr, Ba, and Zn) may also be a biogenic indicator (İzci et al., 2013; Yılmaz-Usta et al., 2019).

It is commonly known that İznik had a successful industry of manufacturing glazed pottery (Kırmızı, 2004; Rice, 1987). The pottery glazes of İznik are characterized by alkaline bases s of tin and lead oxides. Moreover, lead oxide was commonly used as a coloring agent, especially in green and black glazes (Kırmızı, 2004). The high concentration of lead in the soil, and thereby Pb intoxication (Fleming, Blom, 2007) of the population can be considered as a reasonable possibility.

Another considerable subject to discuss is the high accumulation of As in the samples. The As percentage of the soil was calculated as being 19.74 ppm. The reference value expected in modern bone is below 1 ppm. For XRF and ICP-OES the calculated amount of As was also high; 93 ppm by XRF analysis, and 110 ppm by ICP-OES analysis. Rasmussen et al. (2009) claim that the As values of people from Nivaagaard were the result of a marine focused diet. Their initial hypothesis about the accumulation of As in the bones was that of diagenesis, with it originating from impragnated railway sleepers at a nearby railway track. However, soil samples analyzed at different levels disproved their initial hypothesis. In their study, toxicity of the marine animals and seaweed due to the content of As may be corollated with the accumulation in bones, and they also mentioned that As bound in organic forms is far less toxic than inorganic As (Rassmussen et al., 2009).

A high concentration of As is also present in the femurs of the İznik bone samples; femurs are considered to be more durable to diagenetic alteration than other skeletal elements. In the İznik case, an alternative approach to As accumulation rather than diagenesis must be considered.

CHAPTER 5

CONCLUSION

This study includes an archaeometric examination of 21 bones belonging to 19 individuals with different sexes, ages at death, and burial locations excavated from the İznik Roman Theatre. It also includes analysis of five soil samples taken from different parts of the site. of the analyses of the sampled material was conducted utilising several chemical and physical methods.

To understand the diagenetic pattern of the samples, several tests were applied according to the established protocols adapted from the literature including pH, electrical conductivity, and type of the soil analyses, the splitting factor, porosity, gravimetric analysis, and the elemental composition of the bones. The results indicate that the samples analysed in this study were well preserved, but also diagenetically altered to varying levels.

The elemental composition of the İznik bones was determined using XRF (x-ray fluorescence spectrometry) and ICP-OES (inductively coupled plasma optical emission spectrometry) methods of analysis.

Cortical bones (femora) and trabecular bones (costa) were examined separately. The elemental analysis focused on the matrix elements Ca and P, diagenesis related elements Mn, Fe, K, Pb, Al, U, Zr, and Y, and dietary elements Zn, Ba, Mg and Sr. To define uncontaminated bone matrix, the Ca/P mass ratio in the crystal structure of bone hydroxyapatite was calculated.

The Ca/P ratios calculated with the values obtained by XRF analysis were found to be higher than the values obtained from ICP-OES analysis. Although the Ca percentages calculated in the bone apatite have similar values, the P values differ according to the method used. It is important to keep in mind that the differences between the techniques were largely due to differences in the primary calibration standards used,

and the correction factors. However, ICP-OES and any laser ablation method are critically ahead for sub ppm levels of inorganic materials. Furthermore, in archaeology, the main application of energy dispersive XRF is for rapid identification and analysis of metals and their alloys.

The results of the Ca/P from ICP-OES analysis were very similar to those of the reference values. It is significant to find that the obtained results using this method are reliable. With regards to demographic variables such as sex and age at death, and bearing in mind that there is a small sample size, insufficient to obtain a statistical significance, the overall Ca and P values of the samples are slightly less than the reference values, most likely due to diagenetic alterations.

The elemental composition of the İznik bones demonstrated that nine elements (Cu, Pb, U, Al, K, Fe, Zr, Y and Mn) were found in lower amounts in the bone apatite than in the soil. These elements can be considered as accumulative contamination due to diagenesis. With the exception of uranium, it is not unsuitable to conclude that all of these elements were replaced with Ca ions in the apatite. The correlation between these elements was also analyzed by PCA to verify the results.

The PCA analysis of the results from ICP-OES analysis was repeated to reexamine the differences of elemental composition due to location. The results were in correlation with the historical literature about İznik's Roman Theatre, which was used as a deposit for waste materials. The toxic elements considered as contaminants in the bone apatite were reconsidered due to this factor. However, the As values in the soil were surprisingly low, with respect to its presence in bone. According to the literature, As accumulation can possibly be considered as an indicator for a marine based diet.

Since İznik is a well-known location for the manufacture of glazed pottery, and the use of lead oxides as a coloring agent, as well as aglaze stabilizer, the Pb contamination in the bone apatite must be considered by the archaeologists and anthropologists. Although the amount of Pb in the soil samples represents a post

mortem alteration, the amount of Pb in both the bone apatite and soil matrix is considerably high rather than the values for other sites of the same period.

Before drawing any conclusions about any concept of science, in our case a metric approach to archaeology and anthropology, the data needs to be established. Although the elemental analysis of fossil bones has been conducted for over half a century in the world, research here in Turkey is still not extensive, and can be considered to be a work still in progress. Hopefully, this study will provide an important set of data for archaeology, and develop increasing interest in archaeometric studies in Turkey.

REFERENCES

ADAMSON A.W., T. A. ADAMSON, A. P. GAST (1997). "Physical Chemistry of Surfaces." Wiley, 6th Ed. New York, 1997.

AKYOL A.A. (2009). "Material Characterization of Ancient Mural Paintings and Related Base Material : A Case Study of Zeugma Archaeological Area." *Ph.D Thesis* M.E.T.U. Ankara, 2009.

BEHRENSMEYER A.K, A.P. HILL (1980). "Fossils in the Making: Vertebrate Taphonomy and Palaeoecology." *University of Chicago Press*: Chicago.

BERLIN, ADAMS (2017). "Production Ergonomics: Designing Work System to Support Optimal Human Performance." *Ubiquity Press: London* 15-48.

BROADUS E.A. (1990) "Physiologic functions of Calcium, Magnesium and Phosphorus." *Primer on the Metobolic Bone Diseases and Disorders of Bone Mineral Metabolism*. Keyselville CA 29-30.

CZEPIRSKI, L.; BALYS, M. R.; KOMOROWSKA-CZEPIRSKA, E. (2000). "Some generalization of Langmuir adsorption isotherm". *Internet Journal of Chemistry*. **3** (14).

DEMİRCİ Ş., N. KAYATÜRK (1991). "Chemical Analysis of Some Fossil Bones." 111-118.

DEMİRCİ Ş., N. KAYATÜRK (1989)." İstanbul, yarımburgaz mağarasından çıkan bazı kemiklerin analizi." *5. Arkeometri kazı sonuçları toplantısı* 141-146.

DIGANGI E.A., M.K. MOORE (2013). "Introduction to Skeletal Biology". DiGangi and M.K. Edt. Academic Press. Chapter 1. 1-27.

DURSUN, H., M.Y. DİZDAR, Ş. KIRIŞTIOĞLU, İ. ÖZCAN, Y. HAMURKAR, (2008). "Toprak ve Arazi Sınıflaması Standartları Teknik Talimatı ve İlgili Mevzuat", *Tarım ve Köyişleri Bakanlığı Tarımsal Üretim ve Geliştirme Genel Müdürlüğü Yayını*, Ankara, 70.

EISSENSTAT Ç. (1994). "Dietary Reconstruction from Fossil Bones by means of Trace Element Analysis." *Master Thesis, Graduate School of Natural and Applied Science.* M.E.T.U. Ankara, 38-47

ERDAL S.Y. (1996). "İznik Geç Bizans Dönemi İnsanlarının Çene ve Dişlerinin Antropolojik Açıdan İncelenmesi." Hacetttepe Üniversitesi Antropoloji Anabilim Dalı Doktora Tezi Ankara, 1996.

EYİCE S. (1991). "İznik Tarihçesi ve Eski Eserleri." *Sanat Tarihi Araştırmaları Dergisi* İstanbul.

EZZO J. A. (1992). "Dietary Change and Variability at Grasshopper Pueblo, Arizona." *Journal of Anthropological Archaeology* XI 3: 219-289.

EZZO J. A. (1994a). "Putting the 'Chemistry' back into Archaeological Chemistry Analysis: Modelling Potential Paleodietary Indicators." *Journal of Anthropological Archaeology* 13:1-34.

EZZO J.A. (1994b). "Zinc as a Paleodietary Indication: An Issue of Theoretical Validity in Bone-Chemistry Analysis" *American Antiquity*, 59: 606-621.

FLEMING D.E.B., D.E. BLOOM (2007). "Evidence for Lead Diagenesis in Ancient Bones of the Southern Andes." *Nuclear Instruments and Methods in Physics Research* B 263:41-45.

FRIEDEN , E. (1972). “The Chemical Elements of Life” N. KRETCHMER and W. VAN B. ROBERTSON (Eds.), Human Nutrition: Readings from Scientific American. San Fransisco: W.H. Freeman. 148-155.

GARTLEY K.L. (2011). “Recomended Methods for Measuring Soluble Salts in Soil.” *U.S.S.L. Cooperative Bullettin* Washington D.C. 493:87-94

GILL-KING H. (1997). “Chemical and ultrastructural aspects of decomposition.” In Forensic Taphonomy: *The Postmortem Fate of Human Remains*, Haglund WD, Sorg MH (eds). CRC Press: Boca Raton; 93–108.

GOFFER, Z. (1980). Archaeological Chemistry: A Source Book on the Application of Chemistry to Archaeology. New York: John Wiley & Sons.

HEDGES R.E.M., A.R. MILLARD (1995). “Bones and Groundwater: Towards the Modelling of Diagenetic Processes.” *Journal of Archaeological Science* (1995) 22: 155-164

HEDGES R.E.M. (2002). “Bone Diagenesis: An Overview of Processes.” *Archaeometry* 44:319-328.

HEDGES R.E.M. (1976). “Pre-Islamic Glazes in Mesopotamia-Nippur.” *Archaeometry* 18:209-238.

İZCİ Y., S. KAYA, O. ERDEM, C.AKAY, C. KURAL, B. SOYKUT, O. BAŞOĞLU, Y. ŞENYURT, S. KILIÇ, Ç. TEMİZ (2013). “Paleodietary analysis of Human Remains from a Hellenistic-Roman Cemetery at Camihöyük, Turkey” *,* Volume 2013.

JURKIEWICZ A., D. WIECHULA, R. NOWAK, T. GAZDZIK, K. LOSKA, (2004). “Metal Content in Femoral Head Spongious Bone of People in Regions of Different Degrees of Environmental Pollution in Southern and Middle Poland.” *Ecotoxicology and Environmental Safety* 59, 95-101.

JOWSEY J., D. PILL, (1977). “Metabolic Diseases of Bones” *W. B. Saunders Company* Philadelphia, London, Toronto, 3-19.

KACAR B. (2009). “Toprak Analizleri.” *Nobel Yayın Dağıtım*, Ankara 2009 55-67.

KATZENBERG M.A., R.G. HARRISON (1997). “What’s in a Bone? Recent Advances in Archaeological Bone Chemistry.” *Journal of Archaeological Research*, Vol. %, No. 3.

KAYAN İ., (1988). “Arkeolojik Jeomorfoloji Açısından Yenişehir ve İznik Havzalarının Çevre Özellikleri.” *5. Kazı Araştırma Sonuçları Toplantısı II*, Kültür ve Turizm Bakanlığı Yayınları: 211-219.

KILIÇKAYA A., (1981). “Nicaea, Nikaia.” *İznik Tarihi ve Eski Eserleri Kılavuzu*, Eser Matbaası, Bursa.

KIRMIZI B. (2004). “ An Archaeometric Application to a Group of Ottoman Ceramics from İznik” Unpublished Masters Thesis M.E.T.U 2004.

LACHOWICZ J.I., S. PALOMBA, P. MELONI, M. CARBONI, G. SANNA, R. FLORIS, V. PUSCEDDU, M. SARIGU (2016). “Multi Analytical Tecnique Study of Human Bones from an Archaeological Discovery.*” Journal of Trace Elements in Medicine and Biology* 40:54-60

LAMBERT J.B., C.B. SZPUNAR, J.E. BUIKSTRA (1979). “Chemical Analysis of Excavated Human Bone from Middle and Late Woodland Sites” *Archaeometry* 21, 2, 115-129.

LAMBERT J.B., S.M. VLASAK, A.C. THOMETZ, J.E. BUIKSTRA (1982). “A comparative Study of the Chemical Analysis of: Ribs and Femur in Woodland Populations.” *American Journal of Physical Anthropology* 9: 289-294.

LAMBERT J.B., S.V. SIMPSON, C.B. SPUZNAR, J.E. BUIKSTRA (1984). "Ancient Human Diet from Inorganic Analysis of Bone." *Acc. Chem. Res.* 17, 298-305.

LOPEZ-COSTAS O., LANTES-SUARES O., CORTIZAS A.M. (2016). "Chemical Compositional Changes in Archaeological Human Bone Due to Diagenesis: Types vs Soil Environment." *Journal of Archaeological Science* 67; 43-52

MAYS S. (1988). The Archaeology of Human Bones. London and New York: Routledge.

MAYS S. (1998). "The Archaeology of Human Bones." Routledge: London.

MIDDLETON J. (1844). "Comparative Composition of Recent and Fossils Bones." *Lon. and Ed. Phil Mag.* JULY 1884, p.14.

MILLARD A., (2006). "Comment on Martinez-Garcia et al. Heavy Metals in Human Bones in Different Historical Epochs. *The Science of the Total Environment* 348, 51-72.

MILLER E.J. (1985). "Recent Information on the Chemistry of Collagens". *Chemistry and Biology of the Mineralized Tissues*. EBSCO Media Birmingham 83-99.

NIELSEN-MARSH C.M., R.E.M. HEDGES (2000). "Patterns of Diagenesis in Bone I: The Effects of Site Environments." *Journal of Archaeological Science* 27:1139-1150.

NRIAGU J.O., P. BHATTACHYRA, A.B. MUKHERJEE, J. BUNDSCHUH, R. ZAVENHOVEN, R.H. LOEPPERT (2007). "Arsenic in Soil and Groundwater: An Overview. *Trace Metals and Other Contaminations in the Environment, Vol. 9.* Elsevier B.V., Oxford pp.3-60.

NIELSEN-MARSH C.M., GERNAEY A.M., TURNER-WALKER G, HEDGES R.E.M., PIKE A.W.G., COLLINS M.J. (2000). "The chemical degradation of bone." *Human Osteology in Archaeology and Forensic Science*, Cox M, Mays S (eds). Greenwich Medical Media: London; 439–454.

OLESIAK S. E., M. SPONHEIMER, J.J. EBERLE, M.L. OYEN V.L. FERGUSON (2010). "Nanochemical Properties of Modern and Fossil Bone" *Palaeogeography, Palaeoclimatology, Palaeoecology* 289; 25-32.

ÖZBEK M. (1990). "İznik Geç Bizans Çağı İskeletlerinde Hastalık ve Yaralanma İzleri." *Belleten* 54:39-54

ÖZDEMİR K. (2008). "İkiztepe Tunç Çağı Topluluğunda Element Analizleriyle Beslenme Yapısının Belirlenmesi." Unpublished PhD. Thesis Hacettepe Uni.

ÖZDEMİR K., Y.S. ERDAL (2009). " Erken Tunç Çağı İkiztepe Topluluğunda Stronsiyum-Kalsiyum oranı ile Sütten Kesme Yaşının Belirlenmesi." *Çocuk Sağlığı ve Hastalıkları Dergisi,* 52:128-140.

ÖZDEMİR K., Y.S. ERDAL, Ş. DEMİRCİ (2009). "Arsenic Accumulation on the Bones in the Early Bronze Age İkiztepe Population, Turkey." *Journal of Archaeological Science* 37:1033-1041.

PARKER R.B., H. TOOTS (1970). "Minor elements in Fossil Bone" *Geological Society of America Bulletin* 81:925-932.

PARKER R. B., H. TOOTS (1980). "Trace Elements in Bones as Paleobiological Indicators." A.K. BEHRENSMEYER and A. P. HILL (Eds) *Fossils in the Making Chicago*: Chicago University Press. 197-207.

PATE F.D. (1994) “Bone Chemistry and Paleodiet”. *Journal of Archaeological Method and Theory*, Vol 1, No.2. 161-209.

PATE F.D., J.T. HUTTON,(1988). “ The Use of Soil Chemistry Data to Address Post- Mortem Diagenesis in Bone Mineral.” *Journal of Archaeological Science*, 15:729-739.

PATE F.D., J.T. HUTTON, K. NORRISH (1989). “Ionic Exchange Between Soil Solution and Bone: Toward a Predictive Model.” *Appl. Geochem*. 4, 303-316.

POLLARD M., C. BATT, B. STERN, S.M.M. YOUNG (2007). “Analytical Chemistry in Archaeometry.” *Cambridge Manuals in Archaeology*. Cambridge University Press, 47-123.

POSNER A.S. (1969). “Crystal Chemistry of Bone Mineral. “*Physical Review* 49: 760-792.

RASMUSSEN K.L., J.L. BOLDSEN, H.K. KRISTENSEN, L. STKYTTE, K.L. HANSEN, L. MOLHOLM, P.M. GROOTES, M. NADEAU, K.M.F. ERIKSEN (2008). “Mercury Levels in Danish Medieval Human Bones.” *Journal of Archaeological Science* 35:225-230.

RICE P.M., (1987). “Pottery Analysis- A Source Book.” *University of Chicago Press*, Chicago.

SILLEN A. (1986). “Biogenic and Diagenic Sr/Ca in Plio-Pleistoscene Fossils of the Omo Shungura Formation.” *Paleobiology* 12:312-323

SILLEN A., J. C. SEALY and N. J. VAN DER MERWE (1989).”Chemistry and Paleodietary Research: No More Easy Answers.” *American Antiquity* 54: 504-512.

SILLEN A., J. PARKINGTON (1996). “Diagenesis of Bones from Eland’s Bay Cave.” *Journal of Archaeological Science* 23:535-542.

STEEELE D.G., C.A. BRAMBLETT (1998). *Anatomy and Biology of the Human Skeleton.* Texas A&M University Press.

TURNER-WALKER G. (2008). “The chemical and Microbial Degradation of Bones and Teeth, “Advances in Human Paleopathology” Editor(s): Ron Pinhasi, Simon Mays. John Wiley& Sons, Ltd. ISBN: 978-0-470-03602-0.

TORTORA G., M. NIELSEN (2012). “Principles of Human Anatomy”. 12. Edition. John Wiley&Son Inc.

TANRIVERDİ Z. (2018). “Archaeometric Investigation of the Construction Materials of Roman (Caracalla) Bath in Anakara.” Ph. D. Thesis M.E.T.U. Ankara, 2018.

UNDERWOOD, E.J. (1977). Trace Elements in Human and Animal Nutrition. *New York:Academic Press*.

WEINER J.S., O. BAR-YOSEF (1990). “States of Preservation of Bones from Prehistoric sites in the Near East: a Survey.” Journal of Archaeological Science 17:187-196.

WEINER S., H.D. WAGNER (1998). “THE MATERIAL BONE: Structure-Mechanical Function Relations.” *Annual Review of Material Science* Vol. 28:271-298.

VASS A.A. (2001). “Beyond the Grave – Understanding human decomposition.” *Microbiology Today* 28:190-193.

VAN OLPHEN H. (1966). “An Introduction to Clay Colloid Chemistry.” Interscience (Wiley) New York, 1996.

YALMAN B., (1983). “İznik Tiyatro Kazısı 1981.” *IV.Kazı Sonuçları Toplantısı -Ankara 1982*, Kültür ve Turizm Bakanlığı Yayınları, Ankara: 229-235.

YALMAN B., (1986). “İznik Tiyatro Kazısı 1985.” *VII. Kazı Sonuçları Toplantısı -Ankara 1985*, Kültür ve Turizm Bakanlığı Yayınları, Ankara: 579-595.

YALMAN B., (1988). “İznik Tiyatro Kazısı 1986.” *IX. Kazı Sonuçları Toplantısı -Ankara 1987*, Kültür ve Turizm Bakanlığı Yayınları, Ankara: 299-328.

YALMAN B., (1989). “İznik Tiyatro Kazısı 1987.” *X. Kazı Sonuçları Toplantısı -Ankara 1988*, Kültür ve Turizm Bakanlığı Yayınları, Ankara: 339-382.

YALMAN B., (1990). “İznik Tiyatro Kazısı 1988.” *XI. Kazı Sonuçları Toplantısı -Antalya 1989*, Kültür ve Turizm Bakanlığı Yayınları, Ankara: 301-324.

YALMAN B., (1991). “İznik Tiyatro Kazısı 1989.” *XII. Kazı Sonuçları Toplantısı -Ankara 1990*, Kültür ve Turizm Bakanlığı Yayınları, Ankara: 379-404.

YALMAN B., (1992). “İznik Tiyatro Kazısı 1990.” *XIII. Kazı Sonuçları Toplantısı -Çanakkale 1991*, Kültür ve Turizm Bakanlığı Yayınları, Ankara: 377-402.

YALMAN B., (1993). “İznik Tiyatro Kazısı 1991.” *XIV. Kazı Sonuçları Toplantısı -Ankara 1992*, Kültür ve Turizm Bakanlığı Yayınları, Ankara: 181-203.

YILMAZ-USTA N.D., O. BAŞOĞLU, Y. İZCİ, O. ERDEM, C. KURAL, (2019). “ Iasos (Erken Bizans) ve Camihöyük (Helenistik-Roma) Kazıları İskelet Toplulukları Üzerinde Karşılaştırmalı Element Analizi” *Antropoloji* 37:7-14.

ZAPATA J., C. PEREZ-SIRVENT, M.J. MARTINEZ-SANCHEZ, P. TOVAR (2006). “Diagenesis, not Biogenesis: Two Late Roman Skeletal Examples.” *Science of the Total Environment* 369;357-368

APPENDICES

A. Bone Samples

Figure 0.1. ITK 88 43/10

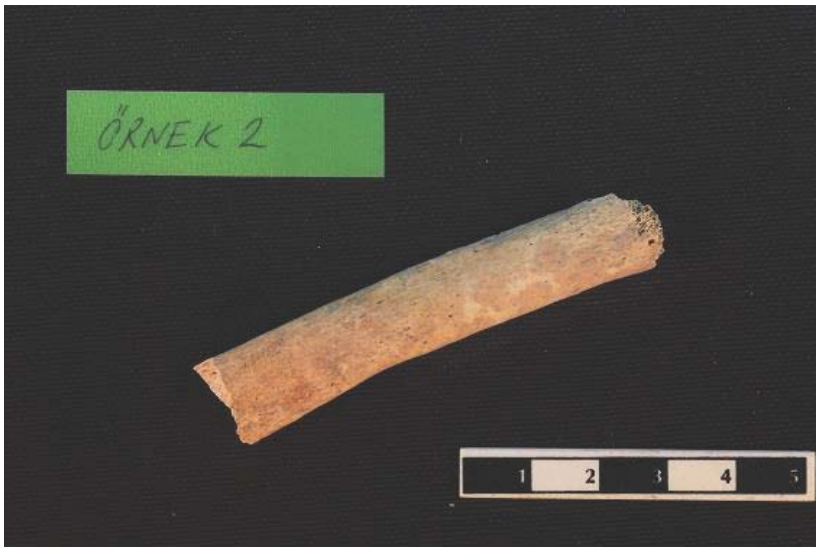

Figure 0.2. ITK 88 41-43/6

Figure 0.3. ITK 41-43/1

Figure 0.4. ITK 89 53/9

Figure 0.5. ITK 89 53/26

Figure 0.6. ITK 89 53/30

Figure 0.7. ITK 90 57/3A

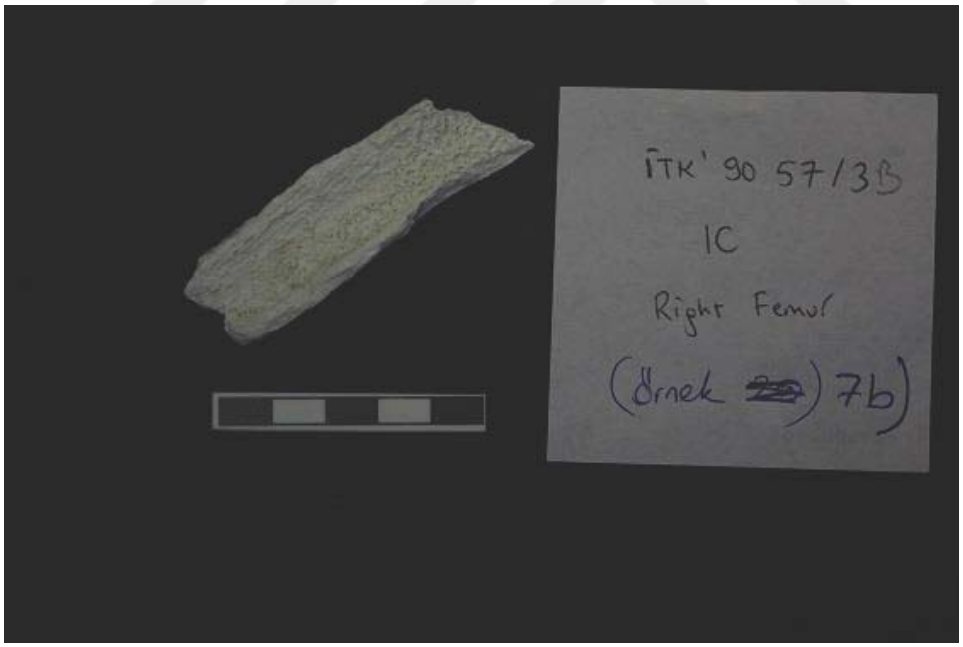

Figure 0.8. ITK 90 57/3B

Figure 0.9. ITK 89 51/24

Figure 0.10. ITK 90 58/7

Figure 0.11. ITK 90 58/3

Figure 0.12. ITK 90 57/11

Figure 0.13. ITK 90 57/8

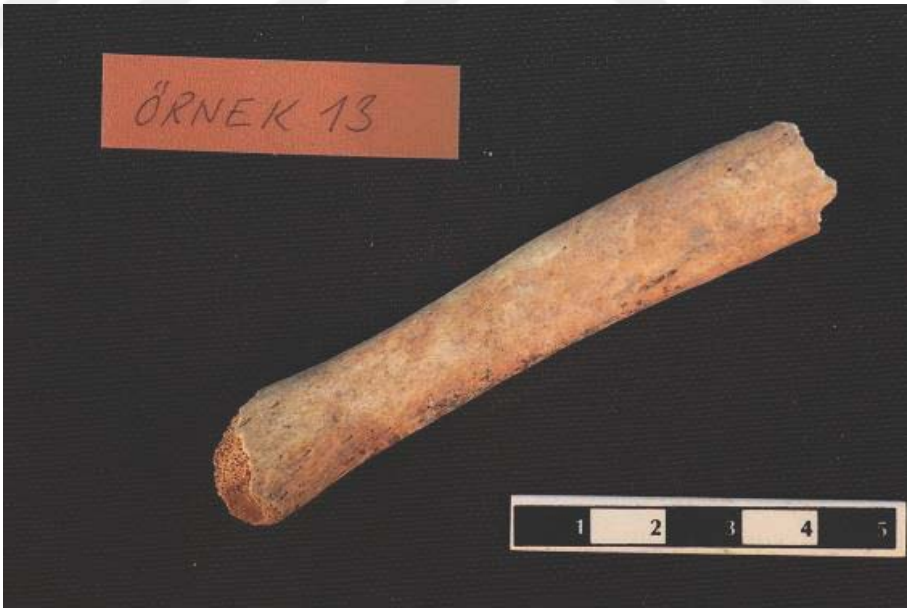

Figure 0.14. ITK 88 43/21

Figure 0.15. ITK 88 43/13

Figure 0.16. ITK 88 43/3

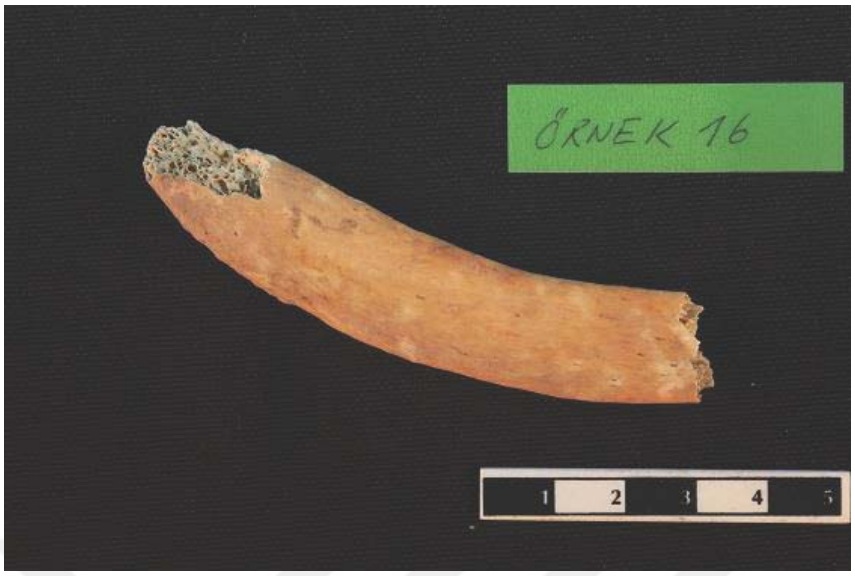

Figure 0.17. ITK 89 41/2

Figure 0.18. ITK 89 53/3

Figure 0.19. ITK 89 53/6

Figure 0.20. ITK 90 58/5A

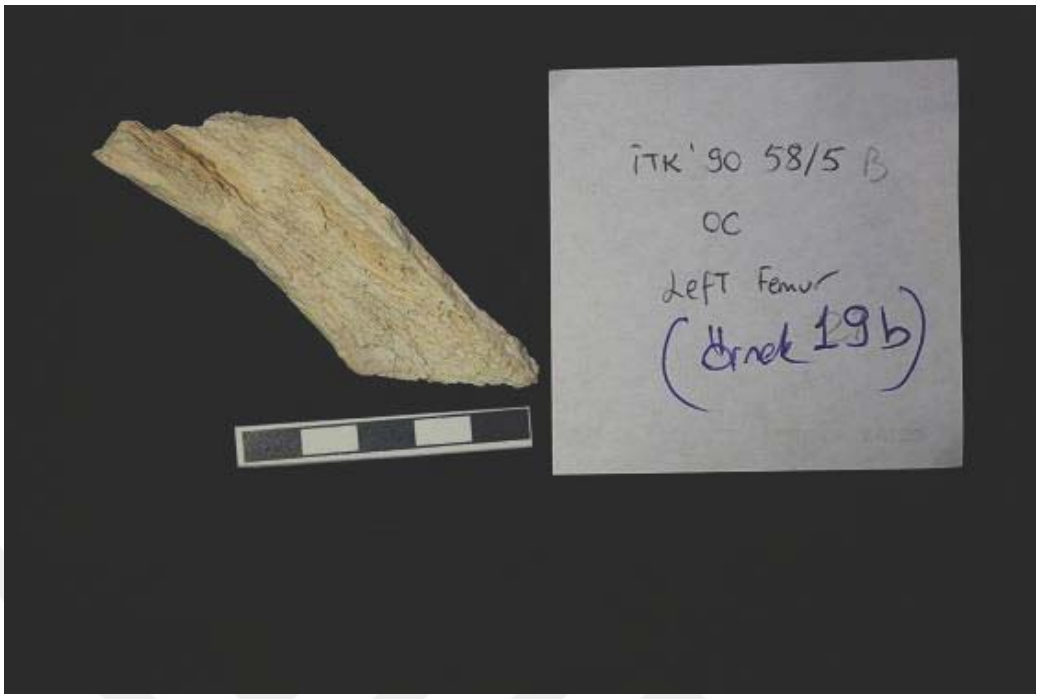

Figure 0.21. ITK 90 58/5B

B. TGA ANALYSIS

SAMPLE 1

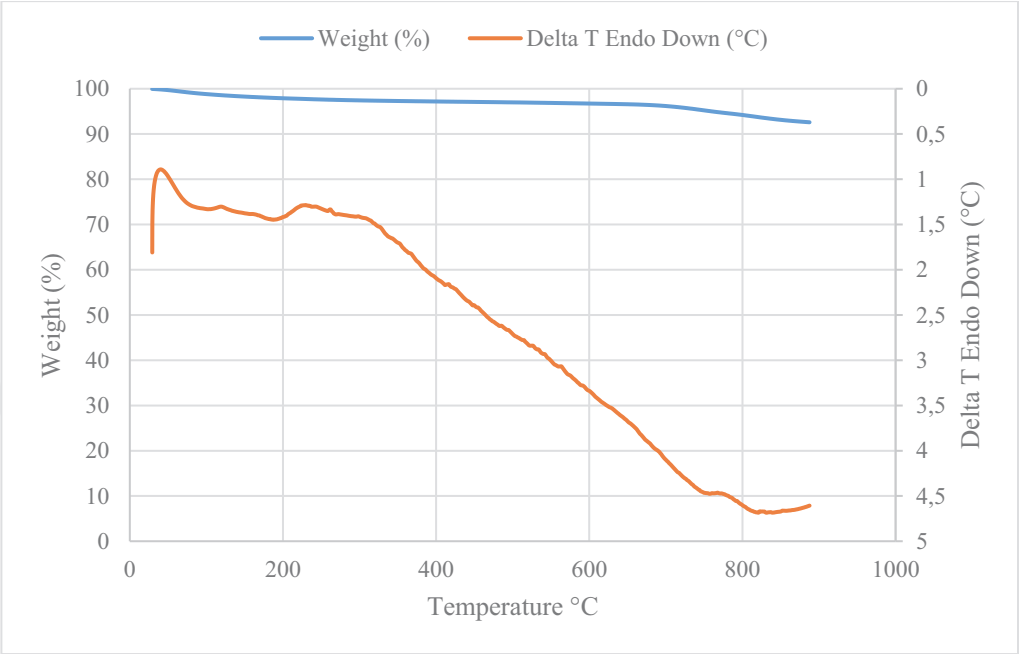

SAMPLE 2

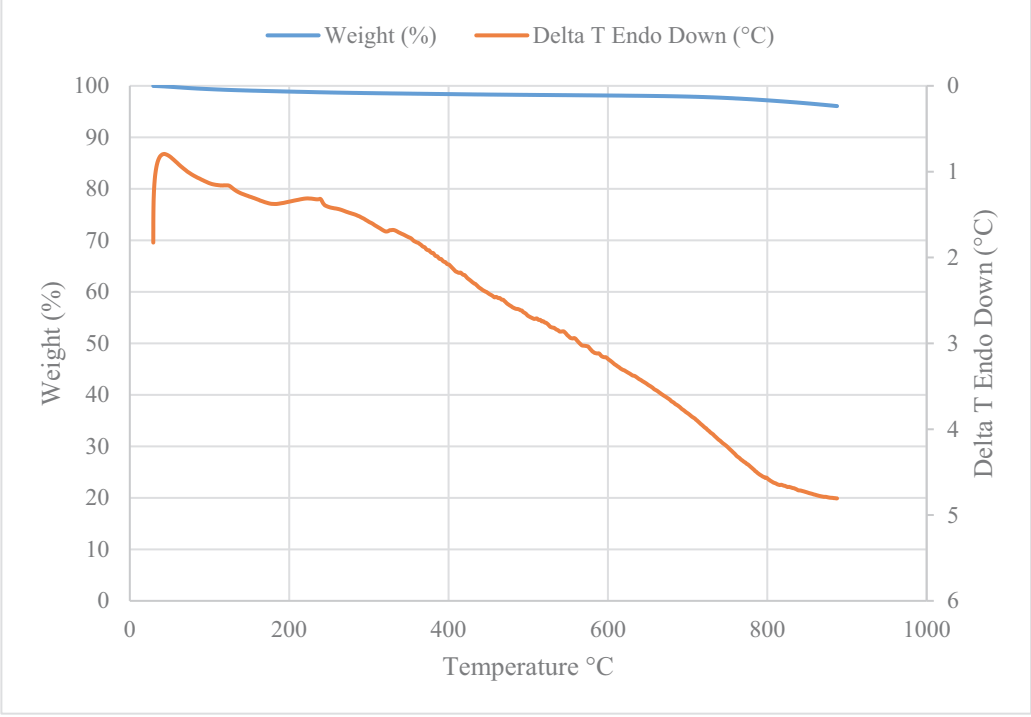

SAMPLE 3

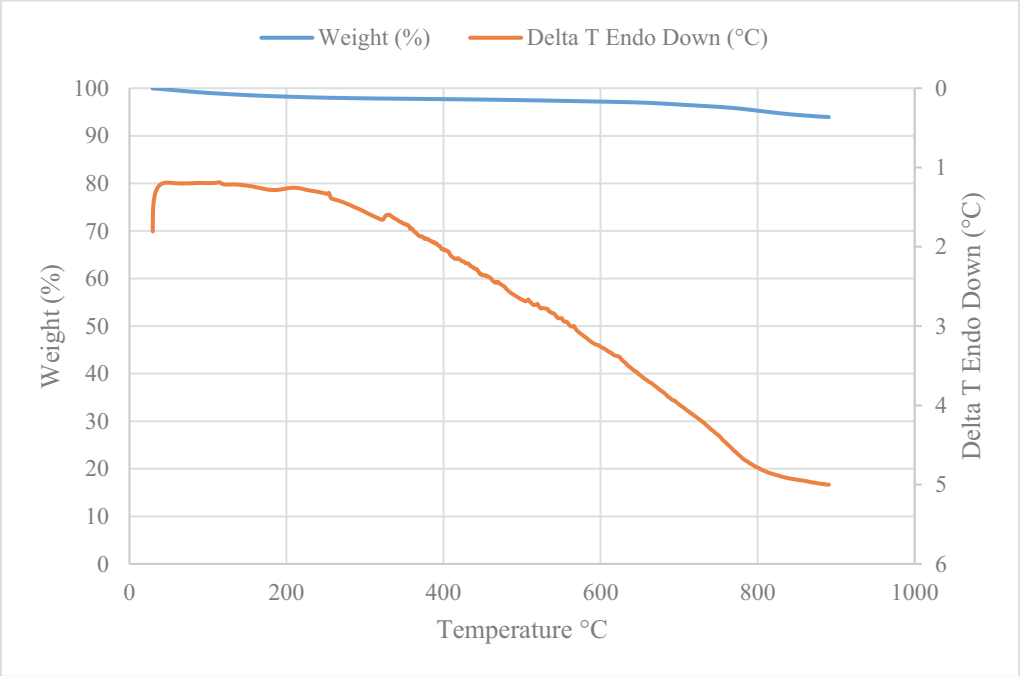

SAMPLE 4

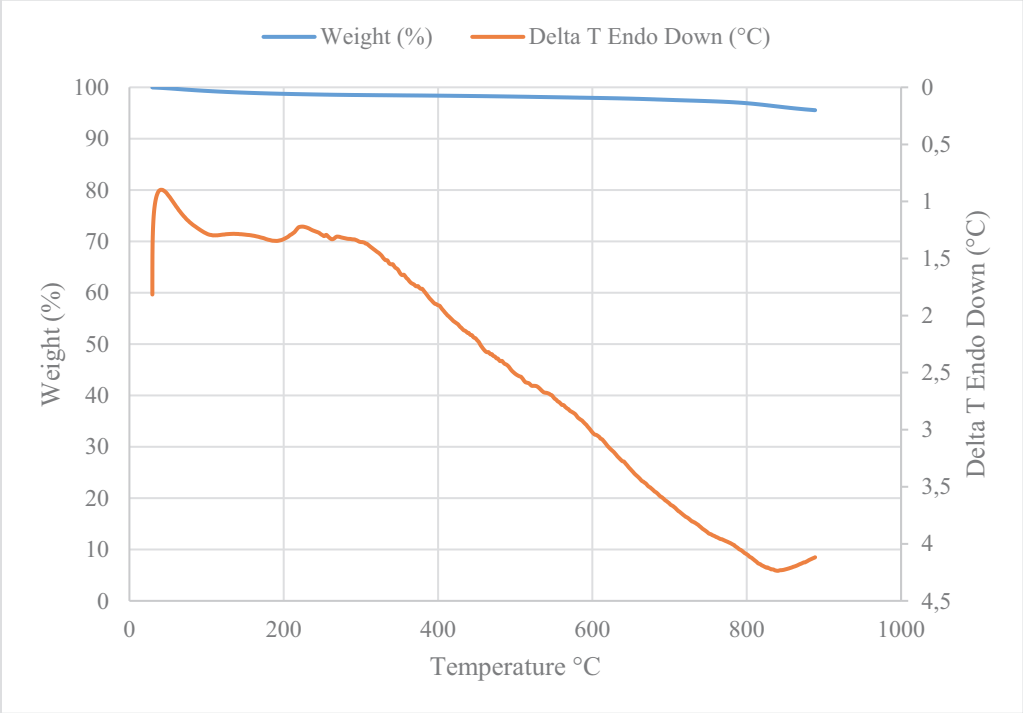

SAMPLE 5

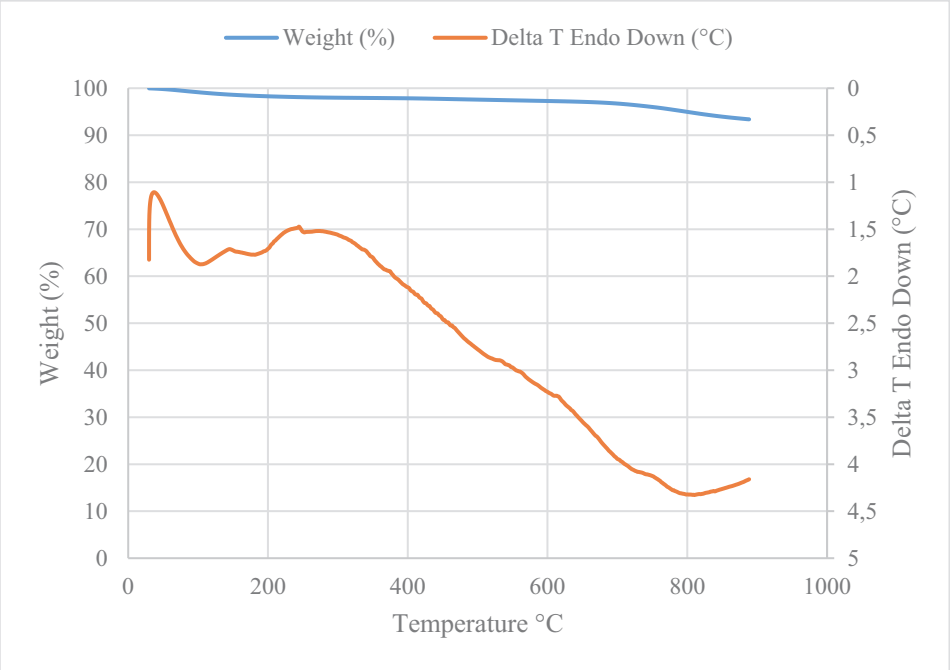

SAMPLE 6

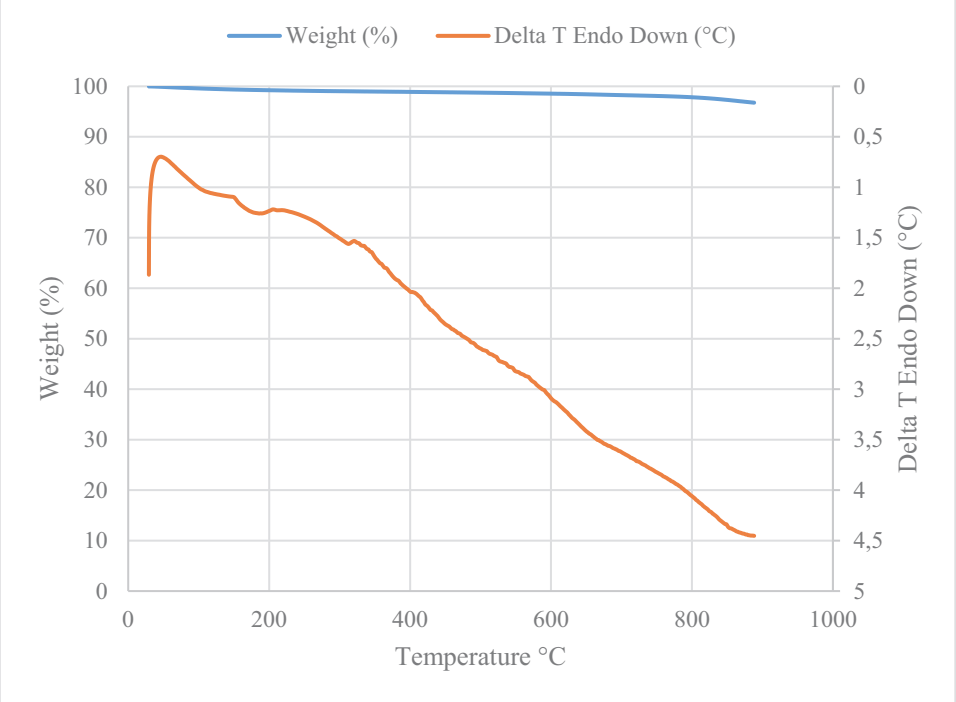

SAMPLE 7A

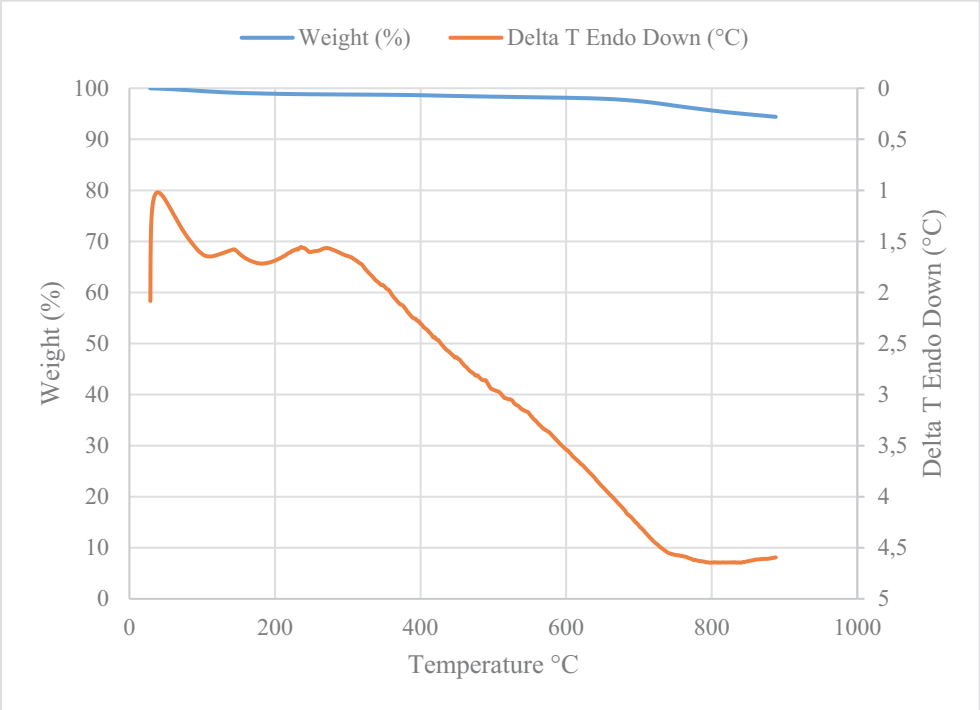

SAMPLE 7B

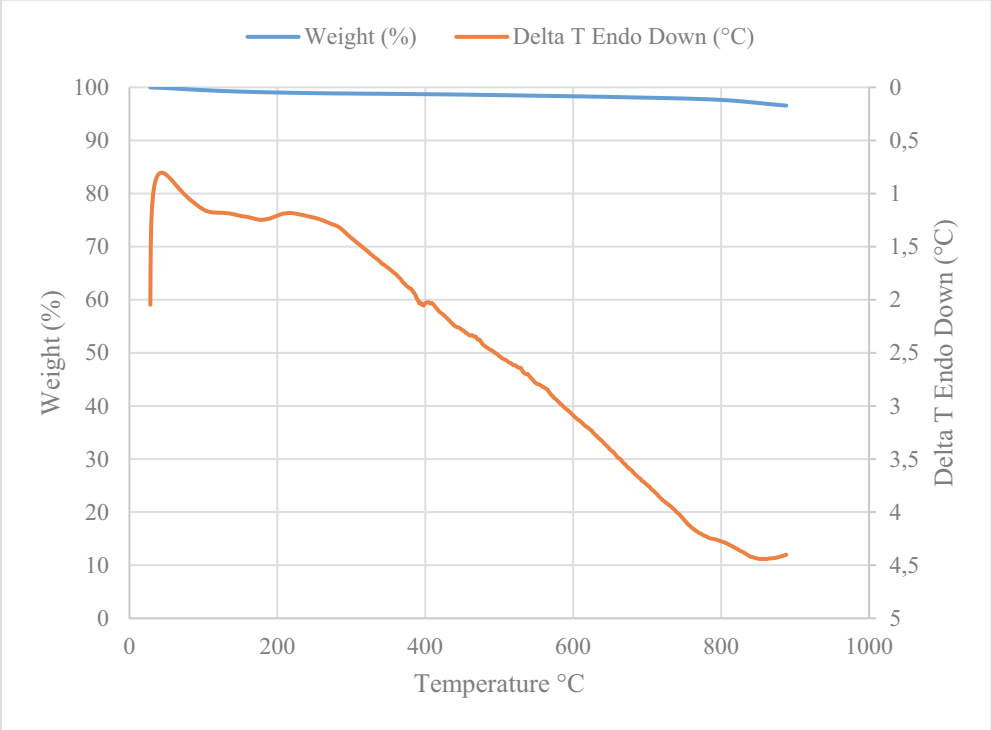

SAMPLE 8

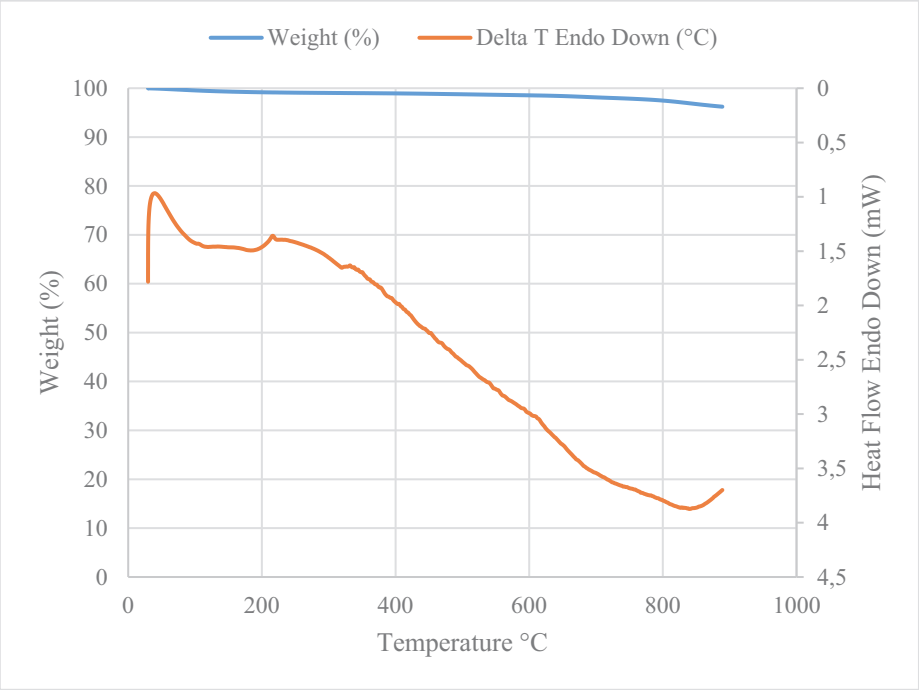

SAMPLE 9

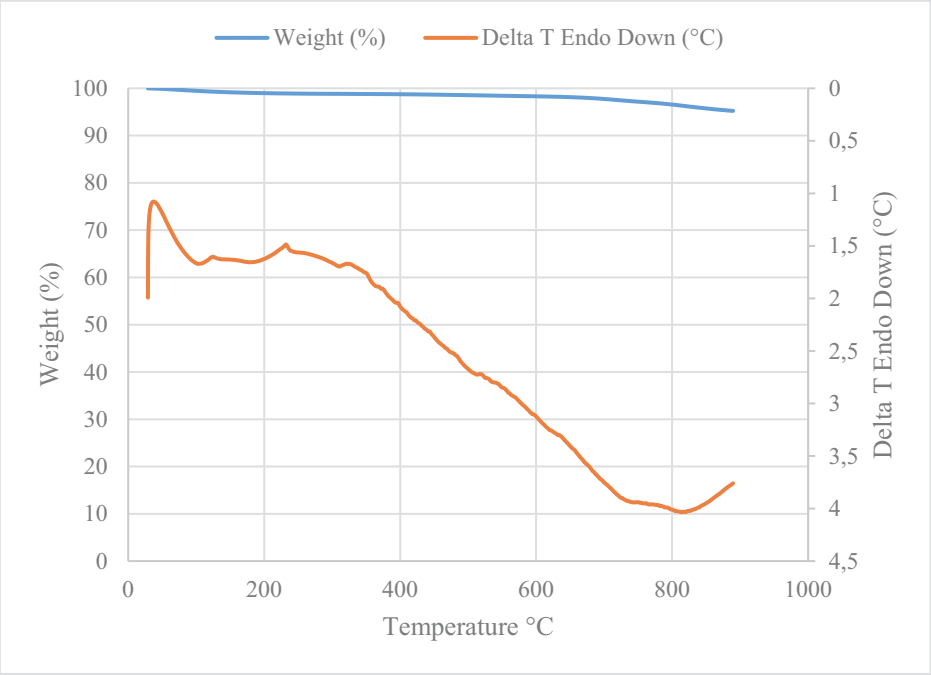

SAMPLE 10

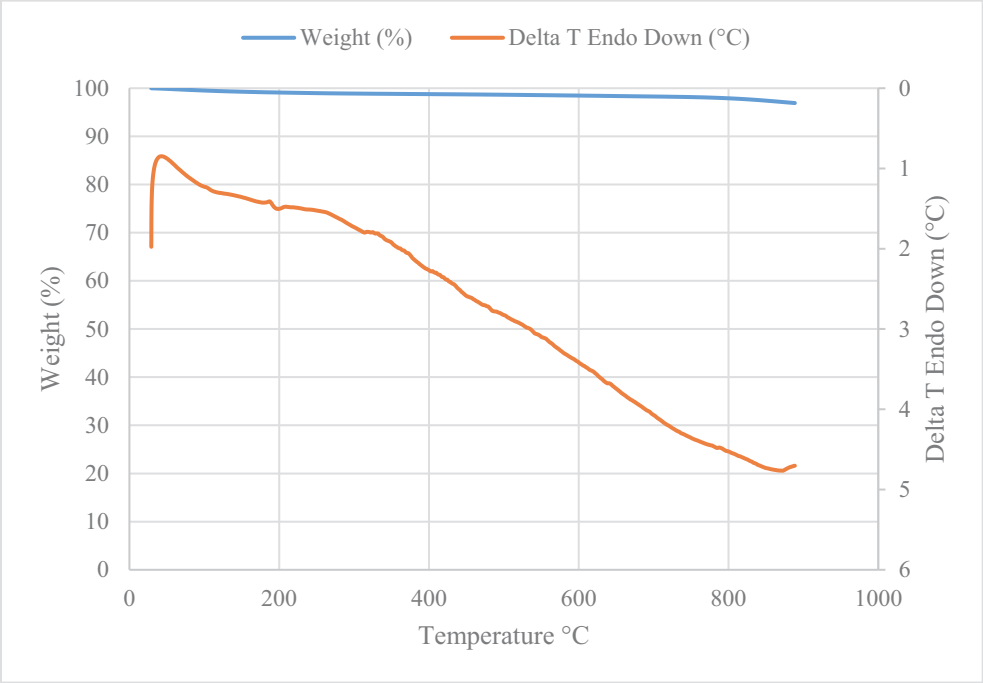

SAMPLE 11

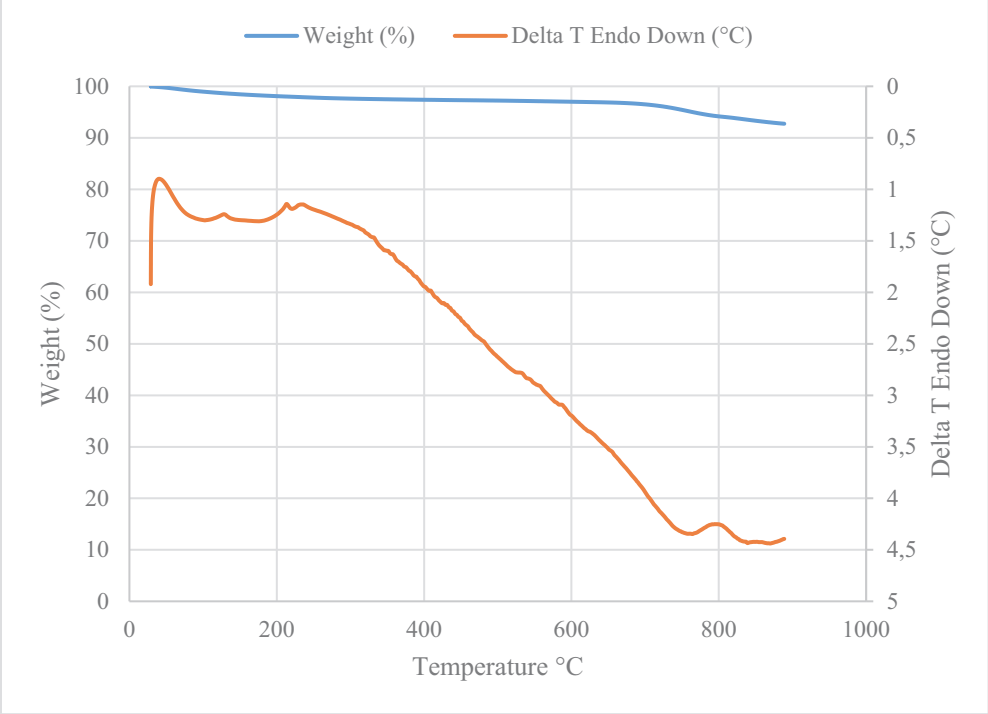

SAMPLE 12

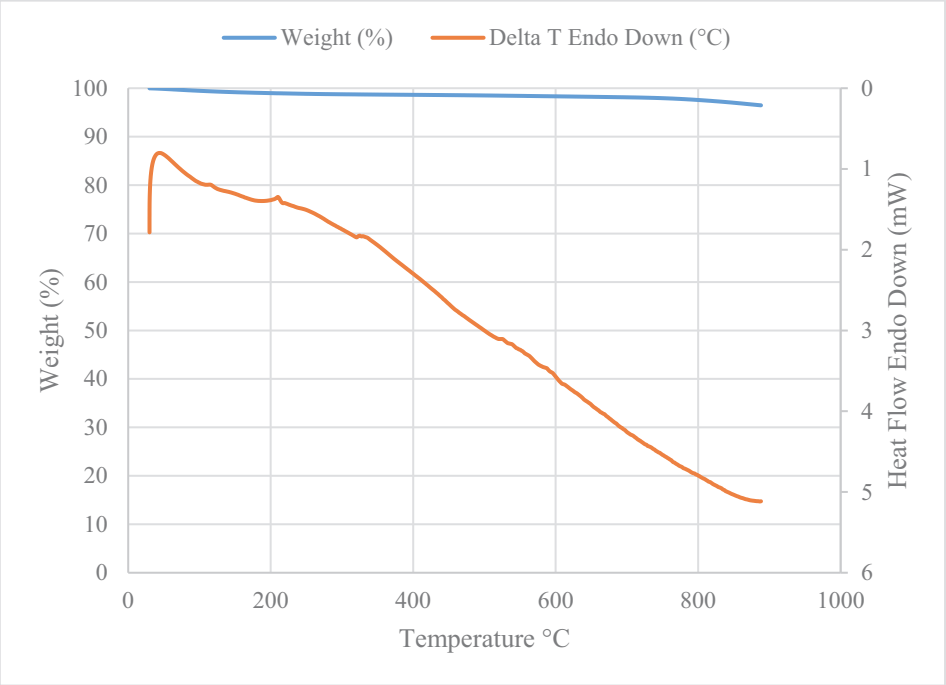

SAMPLE 13

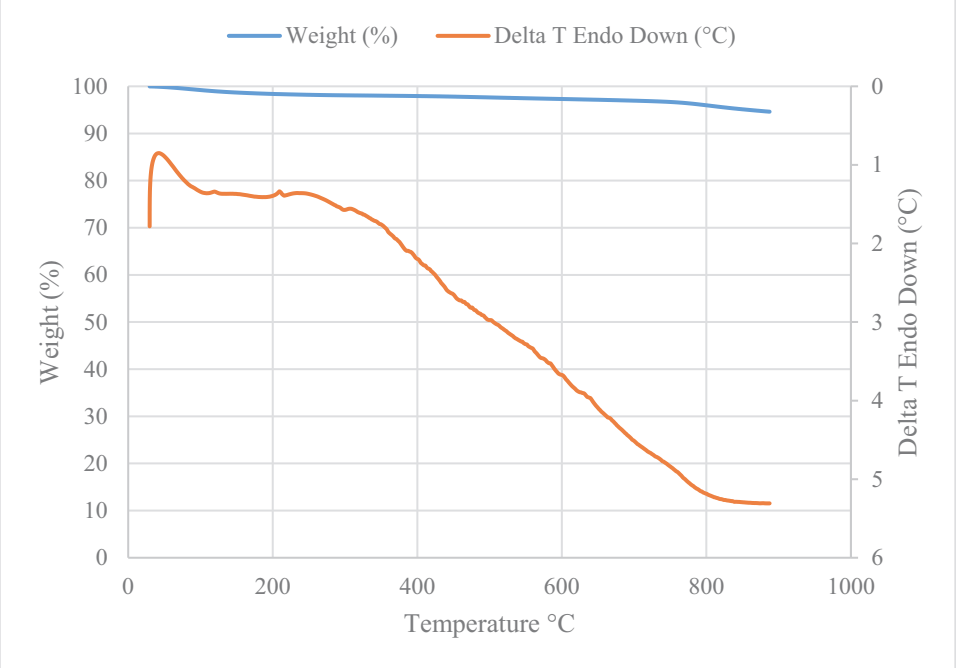

SAMPLE 14

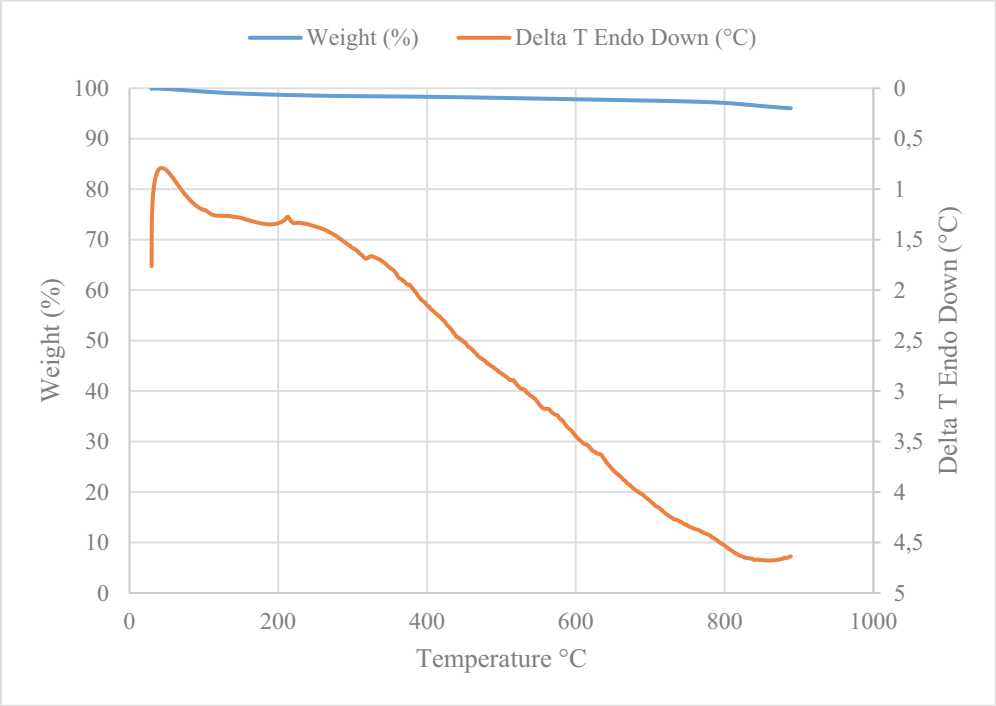

SAMPLE 15

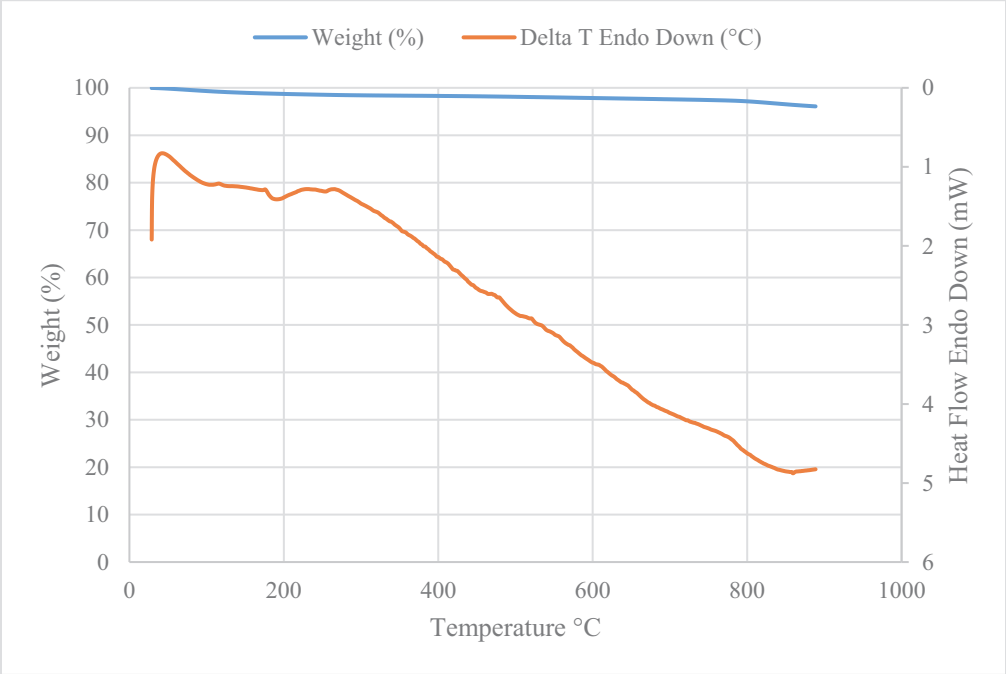

SAMPLE 16

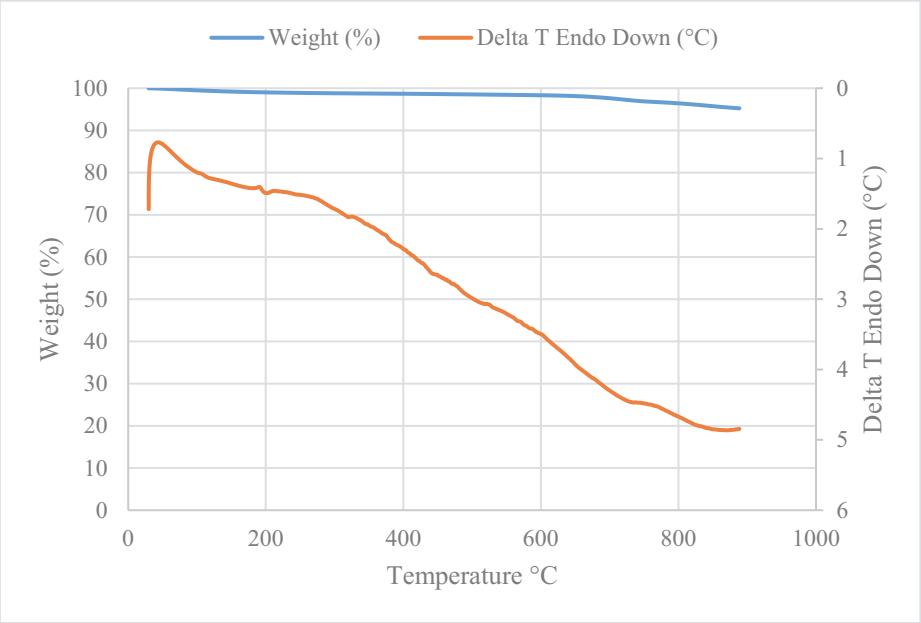

SAMPLE 17

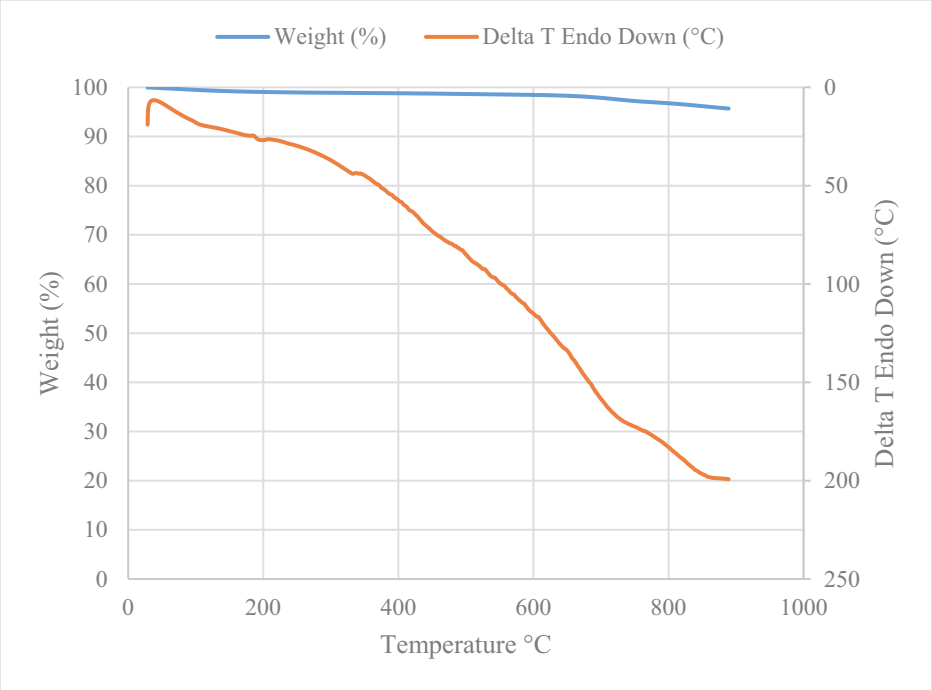

SAMPLE 18

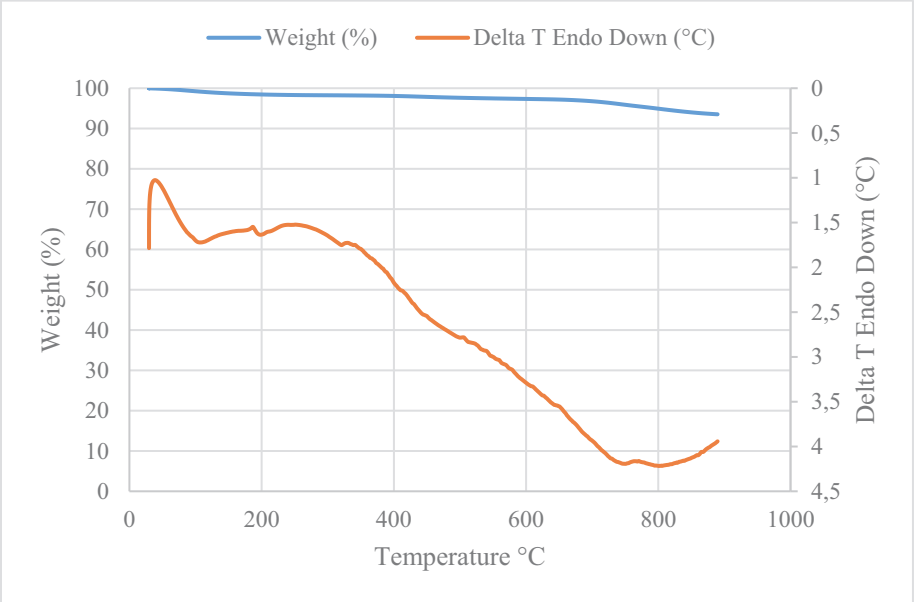

SAMPLE 19A

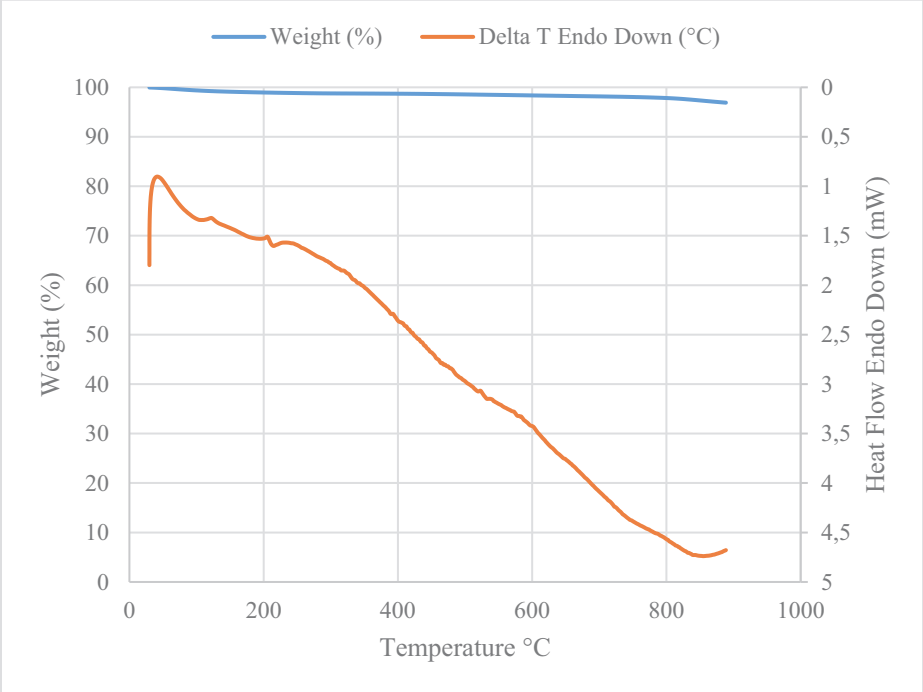

SAMPLE 19B

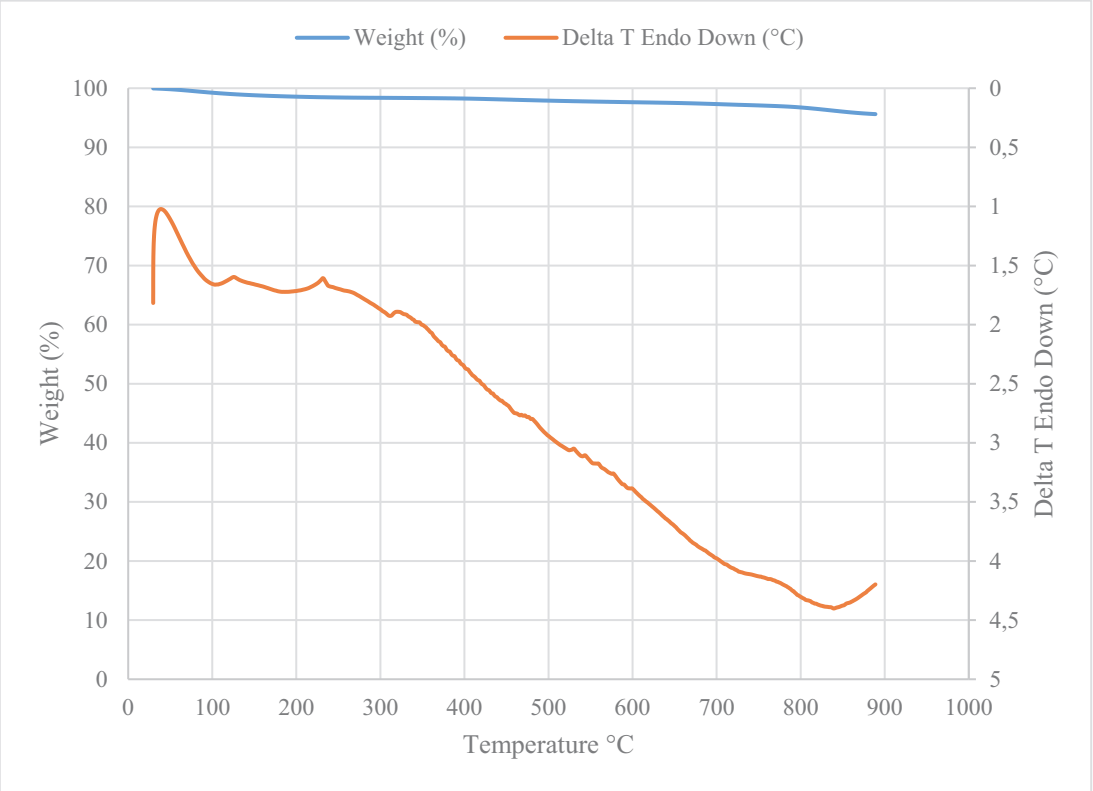
Weight (%)
Delta T Endo Down (°C)
100
90
80
70
60
50
40
30
20
10
0
0
0,5
1
1,5
2
2,5
3
3,5
4
4,5
5
0
100
200
300
400
500
600
700
800
900
1000
Temperature °C
Weight (%)
Delta T Endo Down (°C)

CURRICULUM VITAE

PERSONAL INFORMATION

Surname, Name	: Aksoy, Uğur Bülent
Nationality	: Turkish (TC)
Date and Place of Birth	: 12 July 1974, İstanbul
Phone	: +90 5359372727
E-mail	: e075485@metu.edu.tr

EDUCATION

Degree	Institution	Year of Graduation
MS	METU Archaeometry	2005
BS	METU Dept. of Physics	2002
High School	Kadıköy Anadolu High School, İstanbul	1992

WORK EXPERIENCE

Year	Place	Enrollment
2012-Present	Tenes Gıda LTD.	Owner
2003-2012	Raven Müzik Yapım LTD.	Owner&Operator
1999-2001	Yücegün Turizm LTD.	Owner&Operator

FOREIGN LANGUAGES

Advanced English, Basic German

PUBLICATIONS

HOBBIES

Basketball, Scuba Diving, Gourmet, Music Recording, Movies, Motor Sports